UNIVERSITY OF CALIFORNIA
RIVERSIDE

Kinetics of the Dissolution of Scheelite in Groundwater: Implications for Environmental and Economic Geology

A Thesis submitted in partial satisfaction
of the requirements for the degree of

Master of Science

in

Geological Sciences

by

Stephanie Danielle Montgomery

March 2013

Thesis Committee:

Dr. Michael A. McKibben, Chairperson
Dr. Christopher Amrhein
Dr. Timothy Lyons

The Thesis of Stephanie Danielle Montgomery is approved:

_____

_____

_____

Committee Chairperson

University of California, Riverside

ABSTRACT OF THE THESIS

Kinetics of the Dissolution of Scheelite in Groundwater:
Implications for Environmental and Economic geology

by

Stephanie Danielle Montgomery

Masters of Science, Graduate Program in Geological Sciences
University of California, Riverside, March 2013
Dr. Michael McKibben, Chairperson

Tungsten, an emerging contaminant, has no EPA standard for its permissible levels in drinking water. At sites in California, Nevada, and Arizona there may be a correlation between elevated levels of tungsten in drinking water and clusters of childhood acute lymphocytic leukemia (ALL). Developing a better understanding of how tungsten is released from rocks into surface and groundwater is therefore of growing environmental interest. Knowledge of tungstate ore mineral weathering processes, particularly the rates of dissolution of scheelite ($CaWO_4$) in groundwater, could improve models of how tungsten is released and transported in natural waters.

Our research focused on the experimental determination of the rates and products of scheelite dissolution in 0.01 M NaCl (a proxy for groundwater), as a function of temperature, pH, and mineral surface area. Batch reactor experiments were conducted within constant temperature circulation baths over a pH range of 3-10.5. Cleaned scheelite powder with grain diameters of 106-150μm were placed between two screens in a sample platform and then put inside a two liter Teflon vessel filled with 0.01 M NaCl.

Aliquots of solution were taken periodically for product analysis by ICP-OES. Changes in mineral surface characteristics were monitored using SEM and EDS methods.

The integral method was used to interpret data from experiments and to develop a rate law. The specific rate for the dissolution of scheelite in groundwater is expressed as:

$$\frac{dM_{sch\ overall}}{dt} = k_r\left(K_{sp} - IAP\right)$$

where k_r is the reverse rate constant in units of m/sec, K_{sp} is the solubility product in $(mol/L)^2$, and *IAP* is the ion activity product for scheelite in $(mol/L)^2$. At pH 6.2 and 20°C, the specific rate law for the dissolution of scheelite in a 0.01M NaCl groundwater proxy is:

$$\frac{dM_{sch\ overall}}{dt} = 9.09x10^{-8} m/sec\left(2.63x10^{-10} - IAP\right)$$

The dissolution of scheelite shows variable behavior depending on the pH and temperature. At low pH, the release of Ca and W is disrupted by the formation and adsorption of tungstic acid onto grain surfaces. In groundwater with progressively higher alkalinity, W releases at a higher rate. The reaction also follows typical Arrhenius behavior. These results suggest that the warmer and more basic the groundwater that scheelite is in contact with, the greater the propensity for an elevated level of tungsten within it.

Table of Contents

List of Figures

1. Introduction

1.1 Tungsten Chemistry, Occurrence, and Mineralogy

Tungsten (W) is a grayish white metal with an atomic number of 74 and an atomic weight of 183.84. It is a transition element with a melting point of 3422^{o}C and a density of 19,300 kg/m^{3}. Tungsten is not found as a native element in nature, but rather combined in 14 known minerals (Seiler et al., 2005). Its isotopes are 180, 182, 183, 184, and 186. It is the 54th most abundant element in the Earth's crust. As a member of group VIB of the periodic table, it behaves similarly to molybdenum, arsenic, and chromium and its oxidation states are -2 through 6+. The +6 state is the most stable in water (Baes and Mesmer 1976). It occurs as the tungstate ion, sodium tungstate, tungstic acid, heteropoly acids or volatiles. Tungstate (WO_4^{2-}) is the primary aqueous species and is monomeric between pH 6.9 and 9.3 (Seiler et al. 2005).

Tungstate minerals can be found in magmatic, pegmatitic, placer, skarn, and porphyry deposits. The geological ages of most tungsten deposits range from Archaen to the Cenezoic (Turell 2004). Tungsten minerals are divided into two groups; the wolframite and scheelite group. The wolframite solid solution group consists of hüebnerite (Mn), wolframite (Fe,Mn), and ferberite (Fe). The scheelite group consists of many minerals, but scheelite is the most common and of economic importance (Li and Wang, 1947). W can be deposited as scheelite ($CaWO_4$) when W-bearing magma or hydrothermal fluids come into contact with calcium bearing rocks such as limestone.

Scheelite belongs to the tetragonal crystal system and commonly occurs as tetragonal, bipyramial crystals. Scheelite's structure is composed of flattened WO_4 tetrahedra and polyhedra of CaO_8. The Ca-WO_4 bond is mainly ionic and the W-O bond is mainly covalent (Senyshn et al., 2011). Its color can be white, grey, tan, greenish, or yellowish and it has a vitreous to adamantine luster. It can be transparent to translucent with typically good cleavage. Scheelite fluoresces pale blue under shortwave ultraviolet light but slightly yellowish with increasing impurities. It may alter to yellow tungstic acid, (WO_3) or to hydrotungstate, ($WO_3.nH_2O$) (Klien et al., 1985). It is associated with garnet, epidote, quartz, tremolite, molybdenite and calcite in metamorphic deposits. In high temperature quartz veins, it may be found with wolframite, cassiterite, topaz, fluorite, and apatite. Scheelite is 19.4% CaO and 80.6% WO_3. A molybdenum substitution for tungsten is not uncommon.

1.2 Production, Uses, and Regulations

As the most common tungstate with deposits occurring throughout the world (Figure 1), scheelite is the most mined tungsten mineral followed by the wolframite solid solution. The largest producers of tungsten are China, Russia, Bolivia, Austria and Portugal (Infomine 2012). The United States is not among the top producers of W; however, it is one of the top consumers. W is used to make tungsten concentrates, ammonium paratungstate, oxides and acids, tungsten carbide, ferrotungsten, tungsten metal powder, and more. These intermediate products are then used to make weapons, construction materials, jewelry, aircraft parts, and a wide range of other goods

(Newberry, 1986; Shedd, 2012). Because of tungsten's unique characteristics, such as its high tensile strength and melting point, it is in high demand and used frequently. Inevitably, with its growing popularity, tungsten will have increased interactions with other materials, an increased amount of pathways into the human environment, and a higher likelihood of intentional or accidental releases (Koutsospyros et al., 2006).

There is minimal United States government regulation on the amount of tungsten allowed in drinking water. Of the 126 priority toxic pollutants listed in the Clean Water Act of 1977, tungsten is not included. Tungsten also is not included in the 86 contaminants regulated under the Safe Drinking Water Act of 1986. The Occupational Safety and Health Act does have total weight allowance standards for worker's exposure to tungsten listed as 5 mg/m^3 for soluble compounds and $1mg/m^2$ for insoluble compounds. Tungsten inhalation can be somewhat toxic to humans contingent on its form (elemental and fibrous tungsten trioxide) and the method of exposure. Usually tungsten is not easily absorbed by the human body and until recently it has not been considered to be an important human health hazard (Kerwien et al., 1996). However, great interest in the toxicity and behavior of tungsten has now arisen due to a peculiar occurrence in Fallon, Nevada.

1.3 Leukemia Cluster in Fallon, Nevada

Between 1997 and 2002, 15 cases of Acute Lymphocytic Leukemia appeared in children and teenagers living in Fallon, Churchill County, Nevada. This unusual cluster prompted investigations from multiple government agencies including the United States

Geological Survey (USGS) under the leadership of the Centers for Disease Control and Prevention (CDC). By characterizing the chemistry of the groundwater being used as drinking water, the USGS sought to determine if there was something chemically unique about the groundwater that the cancer victims were drinking. Buccal cells, urine, and blood were also collected from Churchill County leukemia sufferers and their families for genetic and chemical analysis (Seiler et al. 2005). The results revealed that over 65% of the total 205 people tested had urine levels of tungsten higher than the 95^{th} percentile for a United States reference population. The presence of elevated tungsten in urine captured the interest of the residents of Fallon, its city officials and state officials (Seiler et al. 2005).

These results stimulated new carcinogenesis and toxicology studies on tungsten, to evaluate the need for further regulatory control. The aim of the investigations was to determine if environmental (instead of genetic) causes were at the root of the cluster. In the study of Seiler et al. (2005), there was extensive testing of groundwater collected from Churchill County in 2001 and 2002. The goal was to describe the occurrence, distribution, source, and processes leading to the elevated amounts of tungsten in the Fallon groundwater. Seiler et al. (2005) identified four aquifers beneath the Fallon area, three of which are in sedimentary basin-fill strata formed from sediments that accumulated at the bottom of ancient Lake Lahontan. The fourth and youngest aquifer lies within a younger basalt intrusion. Sediments comprising the basin-fill aquifers were transported to the basin by the paleo Carson, Truckee, and Walker Rivers, all of which originated in the W rich eastern Sierra Nevada. Stable isotopic compositions of water

samples suggested that the groundwater used for Fallon's drinking water was derived from the Carson Basin aquifers, implying that the W could have been acquired via water-rock interaction with the sediment hosts. Tungsten can be released into groundwater via the weathering of such sediments, and can exist in aquatic environments in both soluble and particulate form. The soluble form is of greater concern because of its higher mobility and toxicity (Seiler et al., 2005).

The CDC performed a conditional logistic regression to determine a statistical correlation between W exposure and the leukemia clusters. An odds ratio (OR) is a type of statistic used to determine the risk of a certain outcome if a particular factor is present (Crichton 2001). In this case, it is the likelihood of childhood acute lymphocytic leukemia when high levels of tungsten were present in the environment. An OR greater than one suggests an elevated risk and anything lower than one suggests no risk. A p-value is the likelihood that an OR is legitimate. It is calculated by evaluating whether or not opposing circumstances are true. In this situation, it was the chance that W has nothing to do with leukemia in Fallon. The closer the p-value is to zero, the higher the likelihood that the value for the calculated OR is not just by chance and a p-value of less than 0.05 suggests that chance alone is not likely to explain the OR derivation from one. Anything greater proposes the opposite. The tungsten OR was 0.78, suggesting that there was no statistical risk, but the p-value is 0.57 indicating that the OR value could be just due to chance. Children in Churchill County had W in their systems at levels 18.5 times higher than the national average of 0.125ug/L. According to the CDC (2003), people living in communities having similar water and geologic formations to Churchill County

can also expect to have tungsten exposure well above the national average. There is no statistically valid relationship between W exposure and the leukemia cluster. The only sure information is the spatial relationship between the cancer clusters and elevated levels of W in the environment, as supported not only by the leukemia cluster in Fallon, but by other cases of similar childhood cancer clusters that exist in tungsten-rich areas in Sierra Vista, Arizona and Elk Grove, California (Sheppard et al., 2008).

1.4 Alloy Exposure and Cancer

Concerns about "green bullets" (in which W alloys replace toxic Pb and depleted U) created by the United States' Green Armament Technology program have arisen as well, after scientists discovered that tungsten alloy bullets leach W into their surroundings and mobilize lead in soils (Claussen et al., 2009). A second study was prompted when reports showed that people shot with tungsten munitions or hit with tungsten bearing shrapnel developed tumors around their wound sites (Kalnitch et al., 2007).

Because very little is known about the health effects of internalized tungsten, a rodent model system was developed to mimic shrapnel seen in wounded soldiers from the 1991 Persian Gulf War. 1mm x 2mm pellets of weapons grade W alloy pellets (91.1% W, 6.0%Ni and 2.9% Co) were implanted into thigh tissue of Male F344 (general, albino multi-purpose, laboratory grade) rats. The rats implanted with the high dose of tungsten alloy developed highly aggressive tumors surrounding the metal within four to five months of implantation. The rats with a lower dose of implanted tungsten alloy also developed tumors, but at a slower rate. In both cases, the high-grade pleomorphic

rhabdomosarcomas type tumors migrated to the lungs and required euthanasia (Kalnitch et al, 2007).

1.5 Economic Implications

Since 1915 China has been recognized as the world's largest producer of tungsten, with present reserves of over five million tons. W, a strategic metal, is used to make tungsten concentrates, ammonium paratungstate, oxides and acids, tungsten carbide, tungsten metal powder, and more. These products are then used to make high speed cutting tools, weapons, construction materials, jewelry, aircraft parts and a wide range of other goods. Since 2010 China, who produces 80% of the world's tungsten supply, has reduced its tungsten export quota by 600 tons to 15,400 tons annually (Smith 2010) and has completely restricted the export of concentrate and unprocessed ore. With such restrictions, the price of tungsten concentrate has increased from $15,213/mt to $20,000/mt (Montgomery, 2011). The United States imports 70% of its tungsten and an understanding how to better discover tungsten ore would make the U.S. less reliant on foreign supplies. The discovery of unknown domestic tungsten is dependent on determining the location of concealed ore deposits, which can be located by exploring for tungsten anomalies in natural waters, soils and rocks.

Current geochemical models for the dissolution and transport of tungstates are tentative at best due to the lack of thermodynamic and kinetic data (Seiler et al. 2005) and corresponding uncertainty over the mechanisms that mobilize tungsten (Koutsospyros

2006). The goal of this research is to parameterize the rates of reaction of scheelite in shallow aqueous environments into a specific rate law, by determining the dependence of the dissolution reaction on reactant concentration, pH, and temperature. The derived rate law can then be plugged into geochemical modeling software such as the Geochemist's Workbench and PHREEQC, to facilitate modeling efforts on tungsten behavior in shallow aqueous settings.

Previous research on tungsten mobility in shallow natural settings has been focused on its behavior in soils, and its effect on wildlife as an aquatic ecotoxin (Bednar et al., 2009, Clausen et al., 2009, Felt et al., 2011, Thomas et al., 2009, and Strigul, 2010). These studies concluded that tungstic oxide is produced by weathering tungsten-bearing sediment or alloy in soils. It is most mobile in groundwater at around pH 11, but at low pH it has a strong tendency to adsorb to mineral grain surfaces (unless phosphate is present, occupying mineral surface sites where tungsten would otherwise adsorb). As an ecotoxin, it was proved to cause the death of embryos in fish and amphibians when present in aquatic systems at concentrations over 0.05 ppb.

Studies on the aqueous dissolution behavior of scheelite have been predominantly performed in caustic high temperature solutions for various hydrometallurgical applications (Girgin et al. 1993, Guedes de Carvalho et al. 1992, Gurmen et al. 1999, Konishi et al. 1990, Martins et al. 2007, Ozdemidotr et al. 1991). Marinakis et al. (1987) studied the solubility of natural scheelite in distilled water as a function of pH (adjusted with perchloric acid or sodium hydroxide) at a fixed ionic strength of 10^{-2} kmol m^{-3} (which was adjusted with $NaClO_4$). The temperature was kept at 298^{o}C. Their

experiments were not focused on deriving a rate law; however this study does shed light on the potential behavior of scheelite during dissolution. Scheelite crystals were crushed and checked for purity using semi-quantitative X-ray fluorescence spectroscopic analysis. Half a gram of scheelite grains with a surface area of $1.13 m^2 g^{-1}$ were used for each experiment. The grains were placed in 30 cm^3, stoppered centrifuge tubes and equilibrated for three days. He observed that the dissolution of the scheelite was incongruent, with the solubility of the calcium being lower than the tungsten above a pH of 6.

Atademir et al. (1979) conducted a similar experiment with synthetic precipitated microcrystalline scheelite in a solution with a pH of 5-13. Five gram samples with a minimum surface area of $7.5 m^2/g$ were placed in Pyrex flasks with 500ml of doubly distilled water. The chemical reaction was monitored by samples that were taken at 3 hour intervals. Samples of the saturated solution were analyzed for Ca and W content using atomic absorption spectroscopy. The solubility of scheelite was lowest at pH 6.6 within a range of 20-25^oC. Previous research on the dissolution rate of scheelite in shallow groundwater settings does not exist.

2. Methodology

An experimental approach was taken, using Teflon batch reactors (McKibben and Barnes, 1986; McKibben et al., 2008). The specific rate for the batch dissolution of scheelite in groundwater can be expressed as:

$$Rate = -dM_{scheelite}/dt = d[W]/dt = k\,(A/V) \quad (1)$$

where *k* is the rate constant, *A* is the total surface area of the mineral grains, and *V* is the volume of fluid in the Teflon vessel. This equation is used to determine the impact of the mineral surface area and temperature on the dissolution rate of the mineral. If the reaction rate is dependent on pH, then the calculated rate constant will vary with pH and a term incorporating the proton concentration must be added to the rate law. The following descriptions of mineral preparation and experimental design allow for the assignment of values to all variables present in the rate law, within a mock shallow groundwater environment.

2.1 Crushing and Sorting

Crystalline, euhedral scheelite from the Xuebaoding Mine in the Hunan province of China was used for experiments (Figure 2). Bulk scheelite was conjoined to an easily separable muscovite-quartz matrix. The scheelite was crushed down to gravel sized pieces using a hammer and chisel (Figure 3), then separated from the undesirable quartz and muscovite with a pair of tweezers. In a dark box, all visibly high quality pieces of scheelite were viewed under a 254 nm wavelength ultraviolet lamp. Pieces that did not fluoresce white to blue-white were removed because any significant variance in color was representative of a different and undesirable chemical composition. Grains were crushed more finely using a ceramic mortar and pestle, sieved, and then the 106-150μm and the 45-106μm fractions were retrieved. The sized scheelite was further sorted for purity under a binocular microscope. Only grains free of visible impurities were used for further analysis and experiments.

The purified scheelite grains were analyzed using a Shimadzu 3000 Lab X powder x-ray diffractometer (XRD). The diffractogram display and analysis program MacDiff written by Petschick (1996) was used to confirm the mineralogy. The resulting diffractogram coincided with a standard for scheelite confirming that any possible impurities were not major (minerals less than a few percent in abundance may not have been detected) (Figure 4). Elemental composition of the scheelite was further confirmed using an XL30-FEG scanning electron microscope (SEM) and Energy Dispersive X-ray micro analysis software. Only the presence of tungsten, calcium, and oxygen within the scheelite was detected (Figure 5).

2.2 Surface Area Measurement

Surface area is important for quantifying reaction rates in water-rock interactions (Brantley et al. 2008). Freshly crushed and sieved grains were coated with a fine dust which had to be removed, to prevent an inaccurately high surface area measurement, free fines suspended in solution during the experiment, and an erroneous fast initial rate caused by their rapid dissolution. Grains were cleaned by submersing one gram of scheelite powder in a glass beaker containing 35ml of histological grade acetone and then ultrasonicating it for five minutes. The acetone containing suspended scheelite fines was then decanted. Another 35ml of acetone as added to the beaker and along with the scheelite, was ultrasonicated twice more in the same manner until the rinsate was clear. Finally the scheelite was rinsed with ACS grade ethanol within a vacuum filtration system and allowed to completely dry under vacuum for six minutes. SEM

photomicrographs confirmed the success of the cleaning method in removing fines from the grain surfaces (Figure 6).

After cleaning, the scheelite grains' specific surface area was measured by Quantachrome Laboratories using a multipoint Brunauer, Emmett and Teller (B.E.T.) method with Krypton gas at an outgassing temperature of 100.0^{o}C. The measured surface of one gram of 106-150 µm scheelite was .042 m^2 and the surface area of the smaller 45-106 µm fraction measured .060 m^2.

2.3 Ionic Strength Proxy for Groundwater

The solution used as a groundwater substitute was 0.01 NaCl with an ionic strength of 0.01, a level representative of most natural waters (Deutsch 1997, Drever 1982). The sodium chloride used was certified ACS reagent grade with a calcium weight percentage of 0.0005. The water used was twice distilled using a Thermo Scientific Mega-Pure glass still and then processed through a Fisher Scientific EASYpure II LF ultrapure system. The ultrapure system employed a 0.2µm filter to remove micro particles, deionized and filtered the water to a resistivity of 18.2 MΩ cm^{-1}, and killed any microbes present with ultraviolet light. When desired, the pH of the water was adjusted with ACS grade potassium hydroxide.

2.4 Batch Reactor Setup and Accompanying Hardware

Experiments took place within a batch reactor adapted from the reactor design of McKibben and Barnes (1986). To begin, the scheelite had to be secured within a sample

platform (a PVC trap valve fitting). First, a two inch diameter, 20 μm mesh nylon screen round was placed onto the lower portion of the trap valve fitting. Then one gram of cleaned scheelite was gently placed on top of the nylon round. Next a second nylon round was placed atop the scheelite and the cap of the trap valve fitting was screwed onto the lower portion, sandwiching and securing the scheelite between the nylon mesh, within the fitting (Figure 7). The design of the sample platform allows for reactor fluid to circulate through and around the grains.

The PVC ring sample platform was secured with three 3-inch Plexiglas fins in the middle of a two liter Teflon reaction vessel (Figure 8). The vessel was secured shut by a Teflon lid with ports allowing for 3 ml sample extraction, temperature measurements, pH measurements, argon inflow, water inflow, and water outflow. 3ml samples were taken because that volume was best suited for ICP-OES analysis but would not significantly affect the volume of remaining solution for the duration of the experiment. 99.99% pure industrial grade Argon was chosen to percolate through the solution in order to exclude atmospheric CO_2 (which could affect pH and speciation) and because it is more inert than nitrogen gas. The gas was delivered to the vessel by a Teflon tube connected to the regulator of the argon tank on one end, and at the other end to a fritted glass dispersion tube partially submersed in the Teflon vessel. The groundwater was circulated through the vessel by size 73 Masterflex LFL Tygon tubing, connected to a smaller diameter tubing of the same type. The different tubing sizes were connected with tapered barbed connectors and firmly secured from the outside with

electrical tape. Opposite ends of the Teflon tubing were connected to glass inflow and outflow tubes protruding from the sample ports on the reactor lid. The tubing was then looped through the mouth of a Masterflex I/P peristaltic pump. The lower 7/8 of the vessel was lowered into the circulation bath once the vessel setup was completed (Figure 9).

Before experiments, the groundwater proxy was purged with argon at a pressure of 10psi for one hour and fifteen minutes dropping the dissolved oxygen content from ~48% to 1.2%. Purging allowed for the reduction of oxygen and carbon dioxide in solution, the latter of which if present could affect the pH and speciation of W ions. One minute before adding the groundwater to the reactor, the reactor was purged with argon at the same flow rate to prevent interaction with the atmosphere. Throughout the experiment, the gas input was maintained as it constantly exerted a positive pressure against the atmosphere outside the vessel.

Before the water was introduced to the vessel, the peristaltic pump was turned on and set to circulate water at 6,500 ml per minute (a rate determined not to inhibit the ionic transport of reactants, as discussed below). $0.0018m^3$(same as 1.8L) of synthetic groundwater was introduced into the vessel by pouring it through a separator funnel attached to a sample port. As soon as the water circulated through the tubing and came in contact with the scheelite via the inflow tube, the timer was started. The first sample was taken within the first two minutes of the experiment. The blank samples were taken from the initial, argon-purged batch of groundwater.

Samples were taken at intervals ranging from every five minutes at the beginning of the run to every ten minutes in the terminal stages. Accurately determining the initial rate may requires a high frequency of sampling in the initial phases of the experiment. A total of 15 samples per run was the most common with duplicates for the blank, sample 7, and sample 15. The distribution of duplicates allowed the measured concentrations to be verified throughout analysis.

3. Analytical Techniques

Aliquots of solution were taken periodically with a 1ml barrel piston plastic tipped pipette and stored in a polypropylene mailing tube for up to three days. Each sample was diluted with approximately 2ml of ultrapure water one hour prior to analysis (an average dilution factor of 1.6) to bring the sample volume to a level necessary for analysis in the ICP-OES. Acid was not added to the sample so as to insure that nothing in solution would adsorb to the mailing tube or precipitate from the sample. Next, samples were evaluated for W, Ca, Fe, and Mo in a Perkin-Elmer Optima 7300 DV Inductively Coupled Plasma Optical Emission Spectrometer (ICP-OES), to document the changes in product concentration over the duration of the experiment. The detection wavelengths were as follows; Tungsten: 207.912 nm, Calcium: 317.933 nm, Iron: 238.204 nm, and Molybdenum: 202.031 nm. A Multicomponent Spectral Fitting (WinLab32 software) was used for baseline correction. An internal standard of 2.5 ppm Yttrium was added to the samples by mixing into the sample stream between the auto sampler and the nebulizer. Linear calibrations were made using 200 and 1000 µg/L standards for W and 200 and 2000 µg/L standards for the other elements. The limit of

detection for tungsten was 3.5 ppb, calcium: 3.9 ppb, iron: 0.5 ppb and molybdenum: 0.6 ppb.

Atmospheric CO_2 was excluded from runs for the following reasons. The dissolution of scheelite can be assumed to exhibit the following stoichiometry:

$$CaWO_4 \leftrightarrow Ca^{+2} + WO_4^{2-} \quad (2)$$

If the groundwater is not sufficiently purged and the system is not kept with a positive pressure of Argon, the solution might react with the atmosphere and bicarbonate may form from CO_2 hydrolysis (Equation 3) and cause precipitation of calcium carbonate (Equation 4) during scheelite dissolution.

$$CO_2 + H_2O \leftrightarrow H^+ + HCO_3^- \quad (3)$$

$$CaWO_4(s) + HCO_3^- \leftrightarrow CaCO_3(s) + WO_4^{2-} + H^+ \quad (4)$$

If the tungstate ions come in contact with enough free hydrogen in solution, tungstic acid precipitates and adsorbs to the surfaces of the scheelite grains (Equations 5 and 6), restricting the reaction between the scheelite surface and the water, significantly thwarting the dissolution rate. The formation of tungstic acid is shown below.

$$2H^+ + WO4^{2-} = H_2WO_4 \quad (5)$$

$$H_2WO_{4\,(aq)} \leftrightarrow H_2WO_{4\,(s)} \quad (6)$$

For those reasons CO_2 was consistently minimized by maintaining a positive pressure of argon and all experiments were held at a pH of 6.2 or above.

4. Results

Over 80 batch experiments were run over the course of this research. Run data selected for incorporation into the rate law was chosen based upon reproducibility (Figure 10). The experimental data used to derive rate laws are presented in Appendices A and B. Raw data tables for all experiments used may be found in Appendix C.

4.1 Stoichiometry and the Rate Indicating Variable

Initially the dissolution of scheelite is nonstoichiometric. Ca^{2+} ions preferentially release into solution. The preferential leaching of elements from a dissolving mineral is due to a difference in site energies between ions. Nonstoichiometric dissolution could also be caused by impurity phases or zones within the mineral (Brantley et al. 2008). Scheelite behaves like a silicate in that it dissolves non-stoichiometrically at first but eventually reaches stoichiometric dissolution (Figure 11). When there is preferential release of a particular ion from a mineral, the rate should be calculated based on the ion that is not preferentially released (Brantley et al. 2008). Calcium was preferentially released at the beginning of most experiments, except those held at pH above 8.2 and above, where W was preferentially released for the entire duration of the experiment. Graphs of data displaying this behavior can be found in Appendix A. Because the pH of common natural waters ranges from 3 to 9, and because there is particular interest in the release rate of W, W was selected as the rate indicating variable.

4.2 Transport

It is common for researchers to vary the flow rate during dissolution experiments to test for transport control (Brantley et al. 2008). A series of experiments was completed to study the effect of fluid transport on the release rates of W and Ca. Experiments at 20^{o}C, and pH 6.2 were done at pump rates of 5.2; 19.4; 29.4; 91.6; and 108.3ml per second (Figure 12). Results suggest that the release rate of W increased with increasing pump speed (Figure 13). The release rate of tungsten increased with increasing pump speed until 91.6 ml/sec, beyond which the release rate did not increase any further despite a faster pump rate. It can be concluded then that the dissolution of scheelite is transport limited until such a flow rate is reached in the experiments. Subsequently, all experiments were run at rates higher than this.

Base conditions for each experiment were held at the following: pH 6.2, a pump rate of 108.3ml/sec, an argon pressure of ~10 psi, 20^{o}C, 0.0018m^{3} of 0.01M NaCl, with one gram of 106-150µm (0.042m^{2} surface area) scheelite. When experiments to observe the effect of proton concentration were conducted, the pH was adjusted to the desired level with potassium hydroxide. For experiments to investigate the effects of temperature and pump rate, all variables were held constant except for the one of interest.

4.3 The Integral Method

Because the dissolution of scheelite is a reversible reaction it is considered a complicated reaction (Brezonik 1994). To find a rate equation that best describes the reaction, the integral method (Brantley 2008) was used. This method requires that the

reaction of interest be assumed to follow a known rate expression and then the experimental data is used to affirm or disprove that assumption.

Once a rate law is selected, an integrated rate expression must be developed from that law. A characteristic plot of the chosen expression produces a straight line and if the experimental data plot according to the integrated expression, the data (in this case from the dissolution of scheelite) is considered consistent with the corresponding rate equation.

4.4 Choosing a Rate Equation

A theoretical rate equation was derived as follows, using the method of Kamatani et al. (1980). Again, the dissolution of scheelite is a reversible reaction, meaning that there is a forward and reverse reaction taking place simultaneously. Kinetic expressions for reversible reactions include a term for the back reaction (Equation 7)

$$dM_{scheelite\ overall}/dt = R_f - R_r \tag{7}$$

where R_f is the forward rate and R_r is the reverse rate. Since there are two reactions taking place, accordingly, there exists a rate constant for each reaction: k_f for the forward rate constant and k_r for the reverse rate constant. Such forward and reverse rate expressions can be defined independently of each other in relation to the overall rate of dissolution (Equation 8 and 9)

$$R_f = k_f \left(\frac{A}{V}\right) \tag{8}$$

$$R_r = k_r \left(\frac{A}{V}\right) [Ca^{2+}] [WO_4^{2-}] \tag{9}$$

where A is the mineral surface area in m^2, and V is the volume of 0.01M NaCl in m^3, k_f is in mol/m/sec, and k_r is in L^2/mol/m/sec.

The overall dissolution rate of scheelite is defined by combining equations 8 and 9 (Equation 10).

$$dM_{scheelite\ overall}/dt = k_f \left(\frac{A}{V}\right) - k_r \left(\frac{A}{V}\right)[Ca^{2+}]\,[WO_4^{2-}] \tag{10}$$

The next step in developing the theoretical rate equation is to rewrite the expression in terms of the reverse rate constant and the ion activity product (IAP). The concentration of Ca^{2+} multiplied by the concentration of WO_4^{2-} is the IAP under any condition (Equation 11); at equilibrium it becomes the K_{sp} (Equation 12). The K_{sp} calculations and values for each temperature used during experiments can be found in Appendix D.

$$IAP = ([Ca^{2+}]\,[WO_4^{2-}]) \tag{11}$$

$$K_{sp} = [Ca^{2+}]\,[WO_4^{2-}] \tag{12}$$

Likewise, at equilibrium the forward and reverse rates of reaction are equal:

$$k_f \left(\frac{A}{V}\right) = k_r \left(\frac{A}{V}\right)[Ca^{2+}][WO_4^{2-}] \tag{13}$$

$$k_f \left(\frac{A}{V}\right) = k_r \left(\frac{A}{V}\right) K_{sp} \tag{14}$$

Substitution of this expression into equation 10 yields:

$$dM_{scheelite\ overall}/dt = k_r\left(\frac{A}{V}\right) Ksp - k_r\left(\frac{A}{V}\right)[Ca^{2+}][WO_4^{2-}] \quad (15)$$

$$dM_{sch\ overall}/dt = k_r\left(\frac{A}{V}\right)(Ksp - IAP) \quad (16)$$

where the K_{sp} and *IAP* are in $(mol/L)^2$ and the overall rate is in $mol/m^2/sec$.

4.5 Integrating the Rate Expression

Integrated expressions for elementary reactions can be arranged so that rate constants can be found graphically by a plot of concentration versus time (Brezonik 1994). Integration of equation 16 from the start of a dissolution experiment to a theoretical state of saturation (equilibrium) produces a linear equation (Equations 17-19).

$$\int_{t=0}^{t=final} \frac{dM_{sch\ overall}}{dt} = \int_{IAP=0}^{IAP=K_{sp}} k_r\left(\frac{A}{V}\right)(K_{sp} - IAP) \quad (17)$$

$$\int_{IAP=0}^{IAP=K_{sp}} k_r\left(\frac{A}{V}\right)(K_{sp} - IAP) = \ln\frac{K_{sp}}{K_{sp}-IAP} = k_r\left(\frac{A}{V}\right)t \quad (18)$$

$$\ln\frac{K_{sp}}{K_{sp}-IAP} = k_r\left(\frac{A}{V}\right)t \quad (19)$$

When the concentration data for an individual run are plotted in this way, they conform to a straight line (as shown in the graphs of Appendix B), confirming the selection of the correct form of the integrated rate law. It can be seen that $k_r(A/V)$ is the slope (m) of the line in the plot of ln $K_{sp}/(K_{sp}$-IAP) versus time.

$$m = k_r\left(\frac{A}{V}\right) \quad (20)$$

The reverse reaction's rate constant for each experiment is therefore simply calculated from the values of *m*, *A* and *V*:

$$k_r = m\left(\frac{V}{A}\right) \tag{21}$$

An example of the calculation process used to find k_r is shown below for experiment 62, where the slope of the fitted data was $2.12x10^{-6}$ sec^{-1}, the surface area of the grains was $0.042m^2$ and $0.00138m^3$ of 0.01M NaCl was used.

$$k_r = m\left(\frac{V}{A}\right) = \frac{2.12x10^{-6}}{sec}\left(\frac{0.0018\,m^3}{0.042\,m^2}\right) \tag{22}$$

$$k_r = 9.09x10^{-8} m/sec \tag{23}$$

The reverse rate constant can be related to the forward rate constant and the solubility product by the following equation:

$$K_{sp} = \frac{k_f}{k_r} \tag{24}$$

The solubility product for scheelite in distilled water at 20°C is $10^{-9.58}$ (based on entropy and enthalpy values for Ca^{2+}, WO_4^{2-}, and scheelite from Naumov et al., 1974 and Robie et al.1978 as derived in Appendix D). Such a small K_{sp} means that there will be a large k_r, and a small k_f. By plugging in the values for K_{sp} and k_r then rearranging the equation (Equations 25-27) the forward rate constant is calculated to be $2.39x10^{-18}$ m/s.

$$10^{-9.58} = \frac{k_f}{9.09x10^{-9} m/s} \tag{25}$$

$$k_{f=} 10^{-9.58} * 9.09x10^{-9} m/s \quad (26)$$

$$k_{f=} 2.39\text{x}10^{-18} m/s \quad (27)$$

All of the forward and reverse rate constants produced using the integral and initial rate method can be found in Table 1.

Table 1. Slopes and rate constants

Experiment	pH	T (^{o}C)	K_{sp}	Integral Method Slope (sec^{-1})	k_r (m/sec)	k_f (m/sec)
48	6.2	20	2.63E-10	1.22E-07	5.23E-09	1.38E-18
49	6.2	20	2.63E-10	1.38E-07	5.91E-09	1.56E-18
52	6.2	20	2.63E-10	4.06E-07	1.74E-08	4.58E-18
59	6.2	35	4.64E-10	1.58E-06	6.76E-08	3.16E-17
61	6.2	20	2.63E-10	1.72E-06	7.37E-08	1.94E-17
62	6.2	20	2.63E-10	2.12E-06	9.09E-08	2.39E-17
63	6.2	20	2.63E-10	2.09E-6	8.96E-08	2.36E-17
74	7.0	23	2.93E-10	6.00E-06	2.57E-07	7.59E-17
75	8.1	20	2.63E-10	3.03E-06	1.30E-07	3.50E-17
76	8.1	20	2.63E-10	8.64E-07	3.70E-08	9.74E-18
77	6.2	20	2.63E-10	1.19E-06	5.08E-08	1.34E-17
78	6.2	20	2.63E-10	2.42E-06	1.04E-07	2.72E-17
80	6.2	20	2.63E-10	2.88E-06	1.24E-07	3.25E-17
82	6.2	20	2.63E-10	5.39E-06	2.31E-07	6.08E-17
83	6.2	8	1.56E-10	5.32E-08	2.28E-09	3.53E-19
84	6.2	8	1.56E-10	1.21E-07	5.19E-09	8.03E-19
86	10.5	24	3.05E-10	3.41E-06	1.46E-07	4.12E-17
87	8.2	20	2.63E-10	5.52E-07	2.37E-08	6.67E-18
88	10.5	20	2.63E-10	4.16E-06	1.78E-07	5.03E-17
89	10.5	20	2.63E-10	4.39E-06	1.88E-07	5.30E-17
90	6.2	30	3.85E-10	5.39E-06	2.31E-07	8.99E-17

4.6 Effect of Grain Size

In runs conducted at pH 6.2, 20°C, and 106-150µm grains, the rate of the dissolution of scheelite increased with increasing specific surface area of the mineral grains (Figure 14). The same was observed by Girgin (1993).

4.7 Effect of Variations in pH

The effect of pH on the reaction rate was observed from experiments conducted at pH 6.2, 7.0, 7.1, 8.1, 8.2 and 10.5, 20-24°C, and a grain size of 106-150µm. Trial experiments run at a pH below 6.2 quickly developed a yellow coating on grain surfaces (Figure 15) and a yellow gel-like substance was deposited on the sample platform and the bottom of the reaction vessel (Figure 16). Investigation with the SEM (which detected the presence of only W, Ca, and O) and review of previous research led to the conclusion that the precipitate was tungstic acid. Below pH 6, tungstic acid is expected to form on the surfaces of dissolving scheelite (Marinakis et al. 1987). The tungstic acid adsorbed to the scheelite surfaces, hindered the dissolution of scheelite into the surrounding groundwater, and resulted in lower dissolved tungsten concentrations in fluid samples, creating a false (slower) dissolution rate. At pH 6.2, the initial rate of reaction is not stoichiometric but favors the release of calcium (Appendix A, experiments 61, 62, and 80). The release of W and Ca does become stoichiometric with time as observed in experiment 80 (Appendix A), an approximately 24 hour experiment. The pH did not drift much over the course of the run, for example an experiment started at pH 6.2 ended at 6.1. At the highest pH tested, the release of W surpassed Ca continuously. There was no

observable solid reaction products formed at pH values above 6. Reverse rate constants obtained by the integral method showed that though there was a small increase in rate with increasing pH (slope = 0.064), the fit of the data to a line was so poor (R^2= 0.16) that the trend could not be justified (Figure 17). Essentially there appears to be no effect of pH on the rate.

4.8 Effect of Temperature

The effect of temperature on the reaction rate was determined by the reverse rate constants of experiments held at 8°C, 20°C, 30°C, and 35°C and a consistent pH of 6.2. An Arrhenius plot of the temperature data is shown in Figure 18.

The reverse rate constant increased with increasing temperature, had an R^2 of 0.95, a slope of 16752.36, and apparent activation energy (E_a) of 139.28 kJ/mol. Expectedly the reverse reaction had the same slope, r^2 value, and E_a as the forward reaction.

4.9 Calculation of the Rate Law

The integral method's rate law is a correct representation of the relationships between the rate constants, area, volume, and rate. Following equation 16, in settings like those of experiments run at base conditions (pH 6.2, 20°C, and one gram of 106-150µm scheelite), the specific rate law for the dissolution of scheelite is:

$$dM_{sch\ overall}/dt = 9.09x10^{-9} m/sec(2.36x10^{-10} - IAP) \quad (28)$$

5. Discussion

5.1 Implications for Environmental Geology

Seiler found that concentrations of W exceeding 50mg/l are associated with NaCl water types. The p factor, representing a statistical correlation between subjects of interest, was 0.25 for Cl and 0.54 for Na with respect to tungsten. As mentioned earlier, any p value over 0.05 represents a significant correlation. One of the factors affecting the W concentration in Fallon's groundwater is the dissolution of primary tungstates, such as scheelite in sediments. Scheelite in the Carson Desert sediments could be weathering under current conditions, possibly increasing the concentration of W in groundwater. Even with the calculated dissolution rate for scheelite, there is still uncertainty with predicting scheelite saturation and dissolution because of the need for complementary thermodynamic data and rate laws for ammonia, phosphate, and fluoride complexes that include tungstate in their composition.

Of the groundwater samples collected in and around Fallon, all samples with W concentrations above 50mg/L have a pH greater than 8. The only samples that did not follow this trend were taken from areas without significant sources of W. Overall, the W concentrations in Fallon's groundwater increased with increasing pH. The rate data from these laboratory experiments loosely predict the same trend. Seiler also observed that in groundwater with low pH, the adsorption of tungstic acid controls W release, which parallels what was observed in this study's low pH experiments thus demonstrating that tungstic acid absorption increases with decreasing pH.

5.2 Implications for Economic Geology

The specific rate law for the dissolution of scheelite derived from this work may be plugged into computer modeling software and used to model the distribution of aqueous W levels in fluids surrounding valuable tungsten ore. This work suggests that that W from scheelite is soluble at high pH and can be sampled in an aqueous phase within waters with a pH above 6. At a low pH, W is released but quickly adsorbed to other surfaces, therefore sampling for W exploration may be best made using a solid, secondary phase (McKibben 2007) such as an iron manganese oxyhydroxide (Seiler et al., 2005). In the mining industry, scheelite is regarded as having low solubility and aqueous W has not been considered as a good source for pathfinding tungsten ore. The data from this study suggests that W may be a detectable pathfinder in alkaline waters.

6. Future Work

Future work should investigate how other factors present in natural environments affect the dissolution of scheelite. In groundwater there are varying levels of CO_2 present that may have an effect on the reaction beyond what was observed in this research. This would also be interesting to investigate because of the growing popularity of carbon dioxide sequestration in aquifers. This solution used in this investigation was only a groundwater proxy by ionic strength. Future scheelite dissolution experiments might involve a synthetic groundwater which includes major groundwater ions Ca^{2+}, Mg^{2+}, Na^{2+} K^{+}, HCO_3^-/CO_3^- SO_4^-, Cl^- and NO_3^- (Deutsch 1997) so as to observe how dissolution

proceeds with influence by the common ion effect and increased product species in solution.

It would also be useful to define the dissolution rates of hüebnerite and ferberite, the second and third most commonly occurring tungstates which can contribute to the dissolved levels of tungsten in groundwater. Flow through (rather than batch) experiments with scheelite should also take place to observe how the dissolution reaction proceeds at low pH in the absence of layers of adsorbed products on the mineral surface (tungstic acid or calcium carbonate) and to find how the reaction proceeds without the accumulation of ions in solution.

7. Conclusion

The aquatic behavior of tungsten in not well understood. As a potential carcinogen, strategic metal, and indicator metal, discovering its natural source is beneficial both economically and medically. This research satisfies one of the fundamental steps to reaching an understanding of where aqueous tungsten comes from; it identifies how it is released from one of its natural sources, scheelite. Conclusions gathered from this study can be summarized as follows.

1. Subneutral pH inhibits the dissolution rate of scheelite in 0.01M NaCl. At levels below pH 6, dissolution is complicated by the formation and adsorption of tungstic acid. As the pH increases, the release rate of tungsten increases and eventually supersedes that of calcium.
2. The dissolution of scheelite occurs at a greater rate with increasing temperature.

3. The release of tungsten from scheelite is very reliant upon rate of fluid flow. The faster the flow rate, the faster W is released until a flow rate of 91.6ml/sec is surpassed and then the release of W is no longer transport limited.
4. The integral method should be used in reversible reaction analysis, as it gives account of the forward, backward, and overall rates and the corresponding rate constants.
5. The reverse rate constant is much larger than the forward rate constant.

Works Cited

Atademir, M. "The Surface Chemistry and Flotation of Scheelite. I. Solubility and Surface Characteristics of Precipitated Calcium Tungstate." *Journal of Colloid and Interface Science* 71.3 (1979): 466-76. Print.

Baes, Charles F., and Robert E. Mesmer. *The Hydrolysis of Cations*. New York: Wiley, 1976. Print.

Bednar, A.J., R.E. Boyd, W.T. Jones, C.J. McGrath, D.R. Johnson, M.A. Chappell, and D.B. Ringelberg. "Investigations of Tungsten Mobility in Soil Using Column Tests." *Chemosphere* 75.8 (2009): 1049-056. Print.

Brantley, Susan Louise., James David. Kubicki, and Art F. White. *Kinetics of Water-rock Interaction*. New York: Springer, 2008. Print.

Brezonik, Patrick L. *Chemical Kinetics and Process Dynamics in Aquatic Systems*. Boca Raton: Lewis, 1994. Print.

Centers for Disease Control. *Cross-Sectional Exposure Assessment of Environmental Contaminants in Churchill County, Nevada*. Rep. N.p., n.d. Web. Oct. 2011.

Chriton, Nichola. "Descriptive Account: Dealing With Incidence, Prevalence, and Odds Concepts in Undergraduate Epidemiology." *Descriptive Account: â Dealingâ With Incidence, Prevalence, and Odds Concepts in Undergraduate Epidemiology*. Blackwell Science Ltd., n.d. Web. 4 Mar. 2012. <http://www.bioscience.heacademy.ac.uk/journal/vol14/beej-14-7.aspx>.

Clausen, Jay L., and Nic Korte. "Environmental Fate of Tungsten from Military Use." *Science of The Total Environment* 407.8 (2009): 2887-893. Print.

Deutsch, W. J. *Groundwater Geochemistry: Fundamentals and Applications to Contamination*. Boca Raton, FL: Lewis, 1997. Print.

Drever, James I. *The Geochemistry of Natural Waters*. Englewood Cliffs, NJ: Prentice-Hall, 1982. Print.

Felt, D., S. Larson, C. Griggs, C. Nestler, M. Thompson, and R.A. Price. "The Potential for Bioaccumulation of Tungsten in Earthworms - the Effect of Legacy Lead on Biouptake." *Land Contamination & Reclamation* 17.1 (2009): 161-67. Print.

Girgin, I., and F. Erkal. "Dissolution Characteristics of Scheelite in $HClC_2H5OHH2O$ and HClC2H5OH Solutions." *Hydrometallurgy* 34.2 (1993): 221-29. Print.

Guedes De Carvalho, R. "Leaching of Scheelite (CaWO4) under Quasi-stagnant Solution Conditions." *Hydrometallurgy* 28.1 (1992): 45-64. Print.

Gurmen, S. "Acidic Leaching of Scheelite Concentrate and Production of Hetero-poly-tungstate Salt." *Hydrometallurgy* 51.2 (1999): 227-38. Print.

Kalinich, John. "Embedded Weapons-Grade Tungsten Alloy Shrapnel Rapidly Induces Metastatic High-Grade Rhabdomyosarcomas in F344 Rats." *National Center for Biotechnology Information*. U.S. National Library of Medicine, 8 Jan. 1991. Web. Dec. 2011. <http://www.ncbi.nlm.nih.gov/pubmed/15929896>.

Kamatani, A. "Dissolution Rates of Silica from Diatoms Decomposing at Various Temperatures Kamatani, A., 1982. Mar. Biol., 68(1):91–96." *Deep Sea Research Part B. Oceanographic Literature Review* 29.12 (1982): 92-96. Print.

Kerwien, Stacey. "TUNGSTEN ALLOYS - Storming Media." *TUNGSTEN ALLOYS - Storming Media*. U.S. Army Armament Research, Development and Engineering Center, n.d. Web. 3 Jan. 2012. <http://www.stormingmedia.us/keywords/tungsten_alloys.html>.

Konishi, Y., H. Katada, and S. Asai. "Leaching Kinetics of Tungsten from Low-grade Scheelite Ore in Aqueous Na4EDTA Solutions." *Hydrometallurgy* 23.2-3 (1990): 141-52. Print.

Koutsospyros, A., W. Braida, C. Christodoulatos, D. Dermatas, and N. Strigul. "A Review of Tungsten: From Environmental Obscurity to Scrutiny." *Journal of Hazardous Materials* 136.1 (2006): 1-19. Print.

Laidler, Keith J. *Chemical Kinetics*. New York: Harper & Row, 1987. Print.

Li, K. C., and Chongyou Wang. *Tungsten, Its History, Geology, Ore-dressing, Metallurgy, Chemistry, Analysis, Applications, and Economics,*. New York: Reinhold Pub., 1947. Print.

Marinakis, K.I., and G.H. Kelsall. "The Surface Chemical Properties of Scheelite (CaWO4) I. The Scheelite/water Interface and CaWO4 Solubility." *Colloids and Surfaces* 25.2-4 (1987): 369-85. Print.

Martins, J., J. Lima, A. Moreira, and S. Costa. "Tungsten Recovery from Alkaline Leach Solutions as Synthetic Scheelite." *Hydrometallurgy* 85.2-4 (2007): 110-15. Print.

McKibben, Michael A., and Hubert L. Barnes. "Oxidation of Pyrite in Low Temperature Acidic Solutions: Rate Laws and Surface Textures." *Geochimica Et Cosmochimica Acta* 50.7 (1986): 1509-520. Print.

McKibben, Michael A., Bryan Tallant, and Josie Del Angel. "Kinetics of Inorganic Arsenopyrite Oxidation in Acidic Aqueous Solutions." *Applied Geochemistry* 23.2 (2008): 121-35. Print.

McKibben, Michael A. *Release Rates of W and Li from Dissolution of Common Ore Minerals in Aqueous Environments*. 2008. USGS grant proposal.

Montgomery, Michael. "Tungsten." *Price Continues to Rise on China's Tight Export Quota*. n.d. Web. Mar. 2012. <http://tungsteninvestingnews.com/1052-tungsten-price-continues-to-rise-on-chinas-tight-export-quota.html>.

Naumov, G. B., Boris Nikolaevich. Ryzhenko, I. L. Khodakovskiĭ, Ivan Barnes, and Velma Speltz. *Handbook of Thermodynamic Data*. Menlo Park, CA: U.S. Geological Survey, Water Resources Division, 1974. Print.

Newbery, J. E. "Chapter 8. Ti, Zr, Hf; V, Nb, Ta; Cr, Mo, W; Mn, Tc, Re." *Annual Reports Section "A" (Inorganic Chemistry)* 80 (1983): 171. Print.

Petschick, R. *MacDiff*. *MacDiff*. Vers. 4.2.5. N.p., 1991-ongoing. Web. <ftp://servermac.geologie.uni-frankfurt.de/Pub/MacDiff/>.

Robie, Richard A., Bruce S. Hemingway, and James R. Fisher. *Thermodynamic Properties of Minerals and Related Substances at 298.15 K and 1 Bar* [Reston, Va.]: Dept. of the Interior, U.S. Geological Survey, 1979. Print.

Seiler, R. "Comment on "Elevated Tungsten and Cobalt in Airborne Particulates in Fallon, Nevada: Possible Implications for the Childhood Leukemia Cluster" by P.R. Sheppard, G. Ridenour, R.J. Speakman and M.L. Witten." *Applied Geochemistry* 21.4 (2006): 713-14. Print.

Seiler, R., K. Stollenwerk, and J. Garbarino. "Factors Controlling Tungsten Concentrations in Ground Water, Carson Desert, Nevada." *Applied Geochemistry* 20.2 (2005): 423-41. Print.

Senyshyn, Anatoliy, Markus Hoelzel, Thomas Hansen, Leonid Vasylechko, Vitaliy Mikhailik, Hans Kraus, and Helmut Ehrenberg. "Thermal Structural Properties of Calcium Tungstate." *Journal of Applied Crystallography* 44.2 (2011): n. pag. Print.

Shedd, Kim B. "Tungsten Statistics and Information." *USGS Minerals Information: Tungsten*. N.p., 3 May 2012. Web. 9 June 2012. <http://minerals.usgs.gov/minerals/pubs/commodity/tungsten/>.

Smith, Michelle. "China Cuts 2012 Export Quotas For Tungsten." *Tungsten Investing News: Tungsten Price, Tungsten Investing, Tungsten Exploration & Development*. N.p., n.d. Web. Apr. 2012. <http://tungsteninvestingnews.com/1673-china-cuts-2012-export-quotas-tungsten-malaga-kenametal.html>.

Strigul, Nikolay. "Does Speciation Matter for Tungsten Ecotoxicology?" *Ecotoxicology and Environmental Safety* 73.6 (2010): 1099-113. Print.

Thomas, Vernon G. "Assessment of the Environmental Toxicity 2 and Carcinogenicity of 3 Tungsten-based Shot." *Ecotoxins and Environmental Saftey* 72.4 (2009): 1034-037. Web. Feb. 2012.

"Tungsten Mining." - *CommodityMine*. N.p., n.d. Web. 3 Apr. 2012. <http://www.infomine.com/commodities/tungsten.asp>.

Özdemir, S. "Decomposition of Scheelite in Acid-alcohol Solutions." *Minerals Engineering* 4.2 (1991): 179-84. Print.

Figures

Figure 1. A map of scheelite localities around the world. The image was taken from Mindat.com.

Figure 2. Some of the scheelite used for experiments shown in its original state before crushing and sorting. The grayish and white materials on the surface of the orange scheelite crystal are quartz and muscovite. Both were removed during sorting.

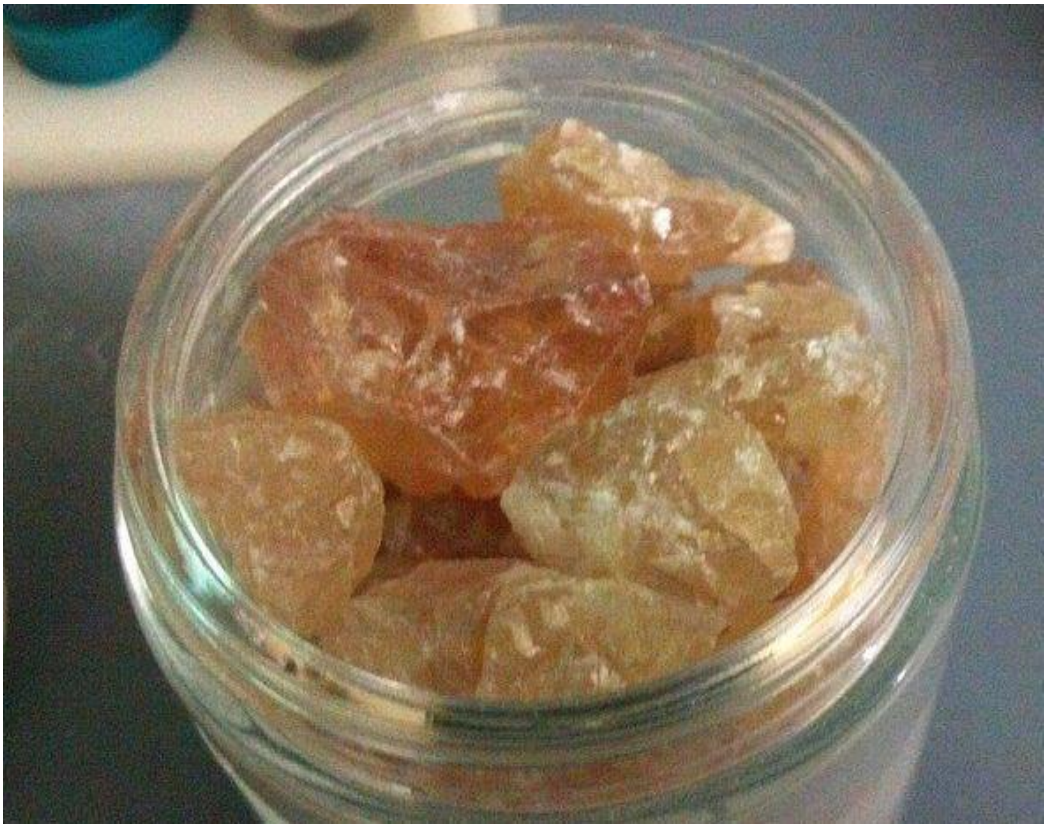

Figure 3. Gravel-sized scheelite to be further crushed and sorted under a microscope.

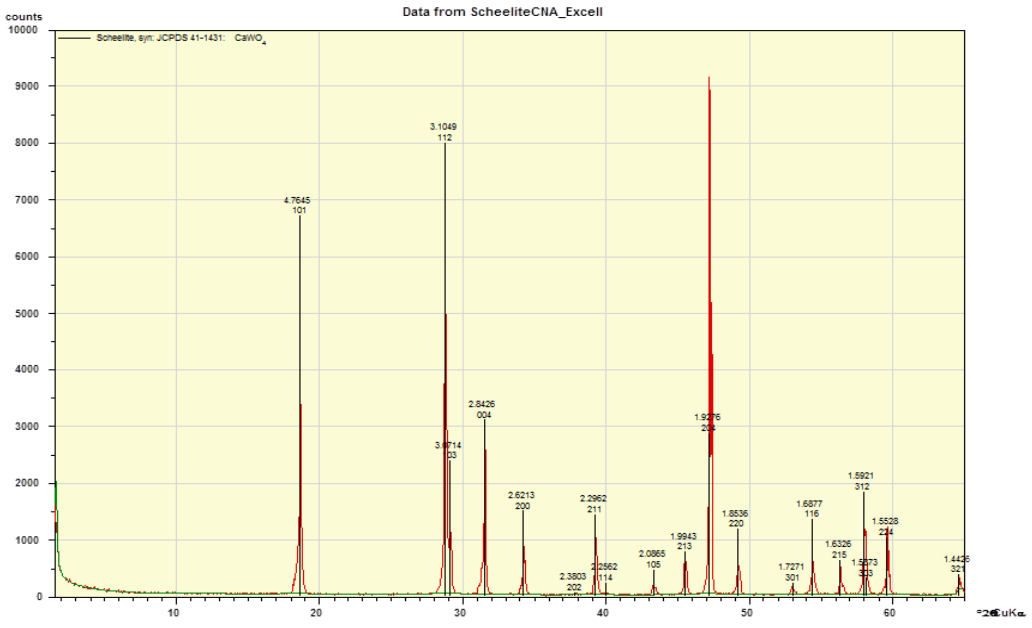

Figure 4. X-ray diffractogram of the scheelite used for experiments. The pattern produced (red peaks), matches the MacDiff standard (black lines).

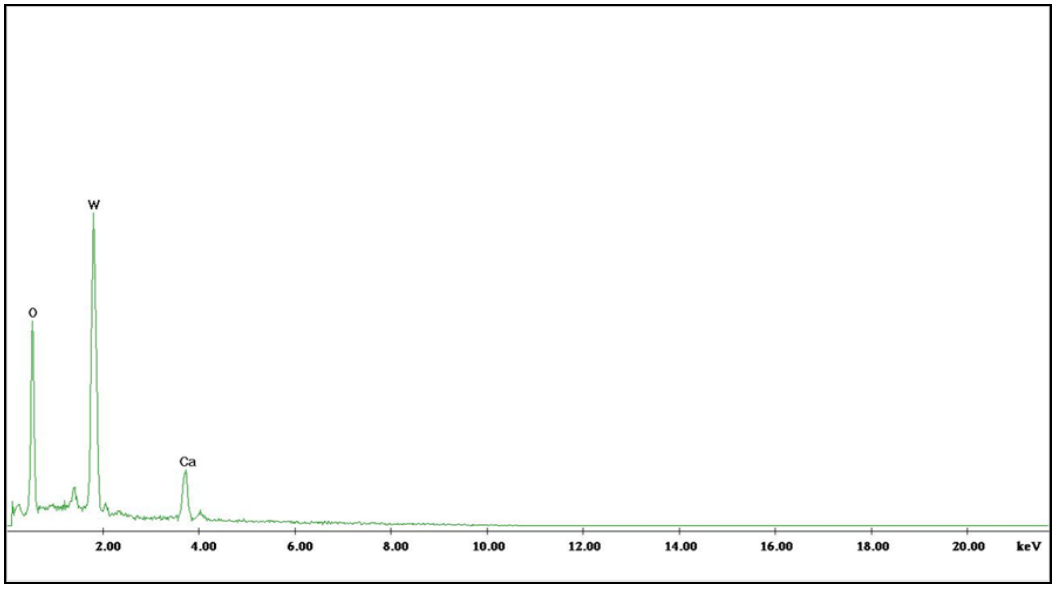

Figure 5. EDS peaks for scheelite. The common scheelite impurities Mo and Fe are not present. The peaks are plotted in counts versus keV. The counts (y axis) are not shown but range from 0 to 3500.

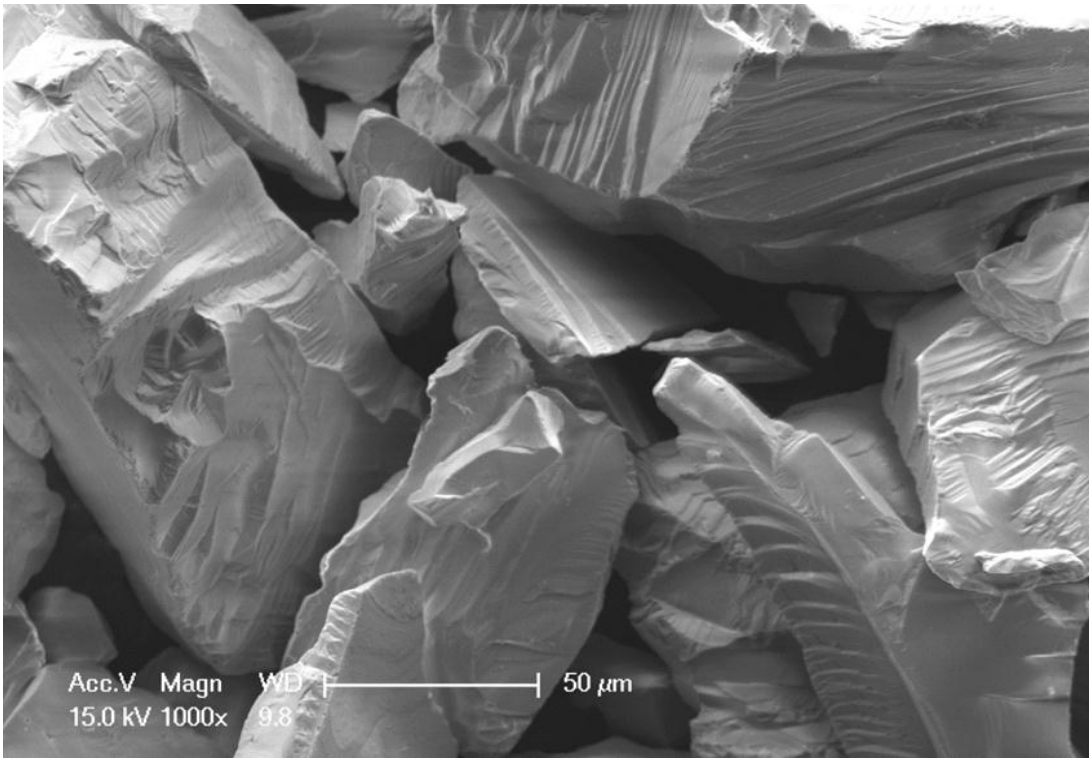

Figure 6. SEM photomicrograph of scheelite grains cleaned with acetone and ethanol. The surfaces are absent of fines.

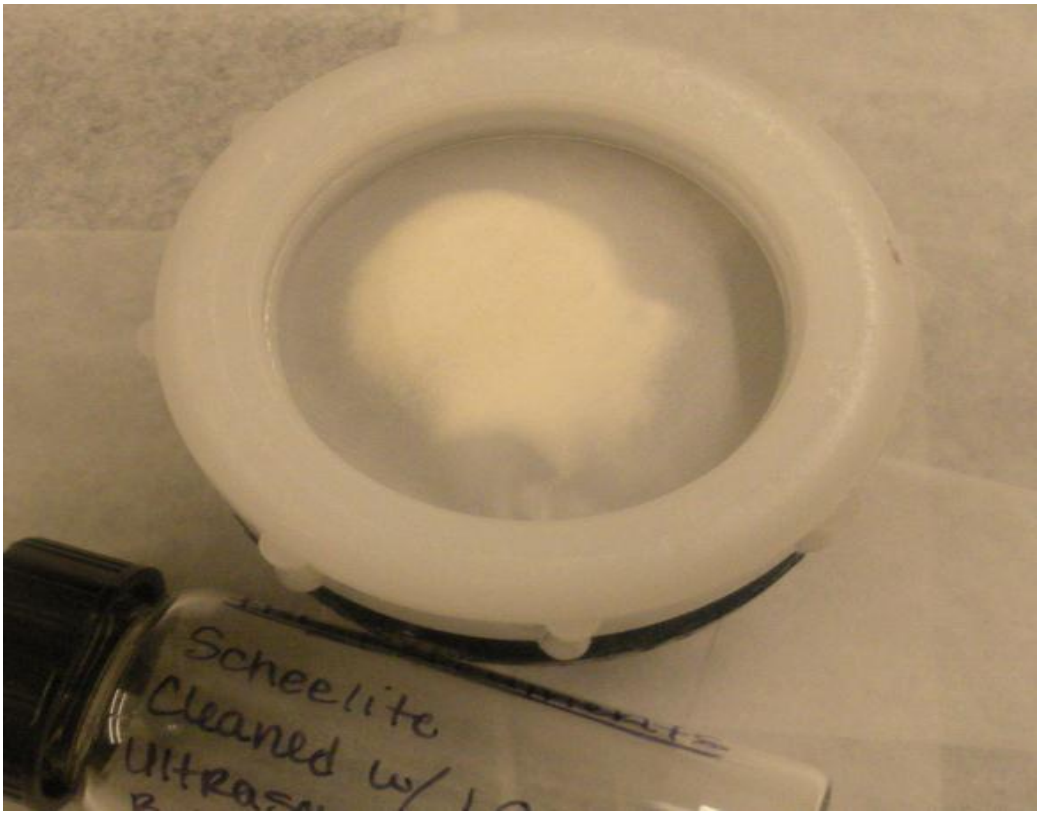

Figure 7. Sample platform (viewed from top) loaded with one gram of scheelite (the fine tan grains in the middle).

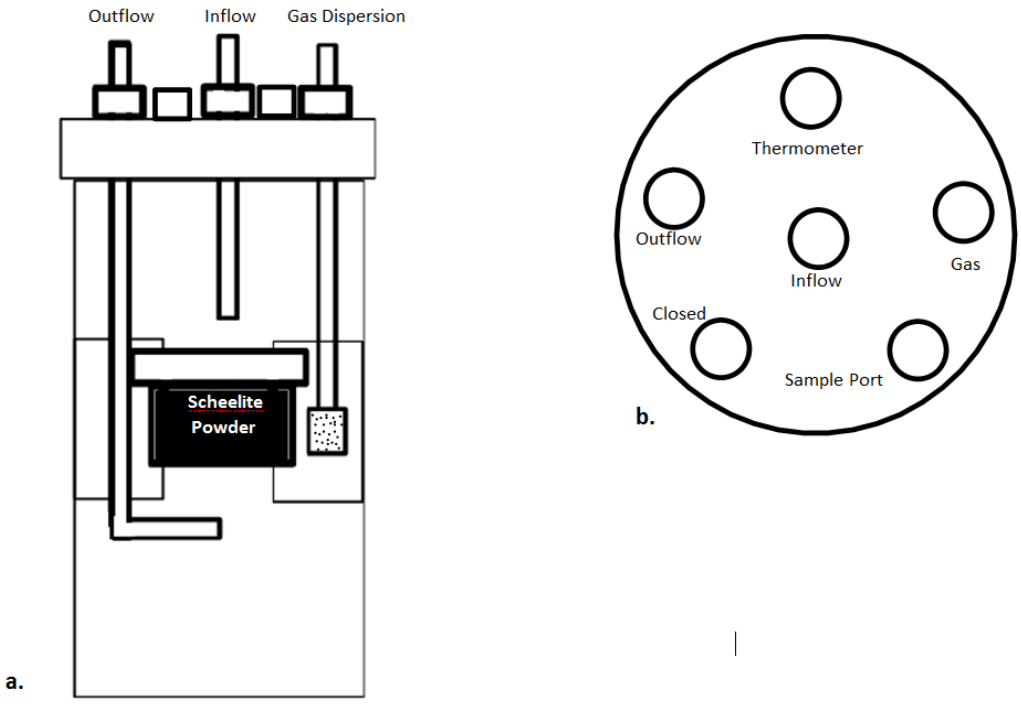

Figure 8. a. A cross-section of the batch reactor assemblage. b. A view of the top of the Teflon vessel and port assignments.

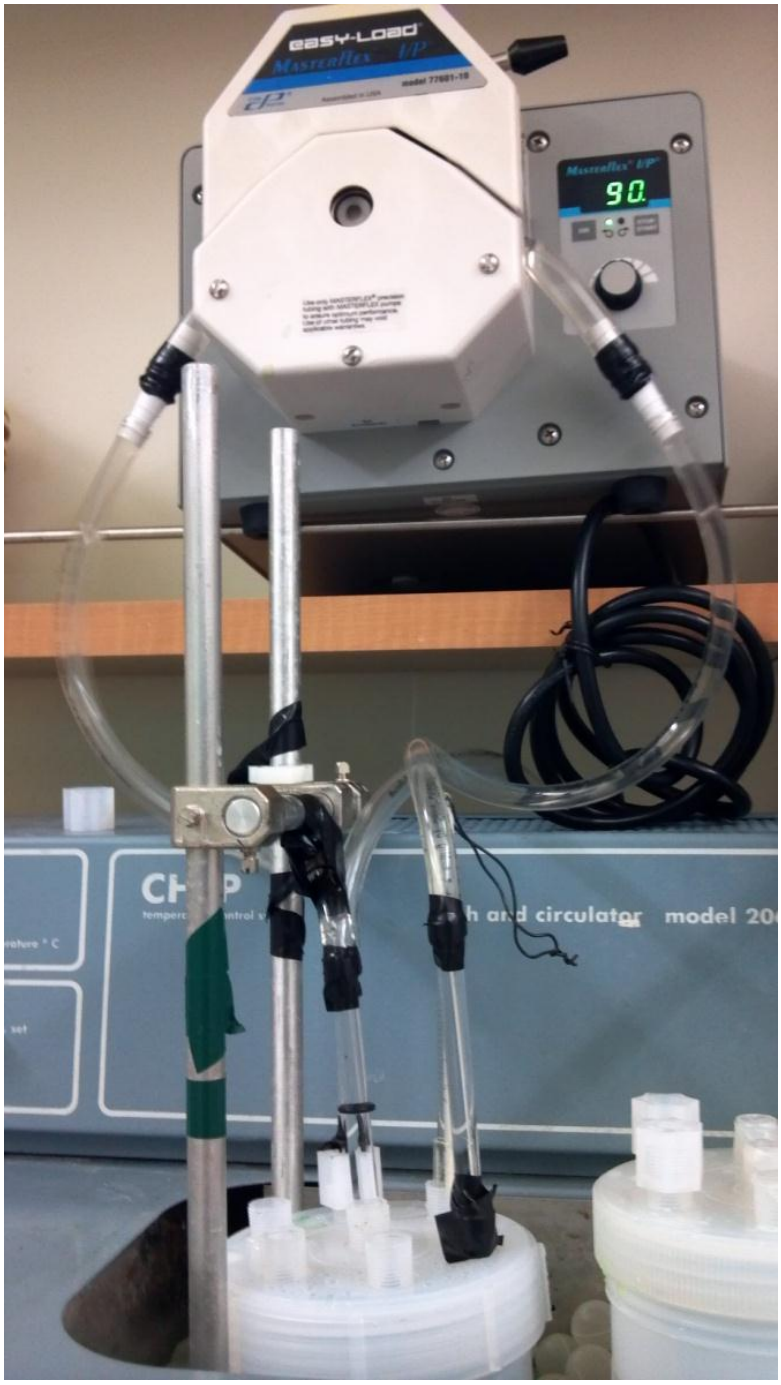

Figure 9. This is a photograph of the Teflon batch reactor resting inside of the antifreeze-filled circulation bath. The reactor is connected to tubing looped through a peristaltic pump.

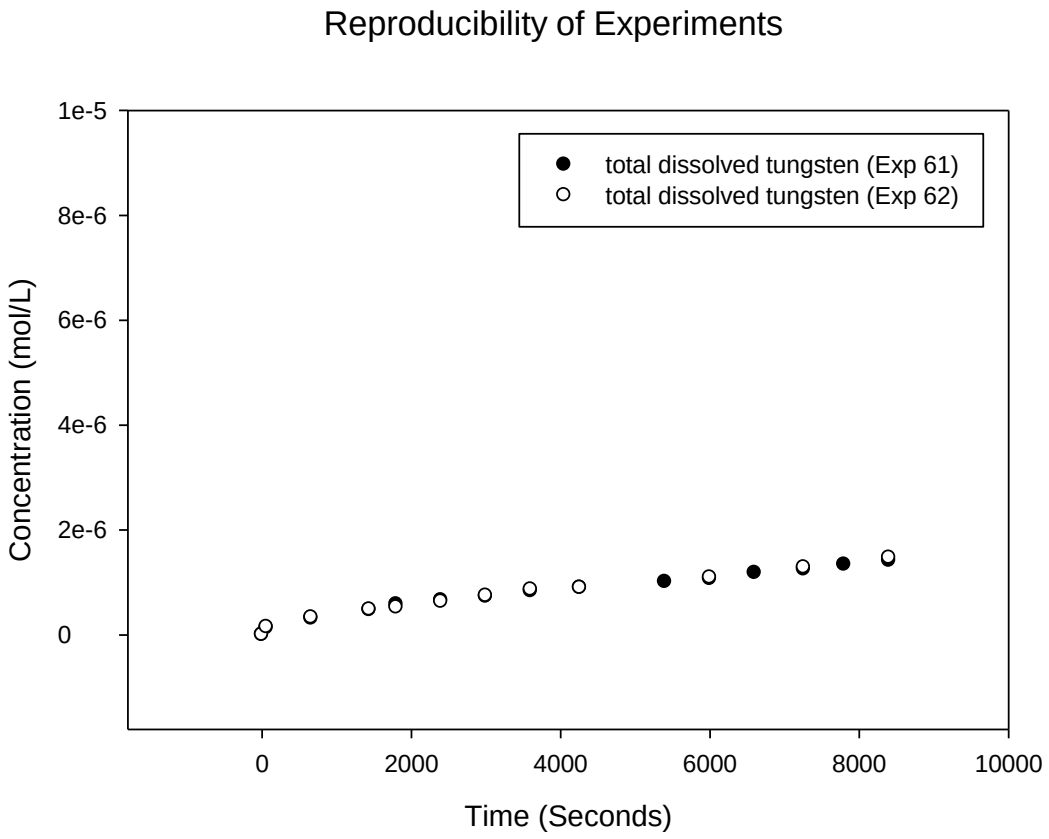

Figure 10. Graph of the concentrations of W for two experiments conducted with the same settings; 1 gram of scheelite at pH 6.2 and 20°C.

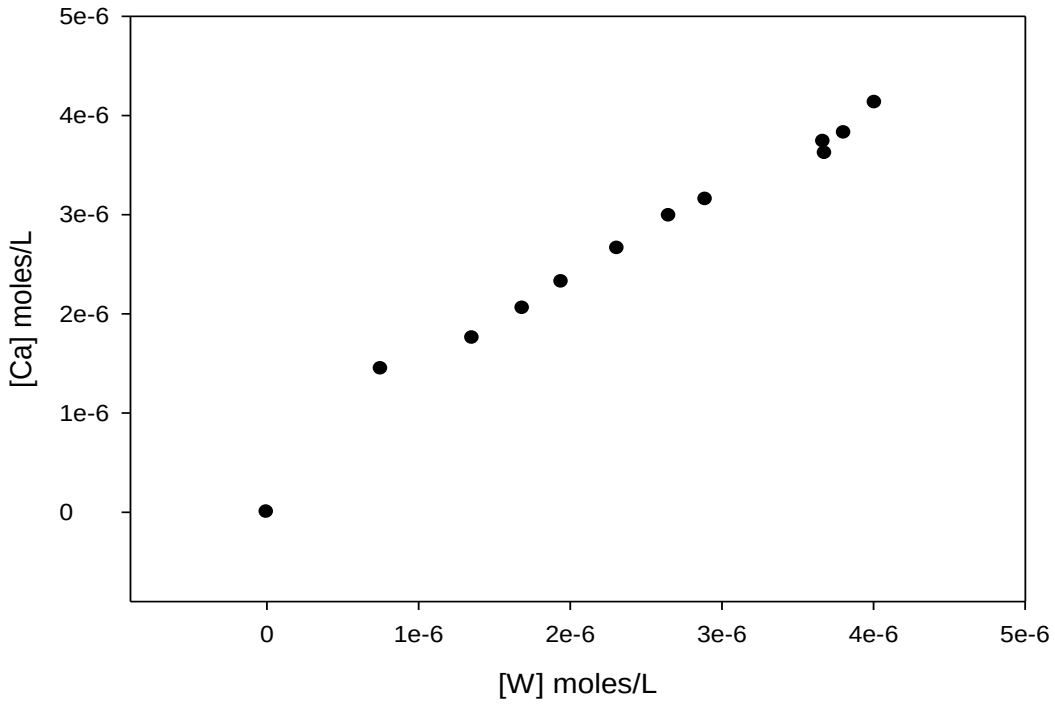

Figure 11. Plot of the non-stoichiometric release of Ca and W from scheelite.

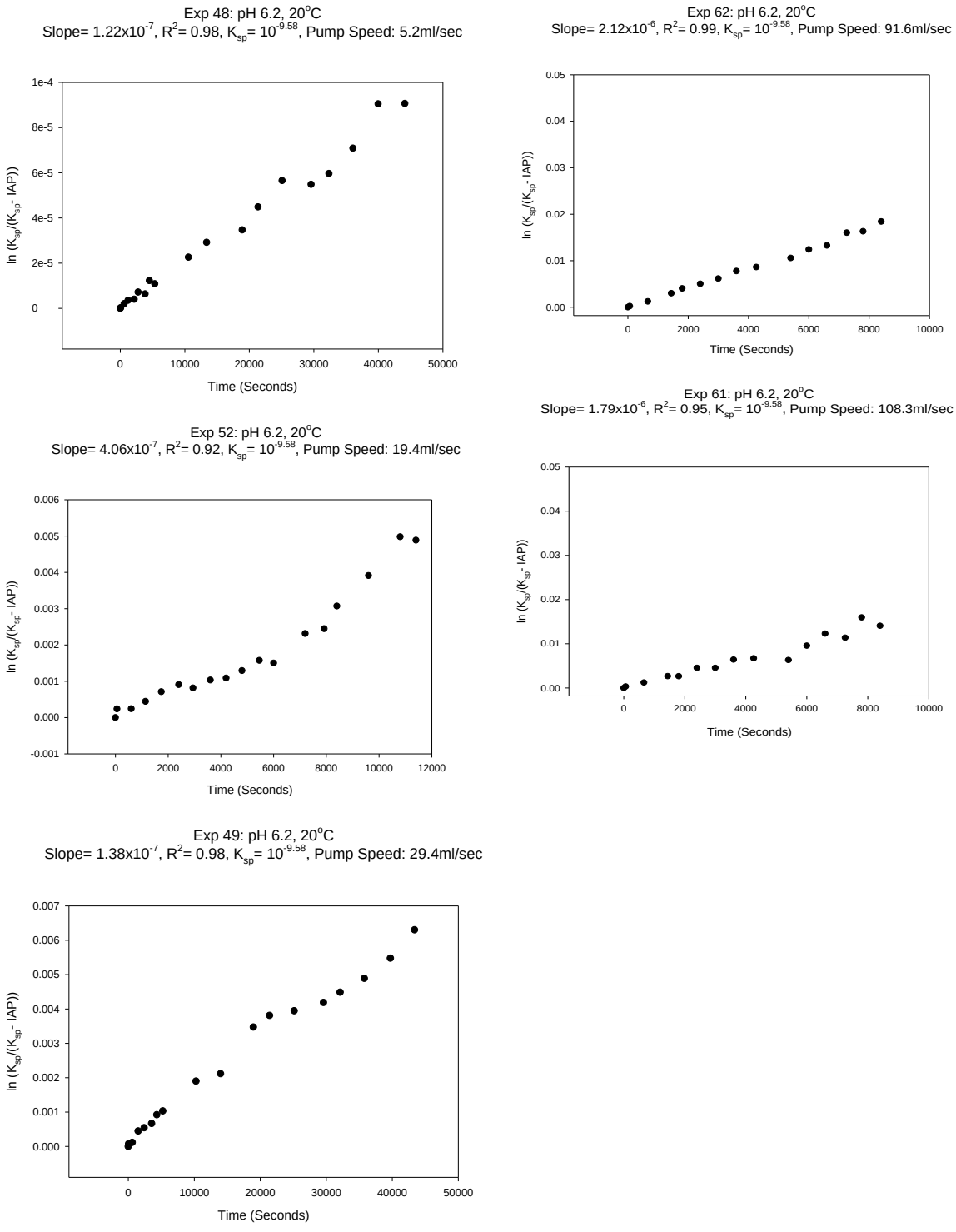

Figure 12. Plots showing the differences in rate per pump speed (in support of Figure 13)

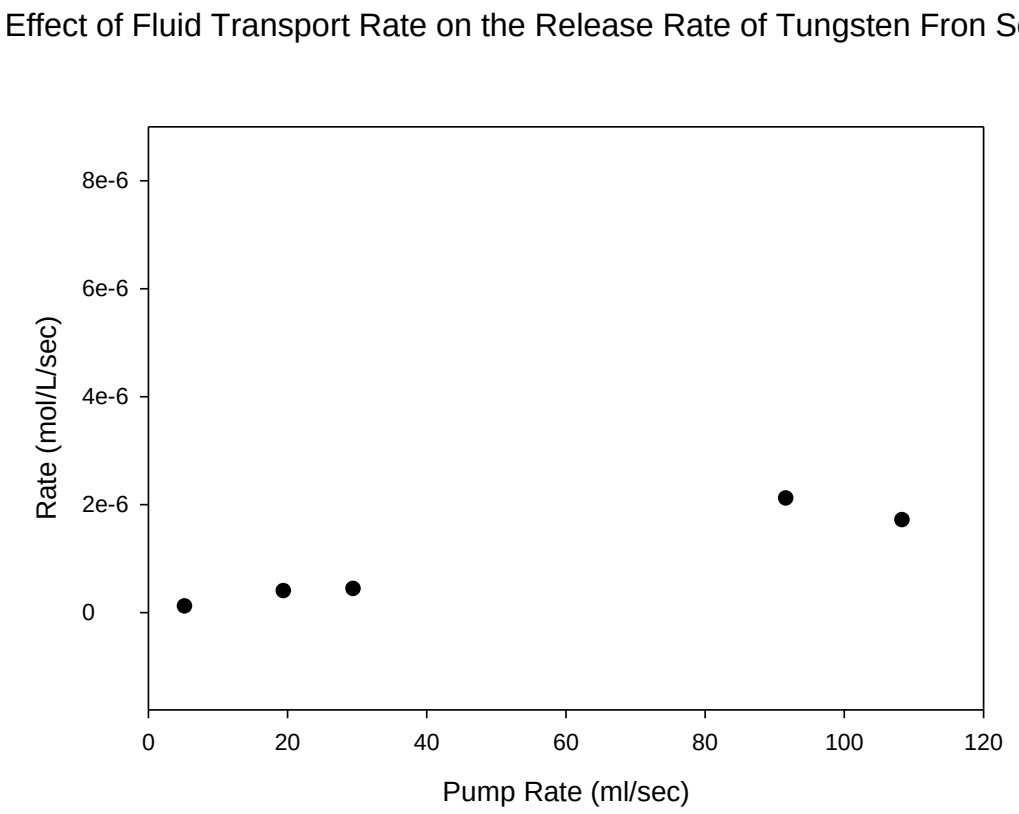

Figure 13. The rate of tungsten release increased with increasing pump speed and water transport rate. The maximum speed represents the fastest flow rate achievable with the available pumps.

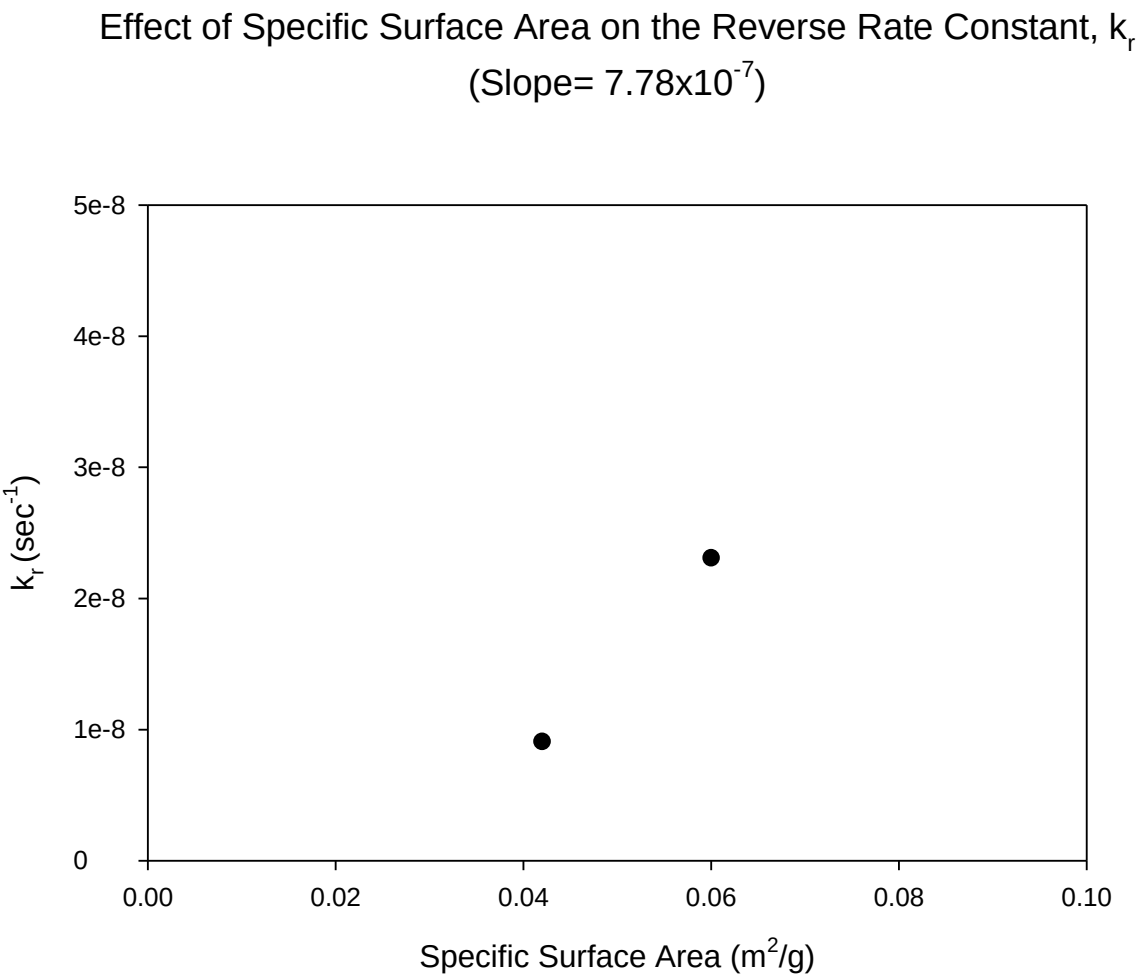

Figure 14. Plot illustrating how an increase in specific surface area is positively correlated to an increase in the reverse rate constant.

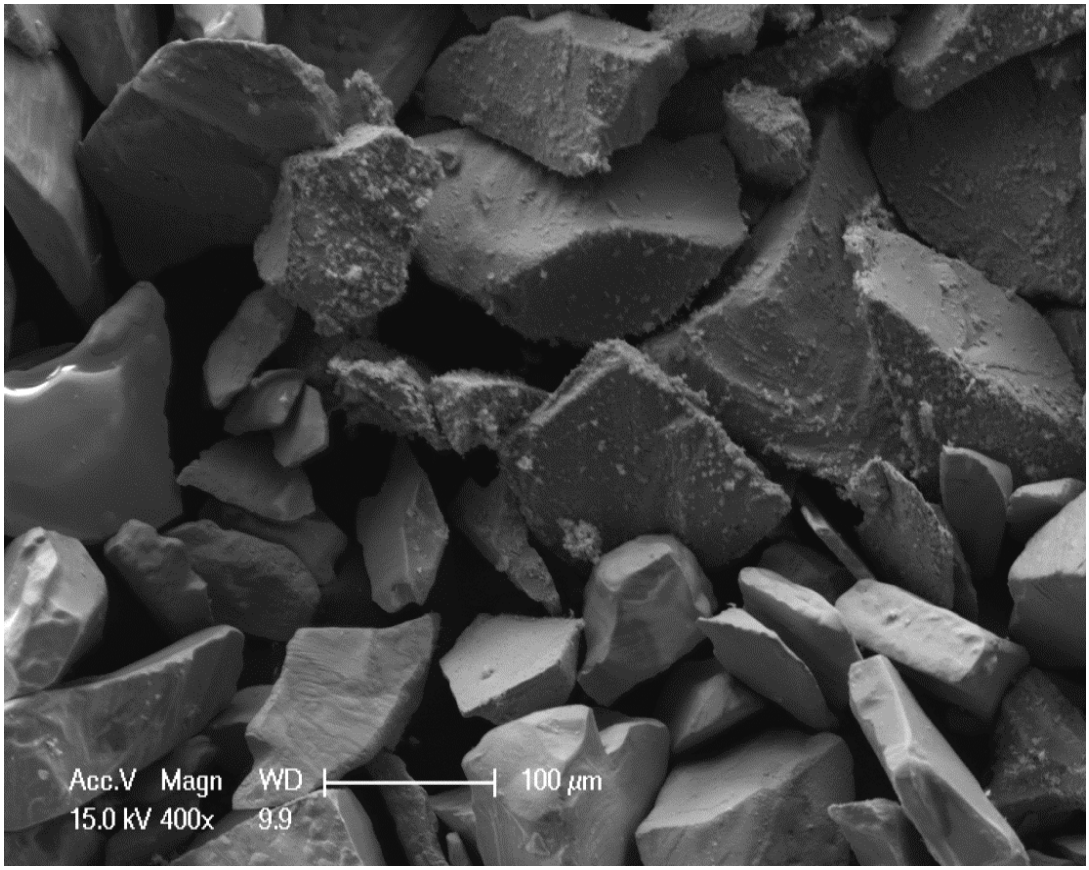

Figure 15. Scheelite coated with tungstic acid after a run at pH 4.0.

a.

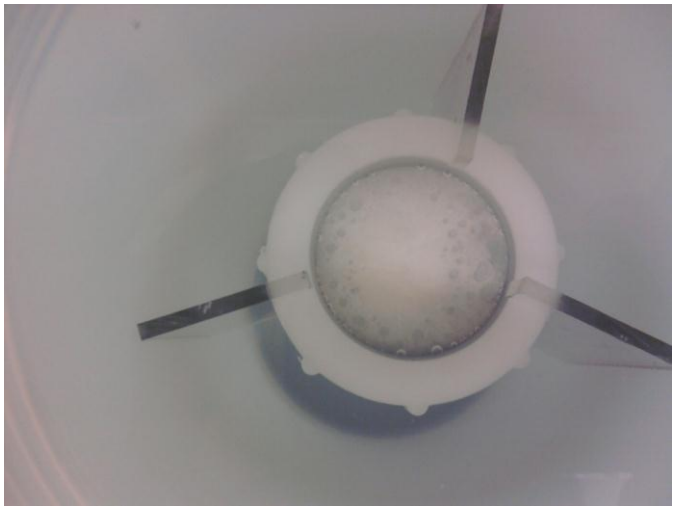

b.

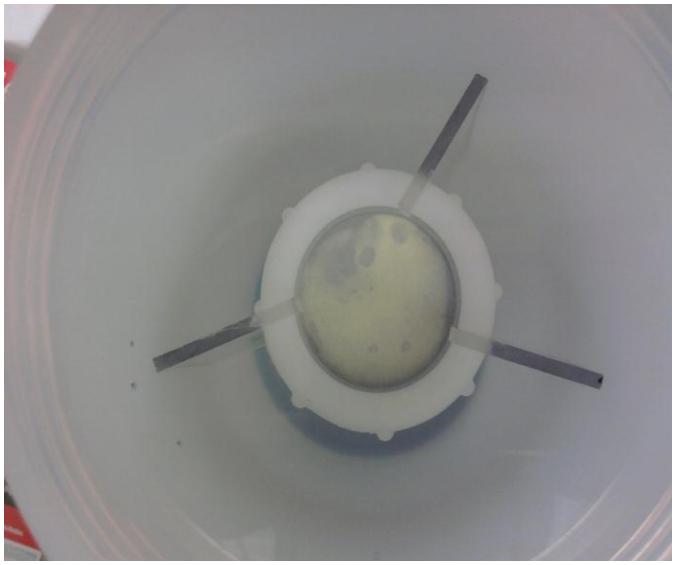

Figure 16. a. Scheelite in the sample platform (looking down into Teflon vessel) after an experiment at pH 6.2. b. Scheelite in the sample platform after an experiment at pH 4.0.

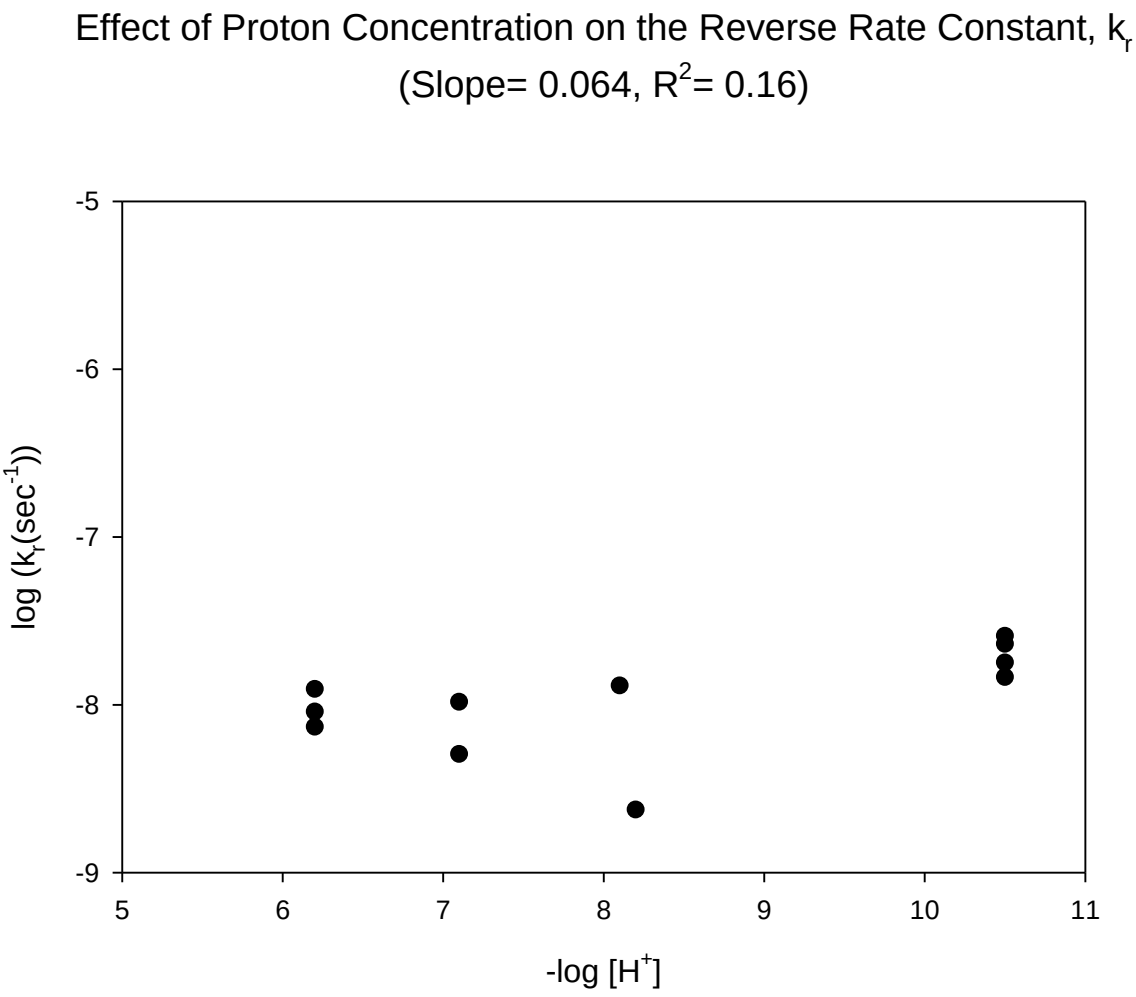

Figure 17. The effect of pH on the reverse rate constant.

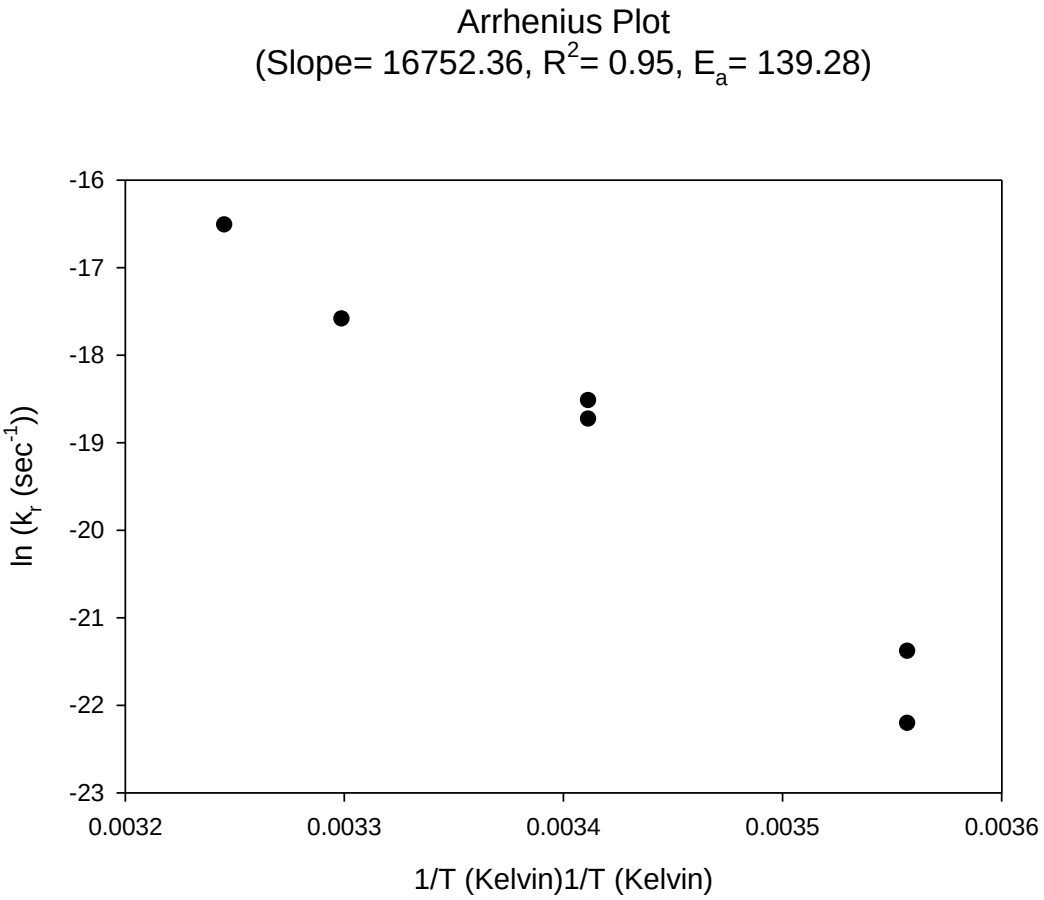

Figure 18. Arrhenius plot showing the effect of temperature on the reverse rate constant.

Appendix A: Raw Data

Exp 48: pH 6.2, 20°C, Pump Speed 5.2ml/sec

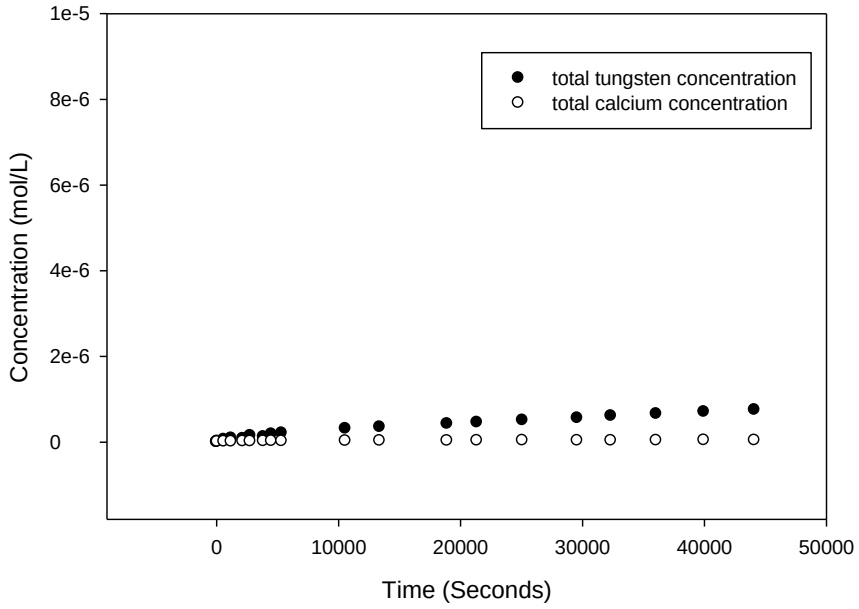

Exp 49: pH 6.2, 20°C, Pump Speed 29.4ml/sec

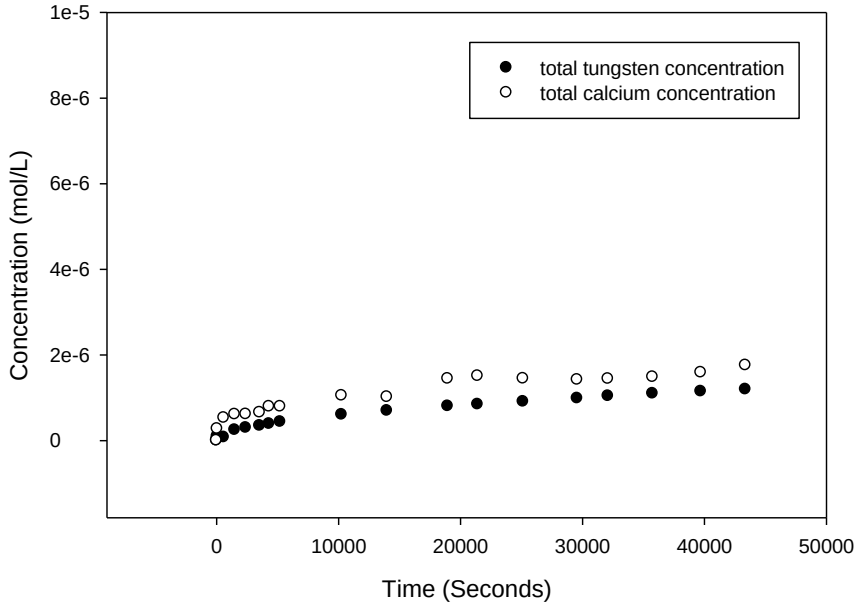

Exp 52: pH 6.2, 20^{o}C, Pump Speed 19.4ml/sec

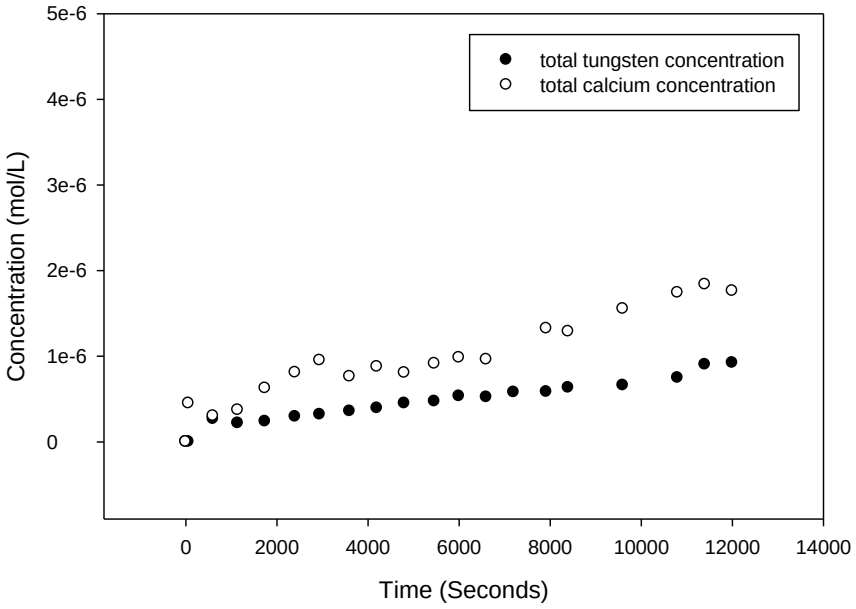

Exp 58: pH 6.2, 15oC

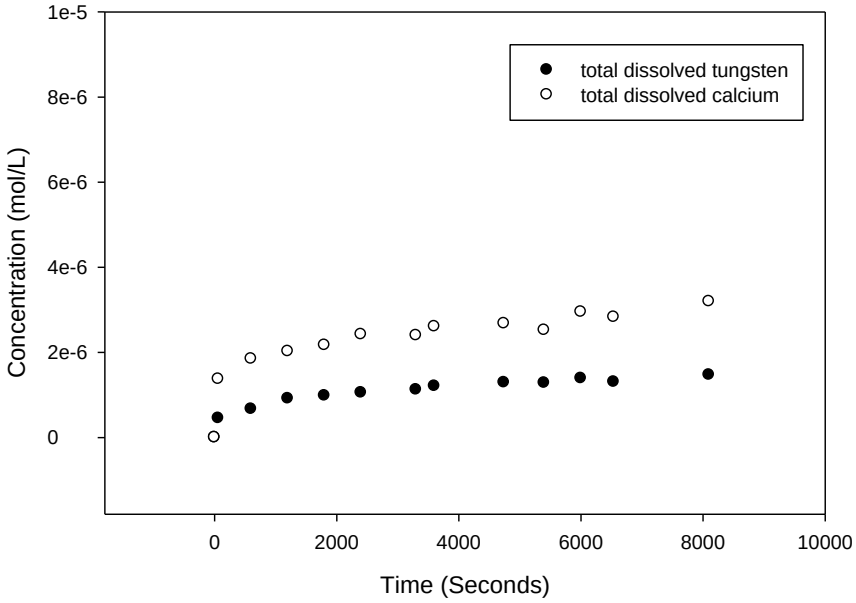

Exp 61: pH 6.2, 20°C

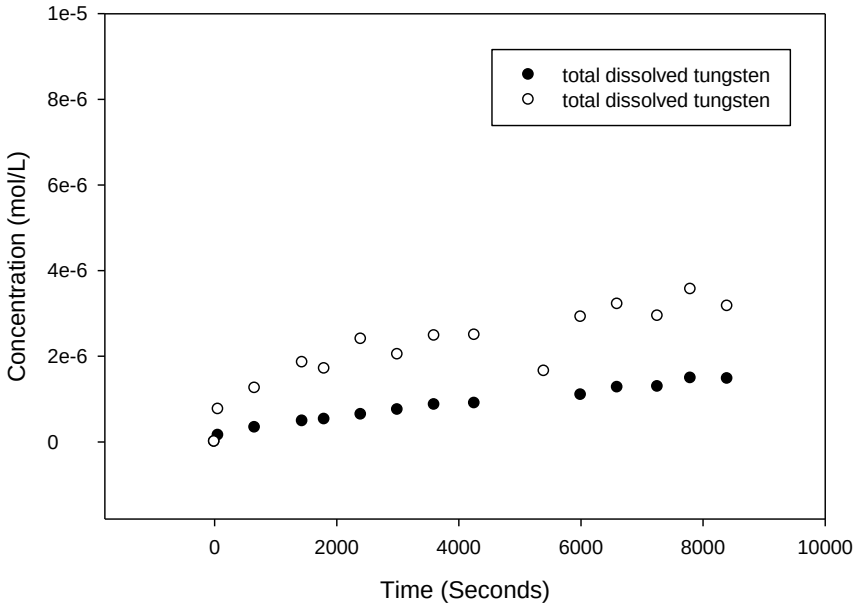

Exp 62: pH 6.2, 20°C

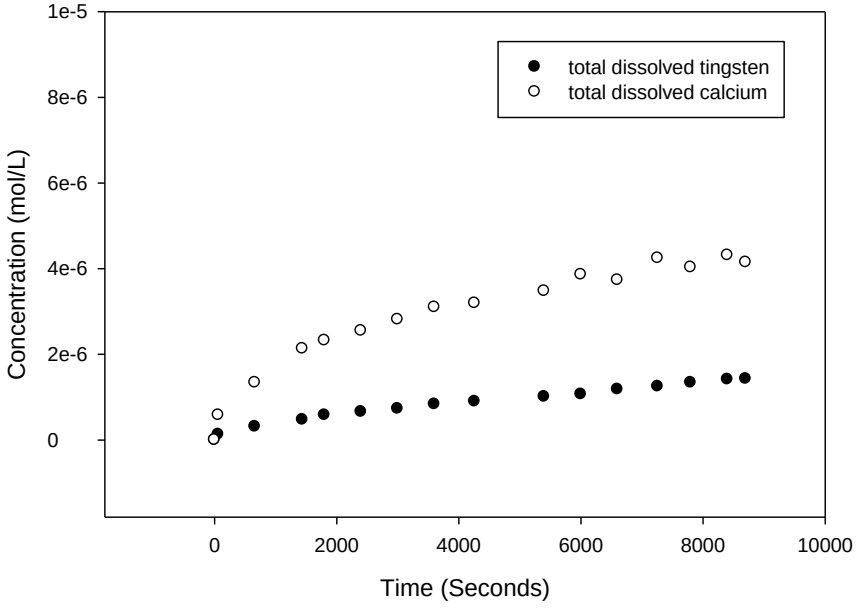

Exp 63: pH 7.0, 20°C

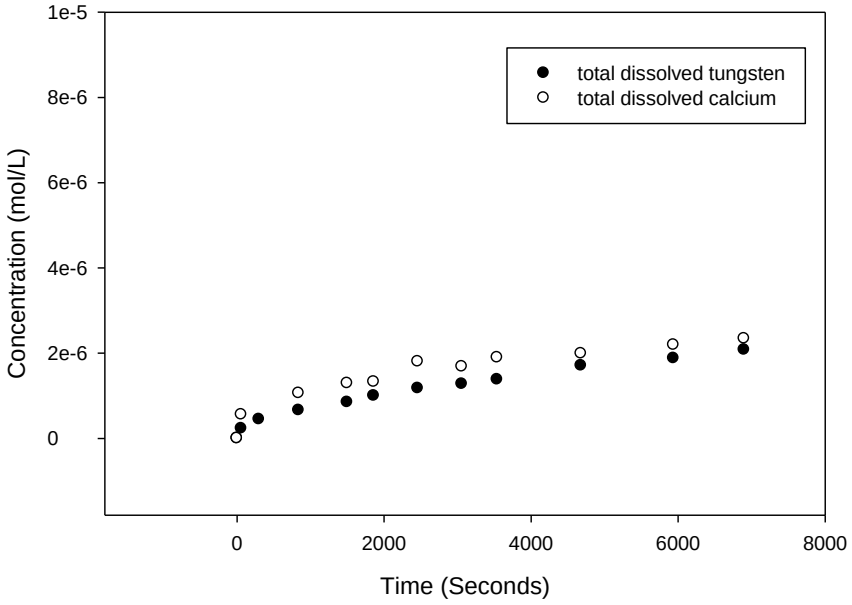

Exp 74: pH 10.5, 20°C

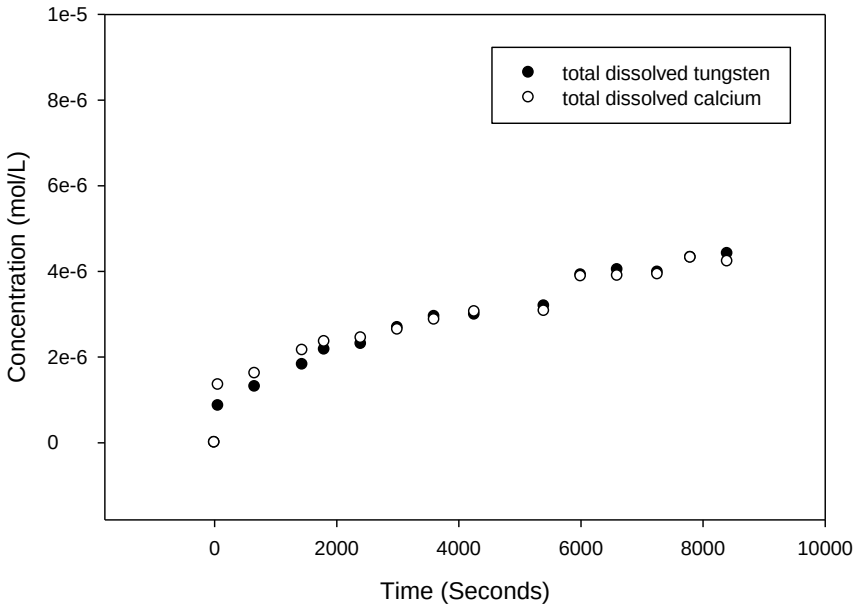

Exp 75: pH 8.1, 21°C

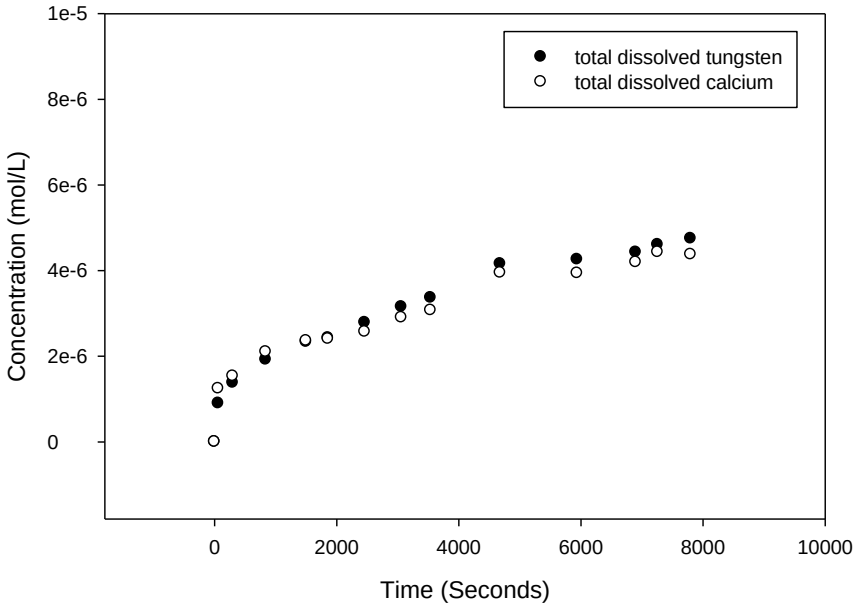

Exp 76: pH 8.1, 21°C

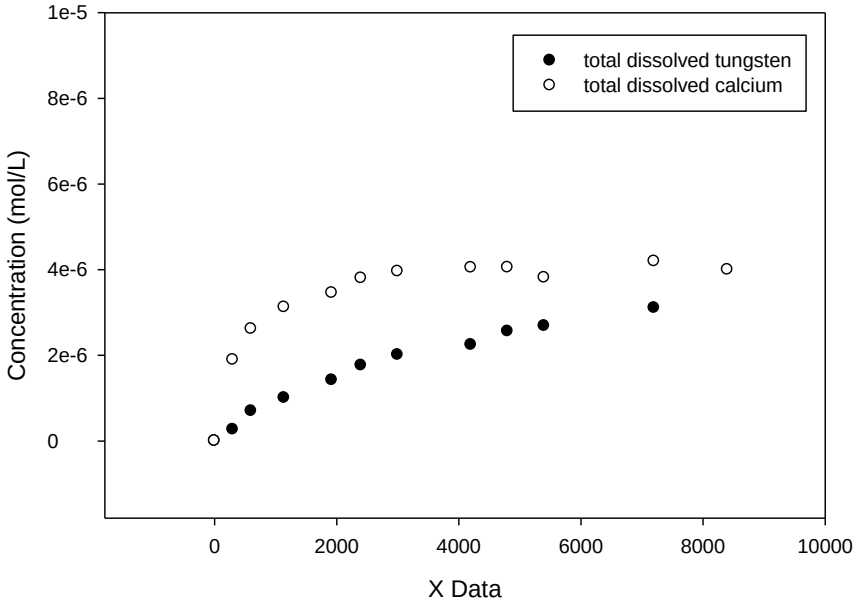

Exp 77: pH 7.1, 20°C

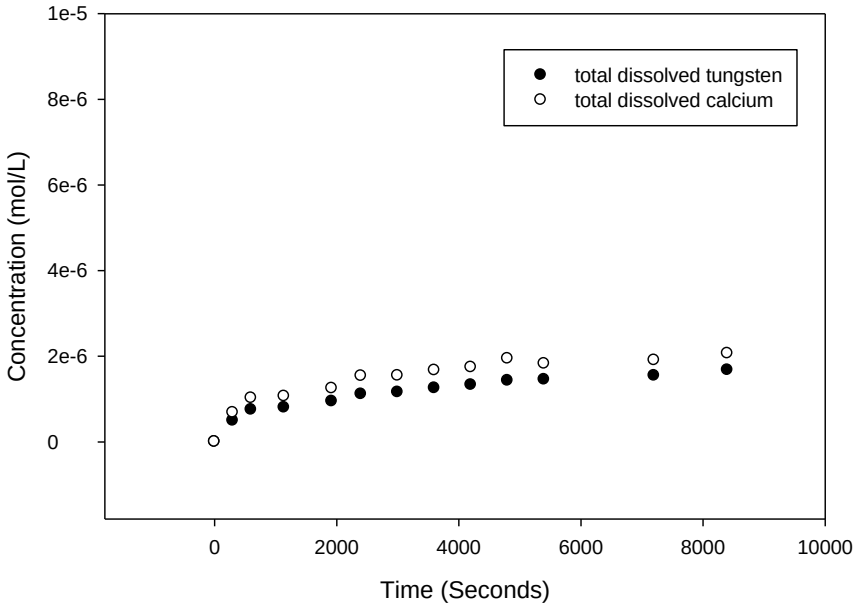

Exp 78: pH 7.1, 20°C

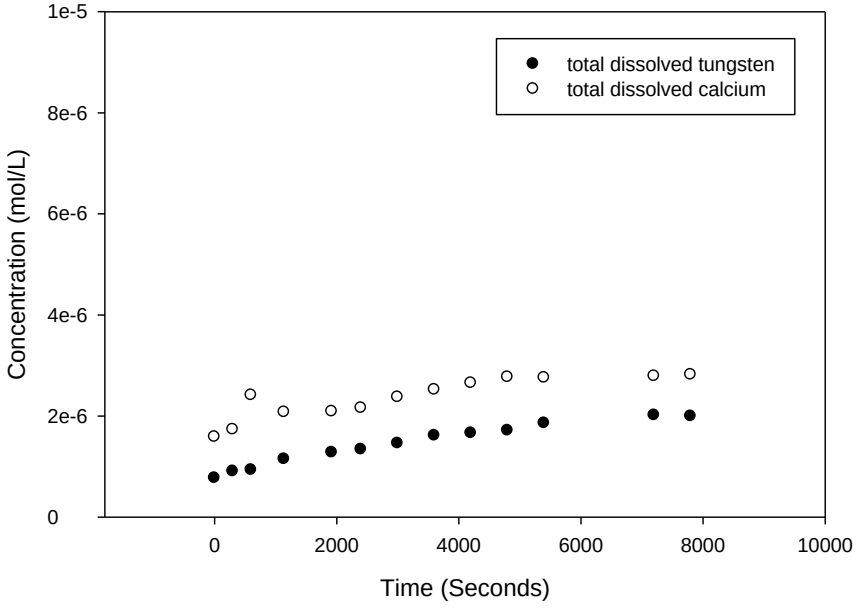

Exp 80: pH 6.2, 20°C

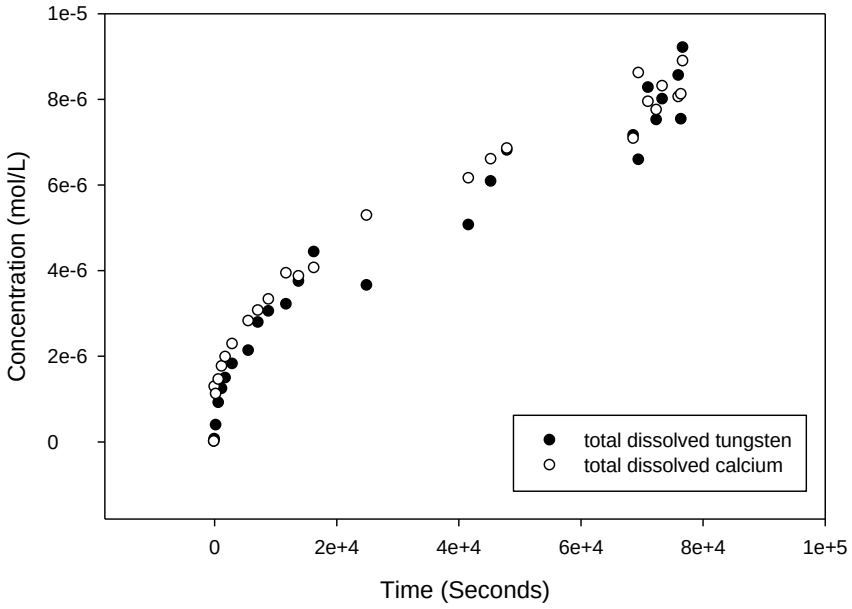

Exp 82: pH 6.2, 20°C, 45-106μm

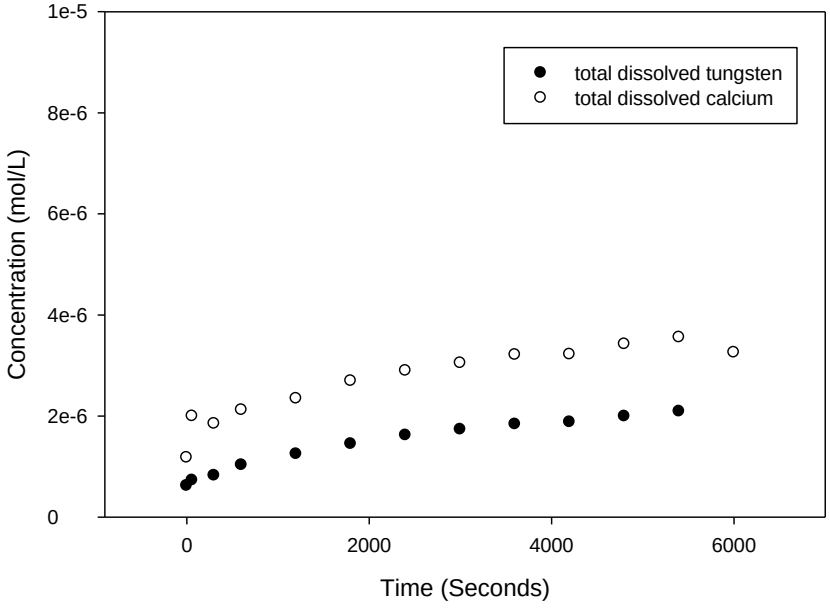

Exp 83: pH 6.2, 8°C

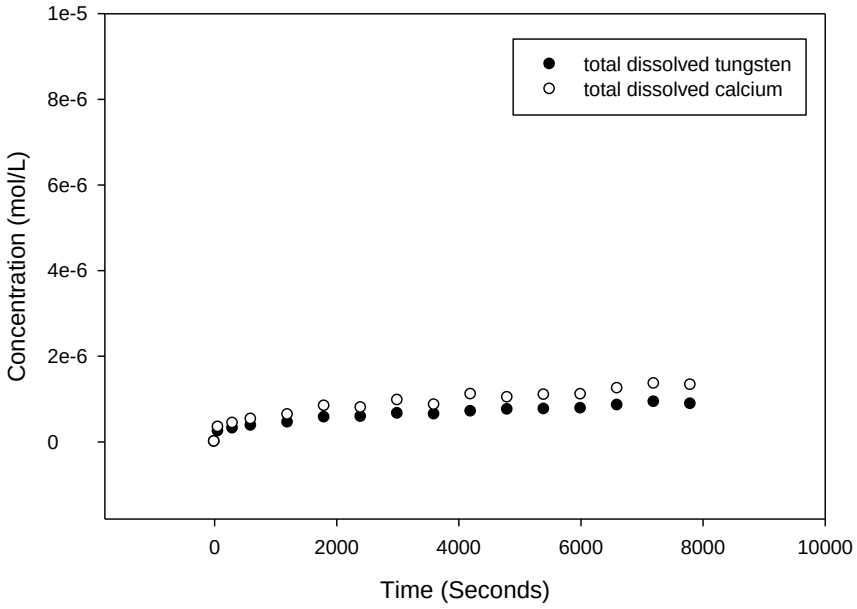

Exp 84: pH 6.2, 8°C

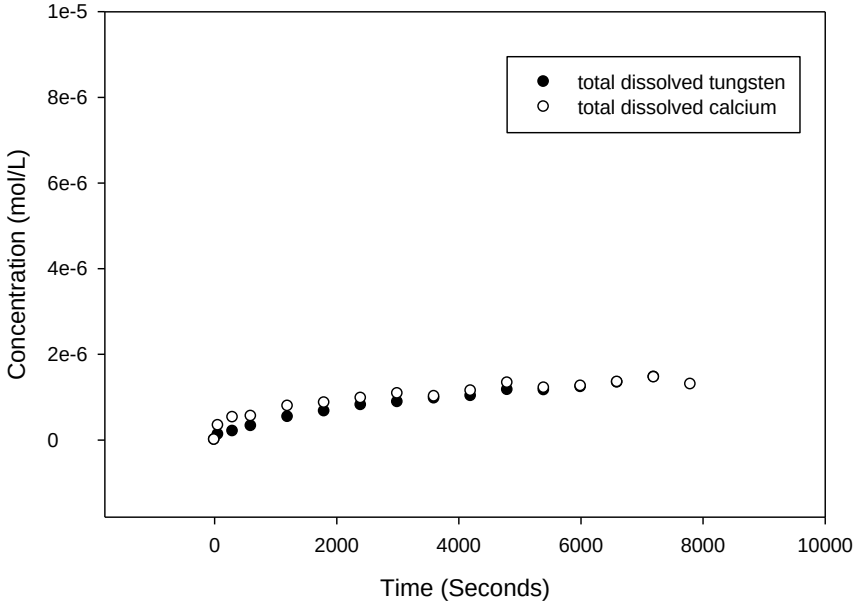

Exp 86: pH 10.5, 24°C

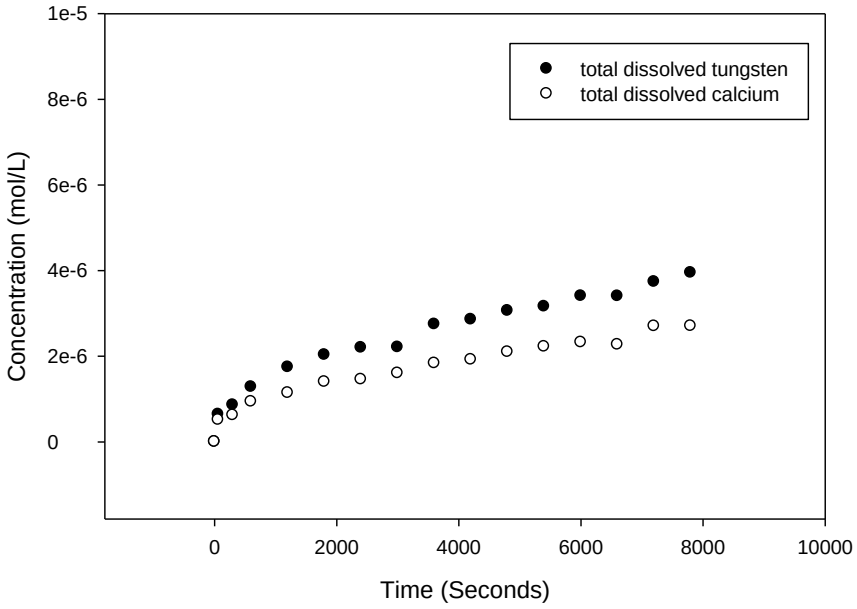

Exp 87: pH 10.5, 24°C

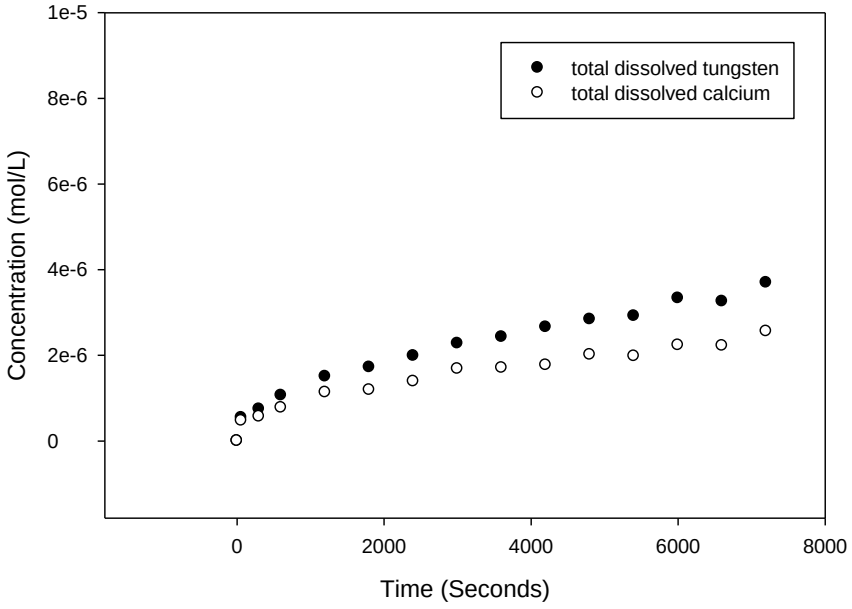

Exp 88: pH8.2, 20°C

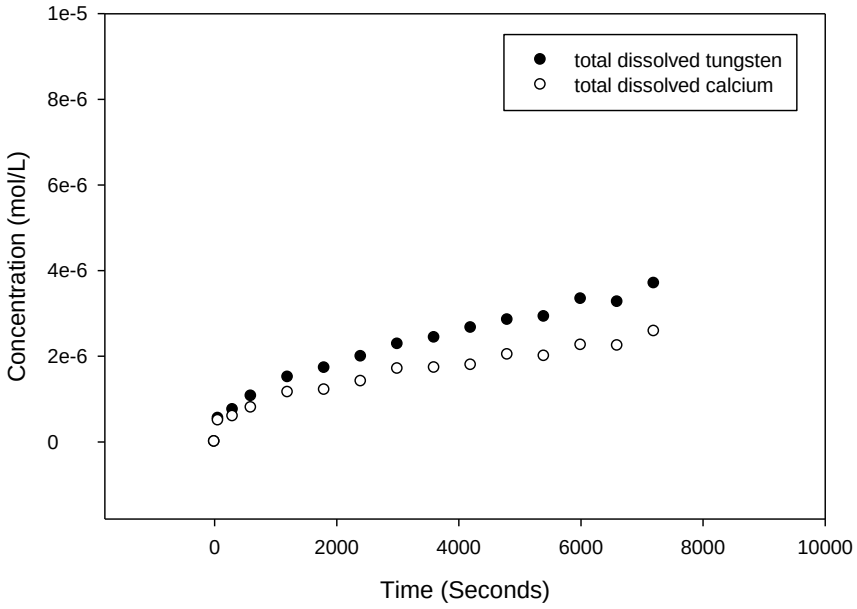

Exp 89: pH 8.2, 20°C

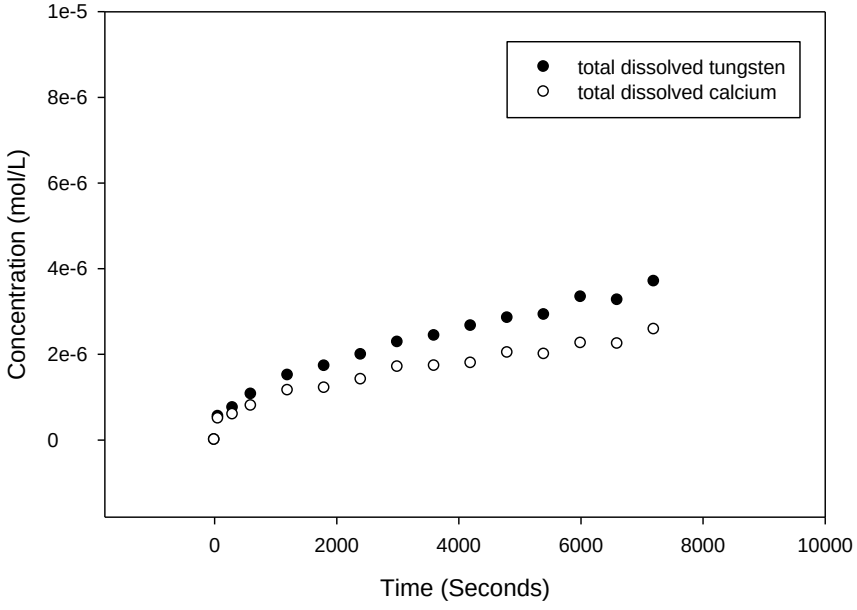

Exp 90: pH 6.2, 30^{o}C

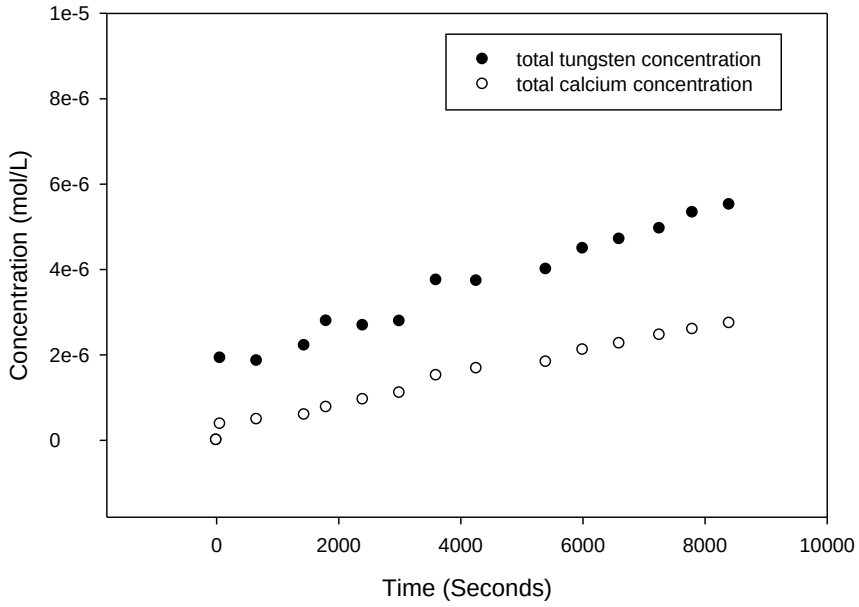

Appendix B: Integral Method Plots

Exp 48: pH 6.2, 20°C

Slope= 1.22×10^{-7}, R^2= 0.98, K_{sp}= $10^{-9.58}$, Pump Speed: 5.2ml/sec

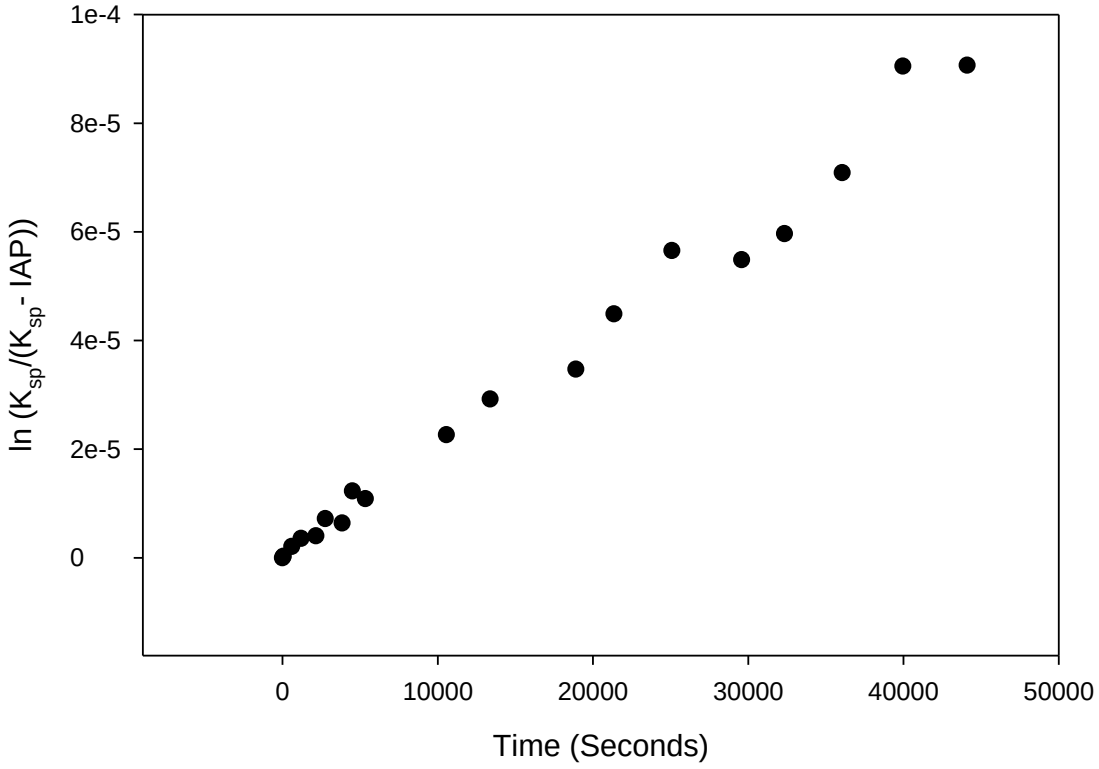

Exp 49: pH 6.2, 20^{o}C

Slope= 1.38x10^{-7}, R^2= 0.98, K_{sp}= $10^{-9.58}$, Pump Speed: 29.4ml/sec

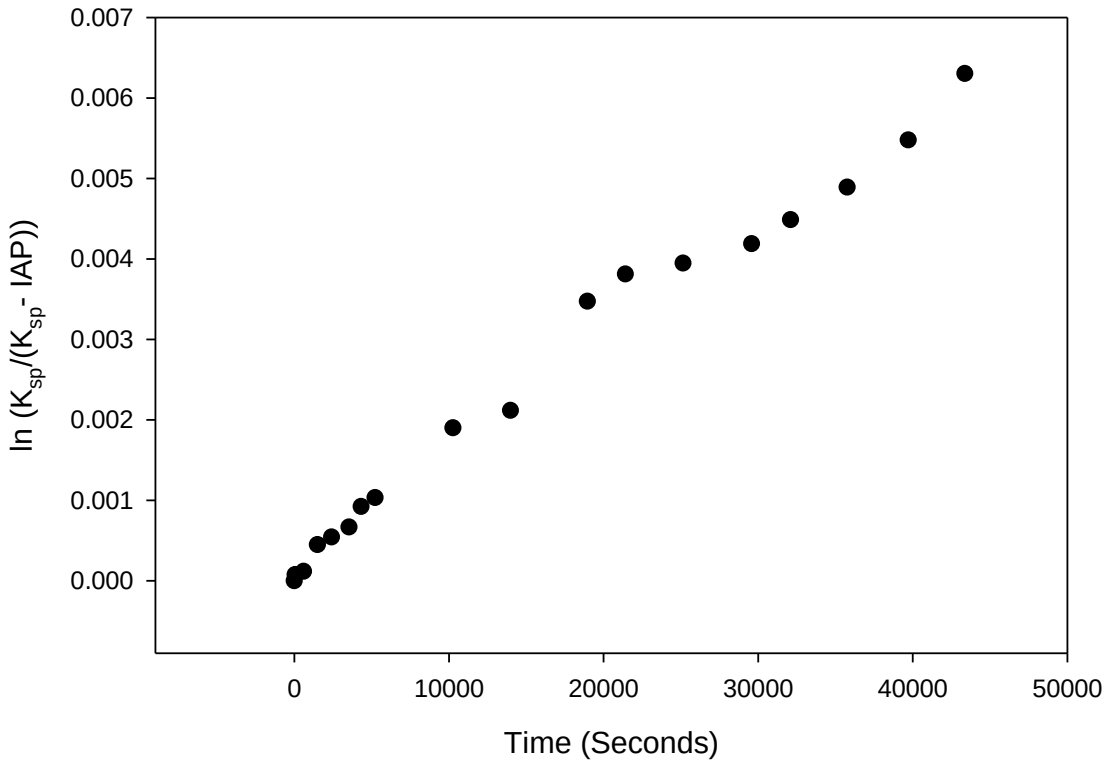

Exp 52: pH 6.2, 20^{o}C

Slope= 4.06x10^{-7}, R^2= 0.92, K_{sp}= 10$^{-9.58}$, Pump Speed: 19.4ml/sec

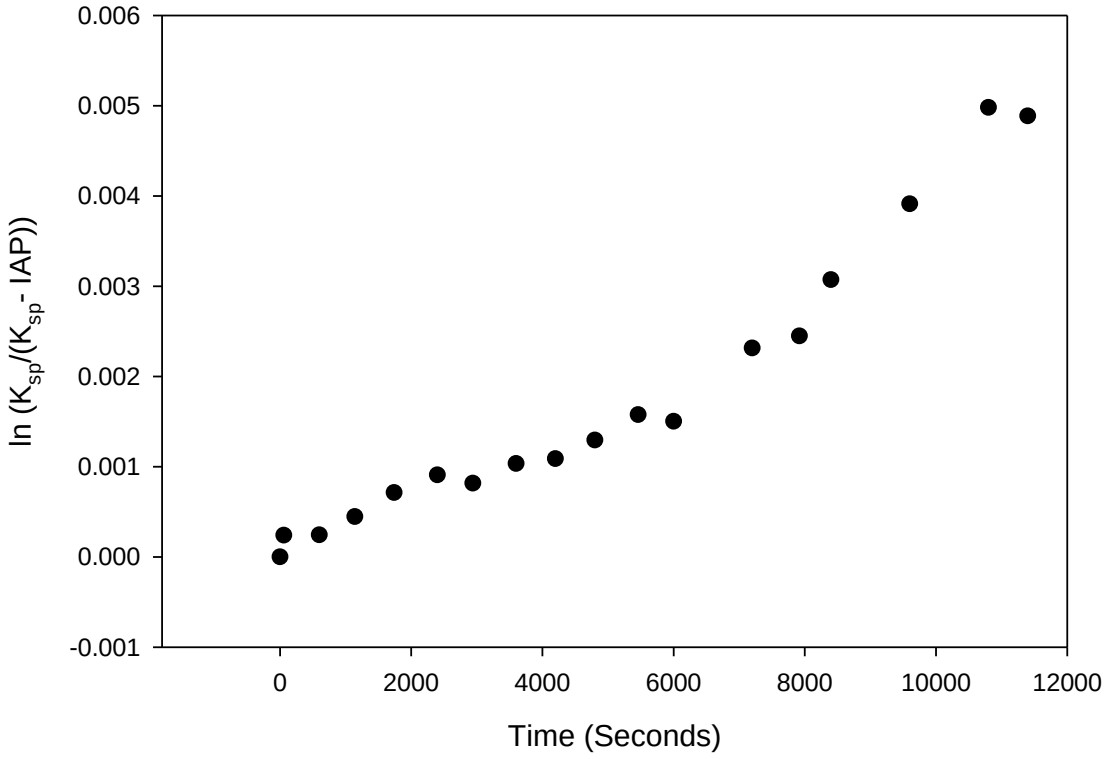

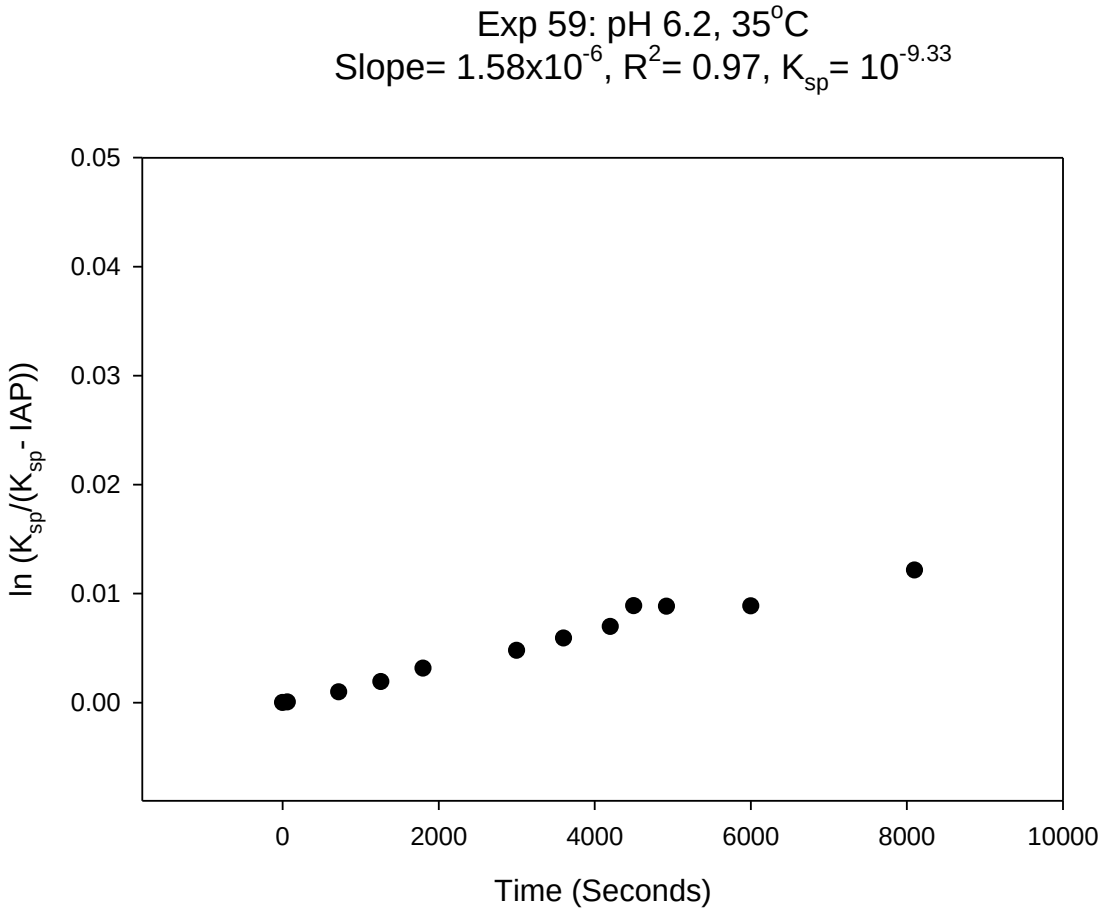
Exp 59: pH 6.2, 35°C
Slope= 1.58x10-6, R2= 0.97, Ksp= 10-9.33
ln (Ksp/(Ksp - IAP))
0.05
0.04
0.03
0.02
0.01
0.00
0
2000
4000
6000
8000
10000
Time (Seconds)

Exp 61: pH 6.2, 20^{o}C

Slope= 1.79x10^{-6}, R^2= 0.95, K_{sp}= $10^{-9.58}$, Pump Speed: 108.3ml/sec

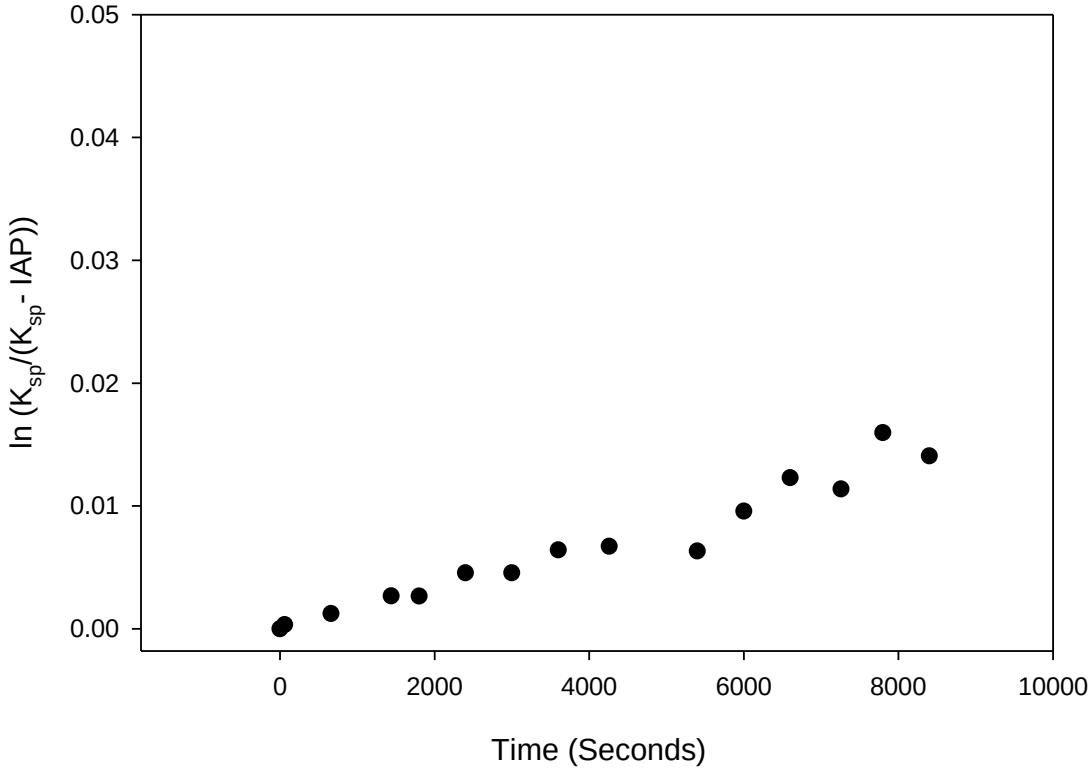

Exp 62: pH 6.2, 20^{o}C

Slope= 2.12x10^{-6}, R^2= 0.99, K_{sp}= 10$^{-9.58}$, Pump Speed: 91.6ml/sec

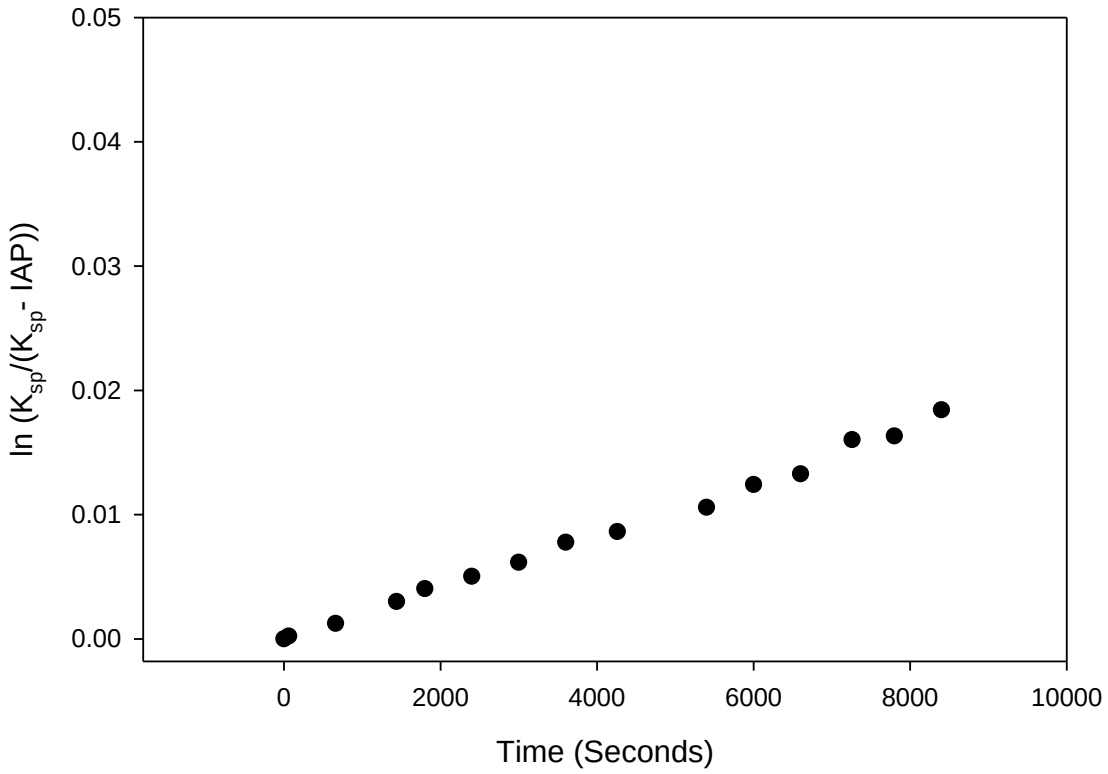

Exp 63: pH 7.0, 20^{o}C
Slope= 2.09x10^{-6}, R^2= 0.99, K_{sp}= 10$^{-9.58}$

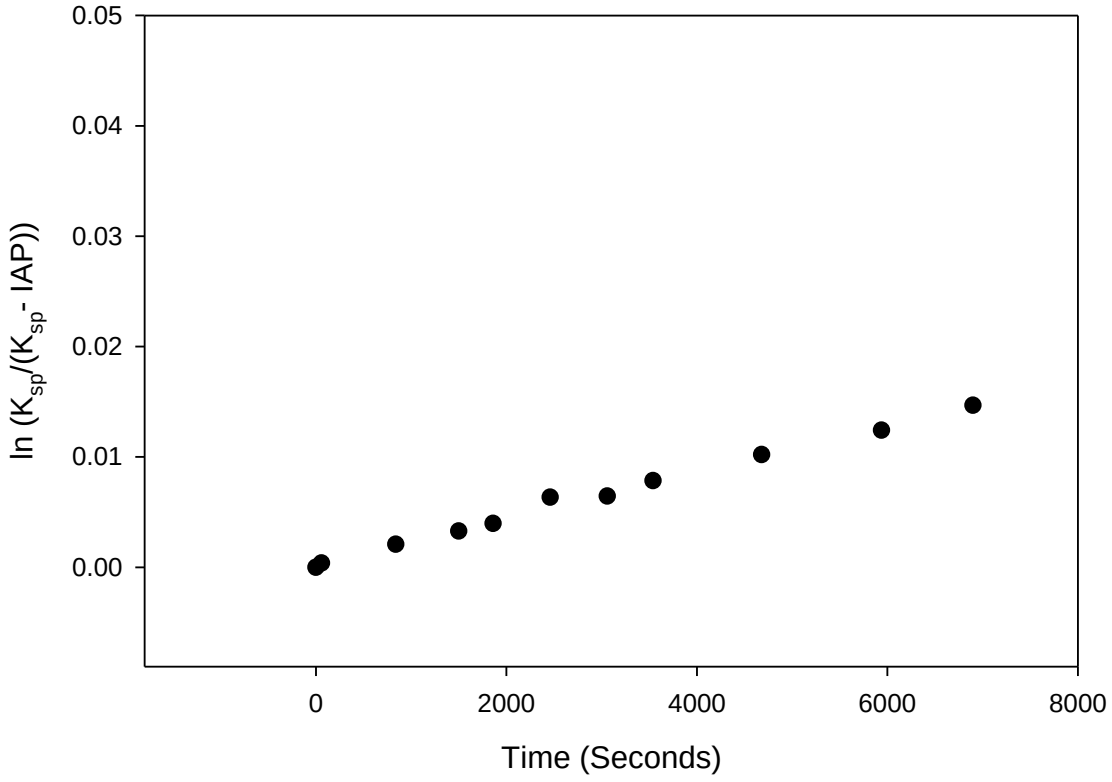

Exp 74: pH 10.5, 23^{o}C

Slope= 6.00x10^{-6}, R^2= 0.97, K_{sp}= 10$^{-9.53}$

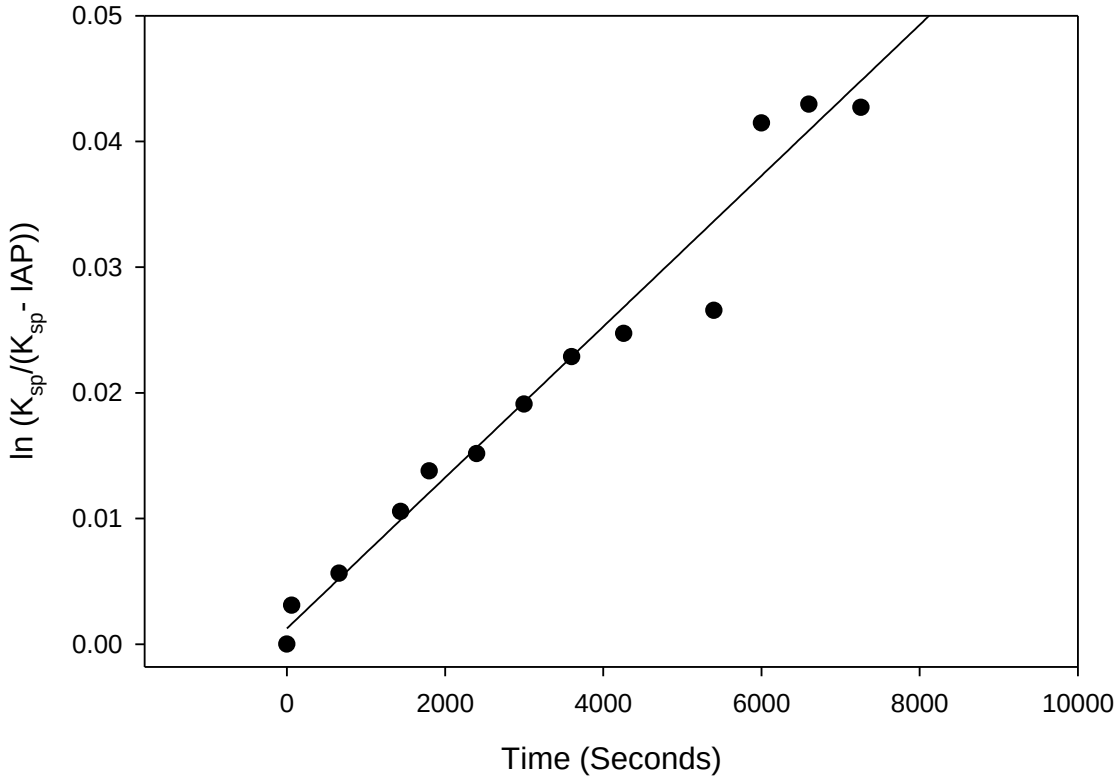

Exp 75: pH 8.1, 21^{o}C

Slope= 3.03x10^{-6}, R^2= 0.97, K_{sp}= 10$^{-9.57}$

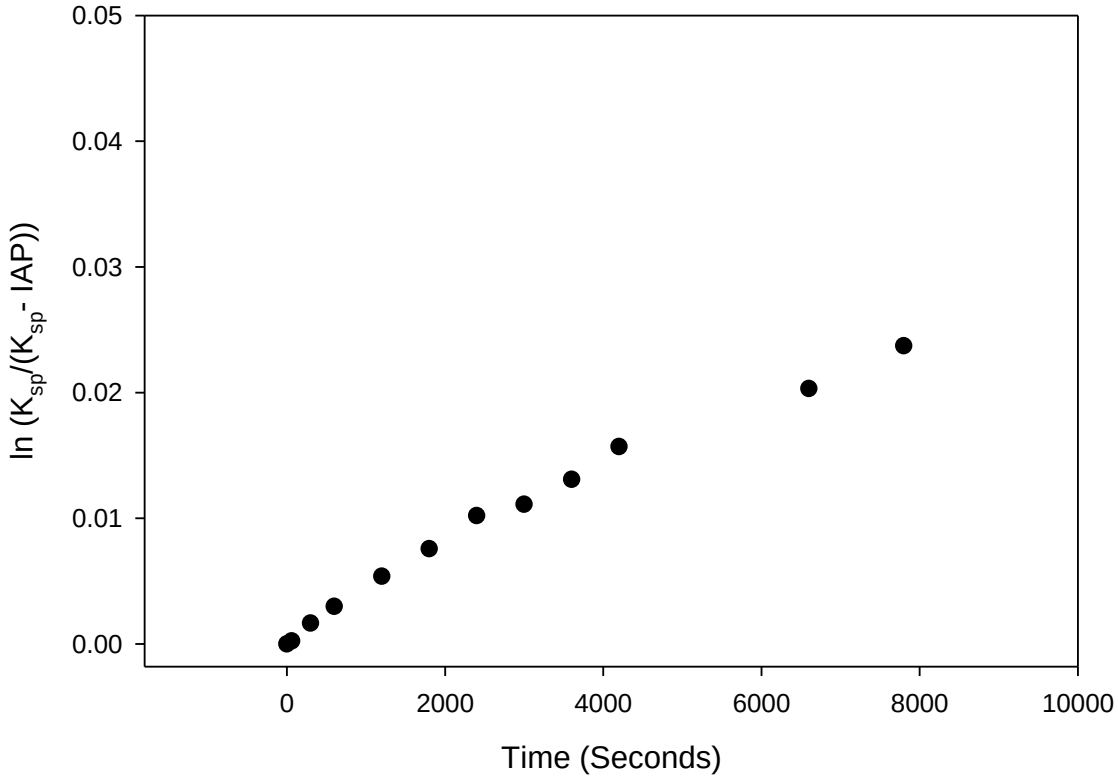

Exp 76: pH 8.1, 20^{o}C

Slope= 8.64x10^{-7}, R^2= 0.91, K_{sp}= 10$^{-9.58}$

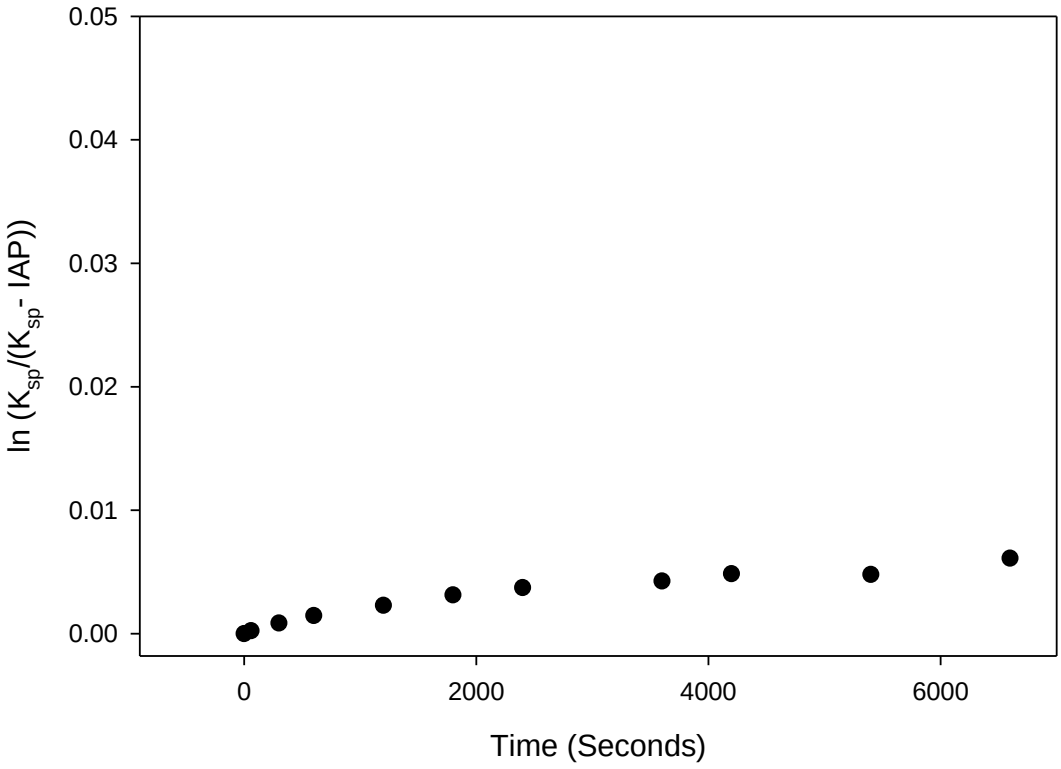

Exp 77: pH 7.1, 20°C

Slope= 1.19×10^{-6}, R^2= 0.93, K_{sp}= $10^{-9.58}$

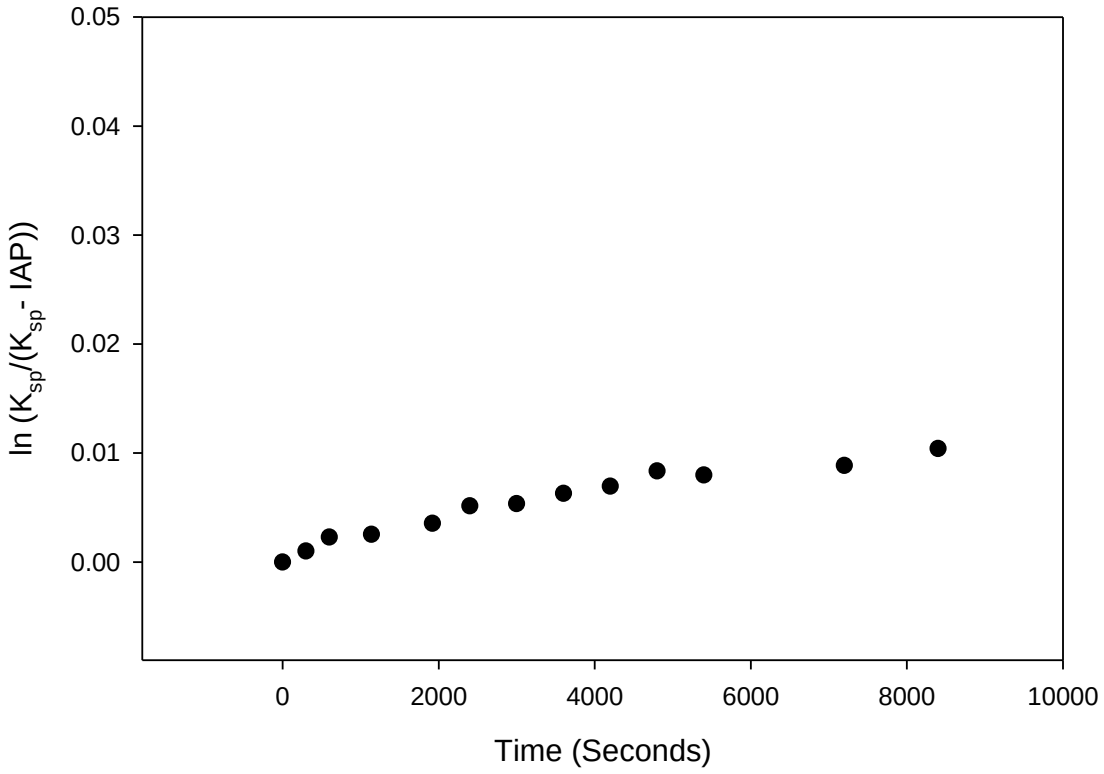

Exp 78: pH 7.1, 20^{o}C

Slope= 2.42x10^{-6}, R^2= 0.93, K_{sp}= 10$^{-9.58}$

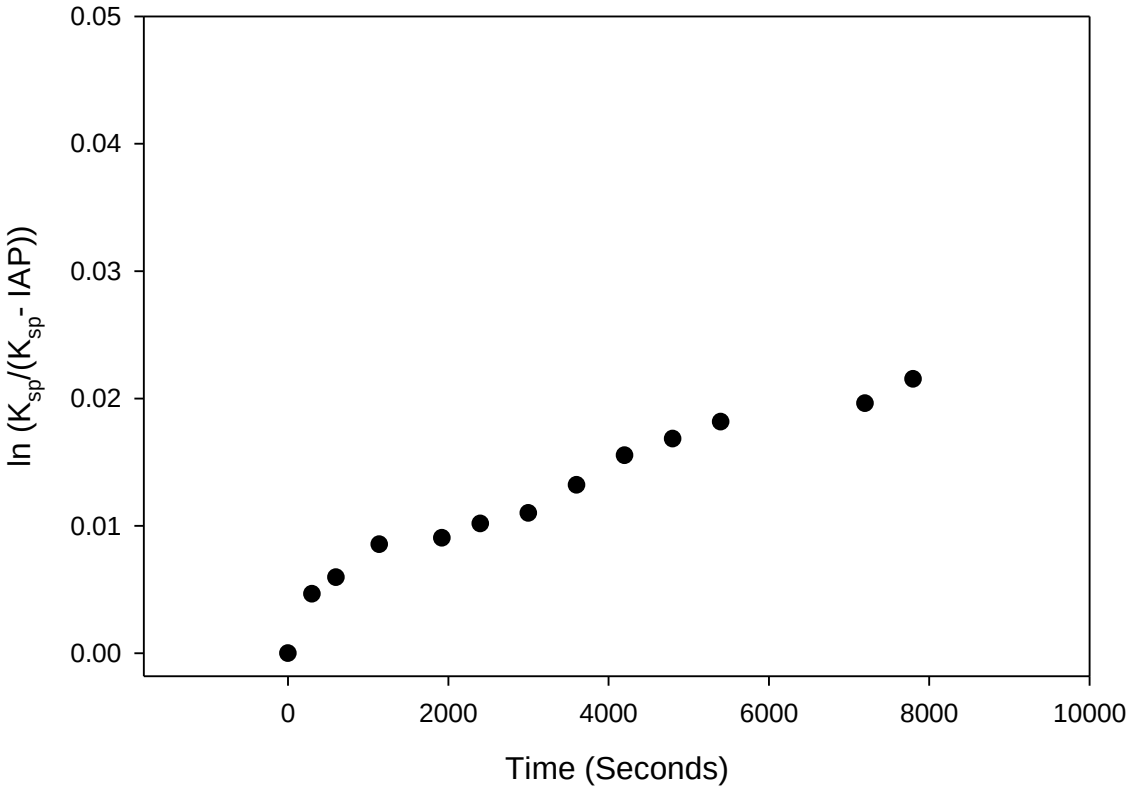

Exp 80: pH 6.2, 20^{o}C

Slope= 2.88x10^{-6}, R^2= 0.96, K_{sp}= 10$^{-9.58}$

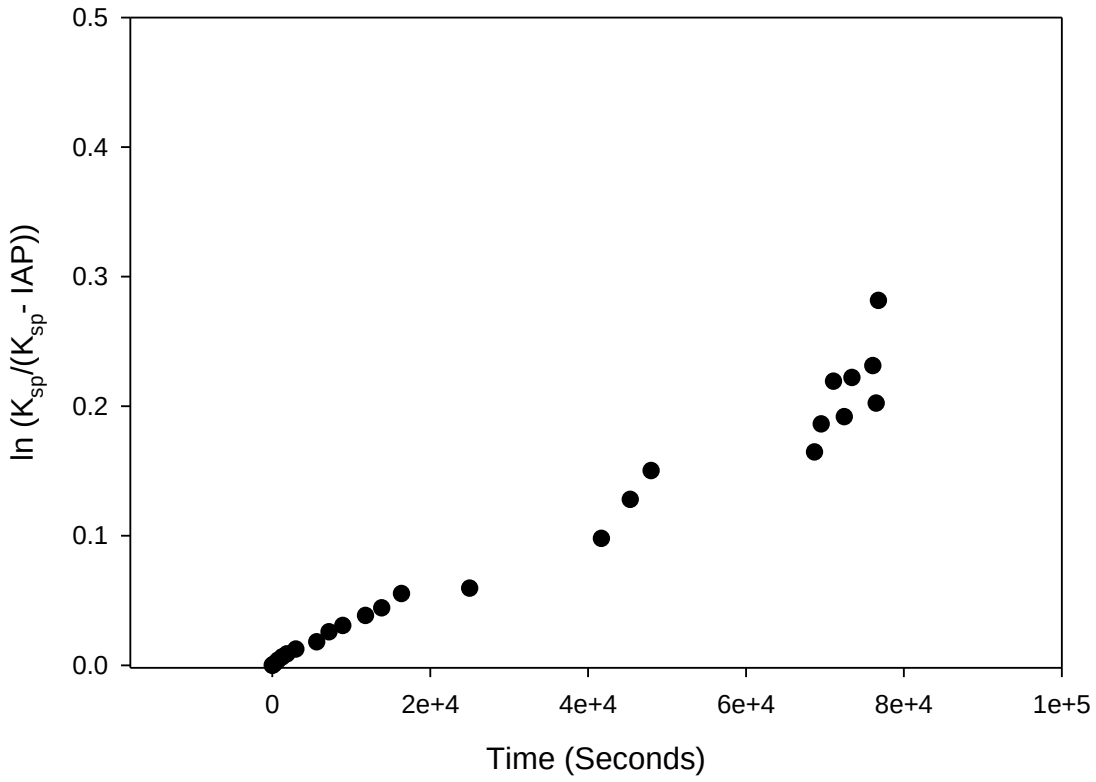

Exp 82: pH 6.2, 20^{o}C

Slope= 5.39x10^{-6}, R^2= 0.97, K_{sp}= 10$^{-9.58}$, 0.06m^2/g

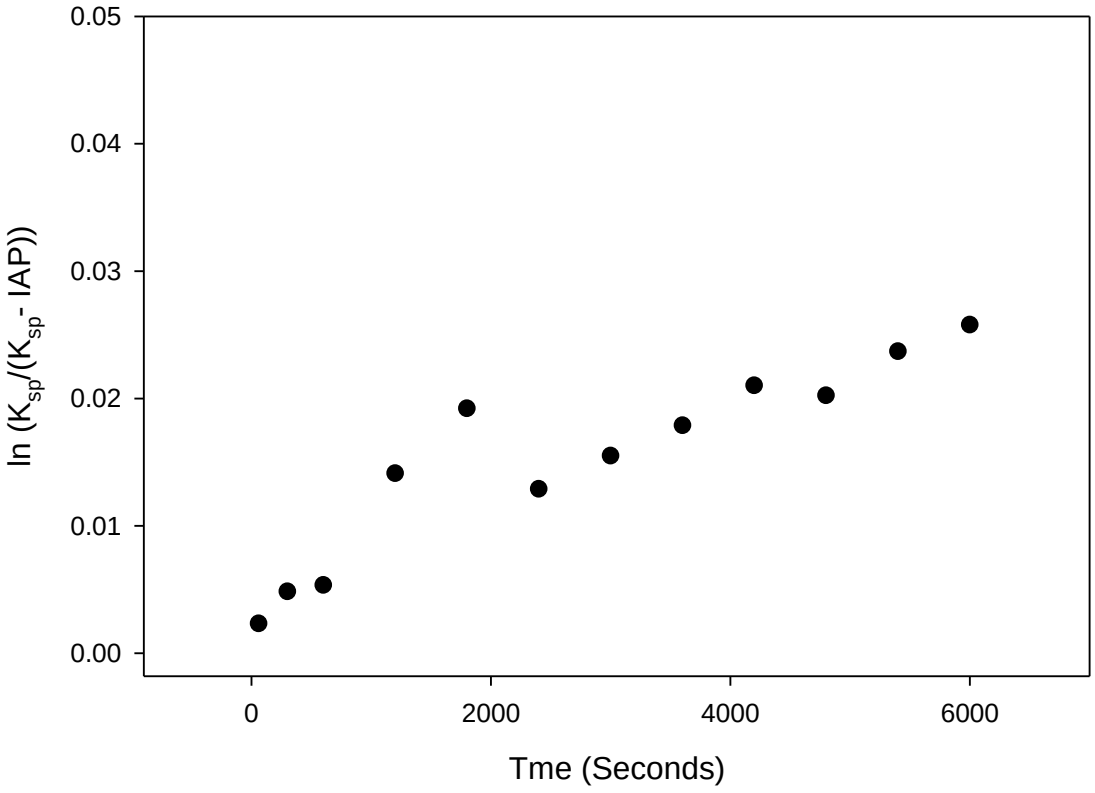

Exp 83: pH 6.2, 8°C

Slope= 5.13×10^{-8}, R^2= 0.94, K_{sp}= $10^{-9.81}$

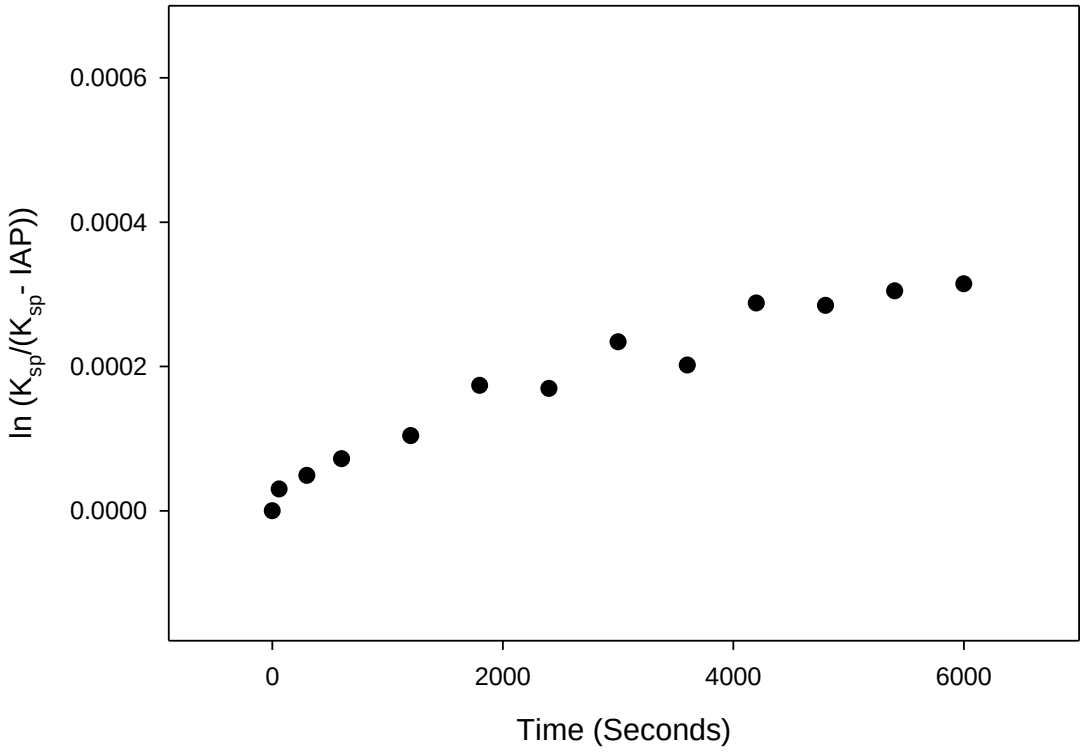

Exp 84: pH 6.2, 8°C
Slope= 1.21×10^{-7}, R^2= 0.94, K_{sp}= $10^{-9.81}$

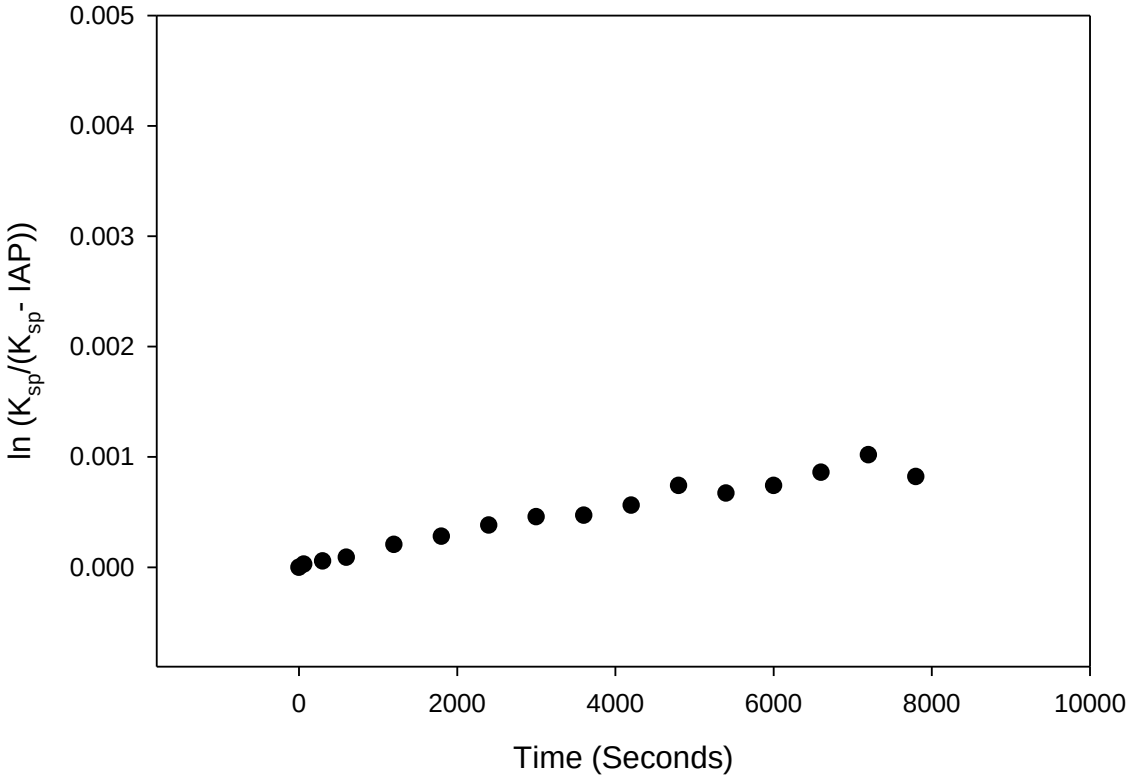

Exp 86: pH 10.5, 24°C

Slope= 3.41×10^{-6}, R^2= 0.98, K_{sp}= $10^{-9.52}$

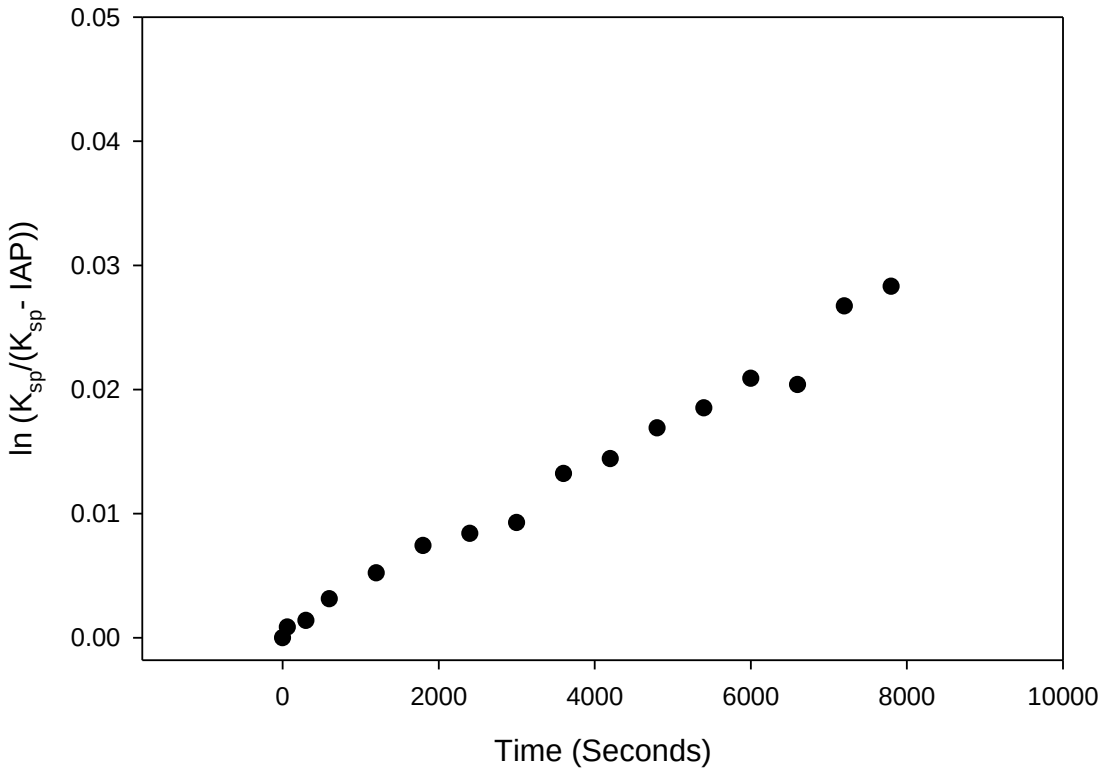

Exp 87: pH 8.2, 20^{o}C

Slope= 5.52x10^{-7}, R^2= 0.98, K_{sp}= 10$^{-9.58}$

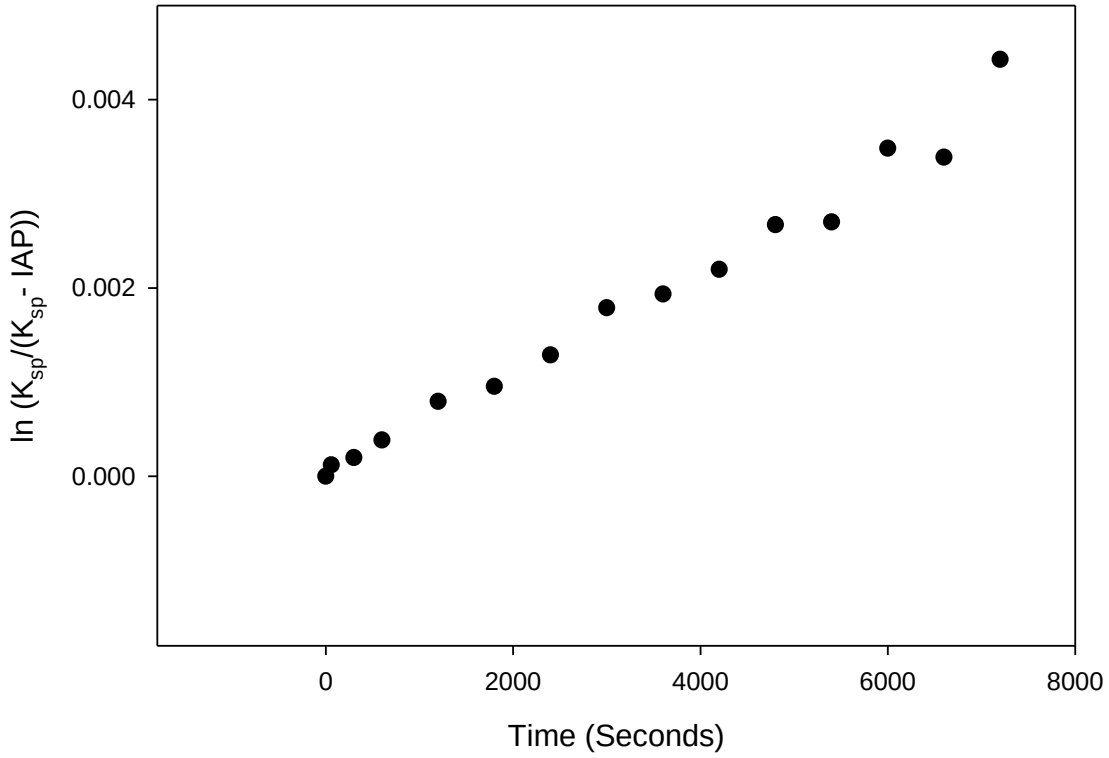

Exp 88: pH 10.5, 20^{o}C
Slope= 4.16x10^{-6}, R^2= 0.98, K_{sp}= 10$^{-9.58}$

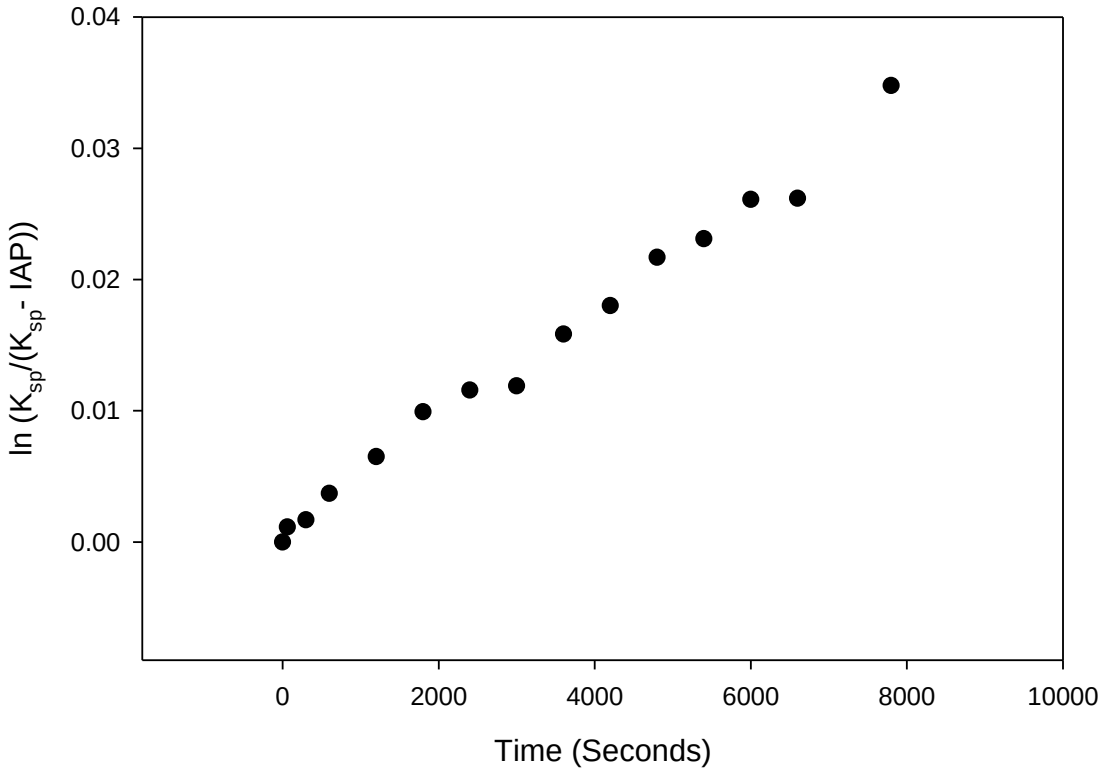

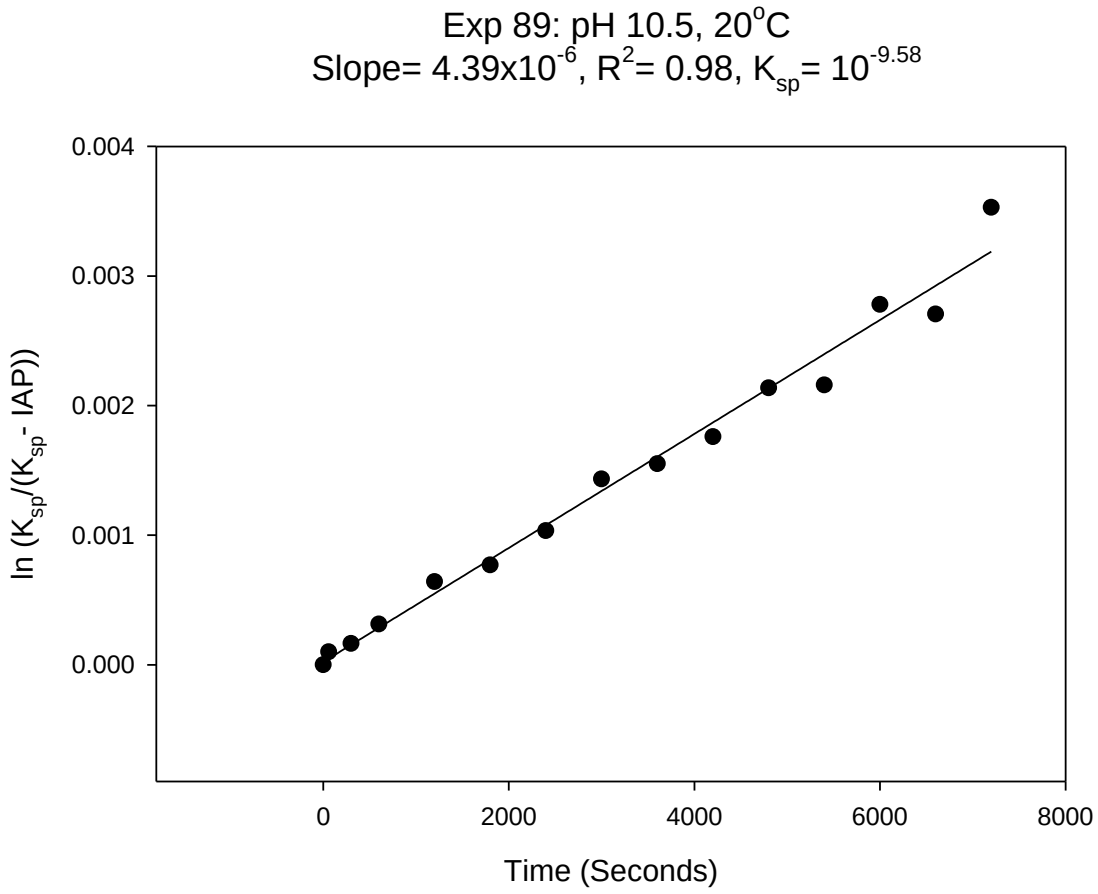
Exp 89: pH 10.5, 20°C
Slope= 4.39x10-6, R2= 0.98, Ksp= 10-9.58
ln (Ksp/(Ksp- IAP))
0.004
0.003
0.002
0.001
0.000
0
2000
4000
6000
8000
Time (Seconds)

Exp 90: pH 6.2, 20^{o}C
Slope= 5.39x10^{-6}, R^2= 0.97, K_{sp}= 10$^{-9.58}$

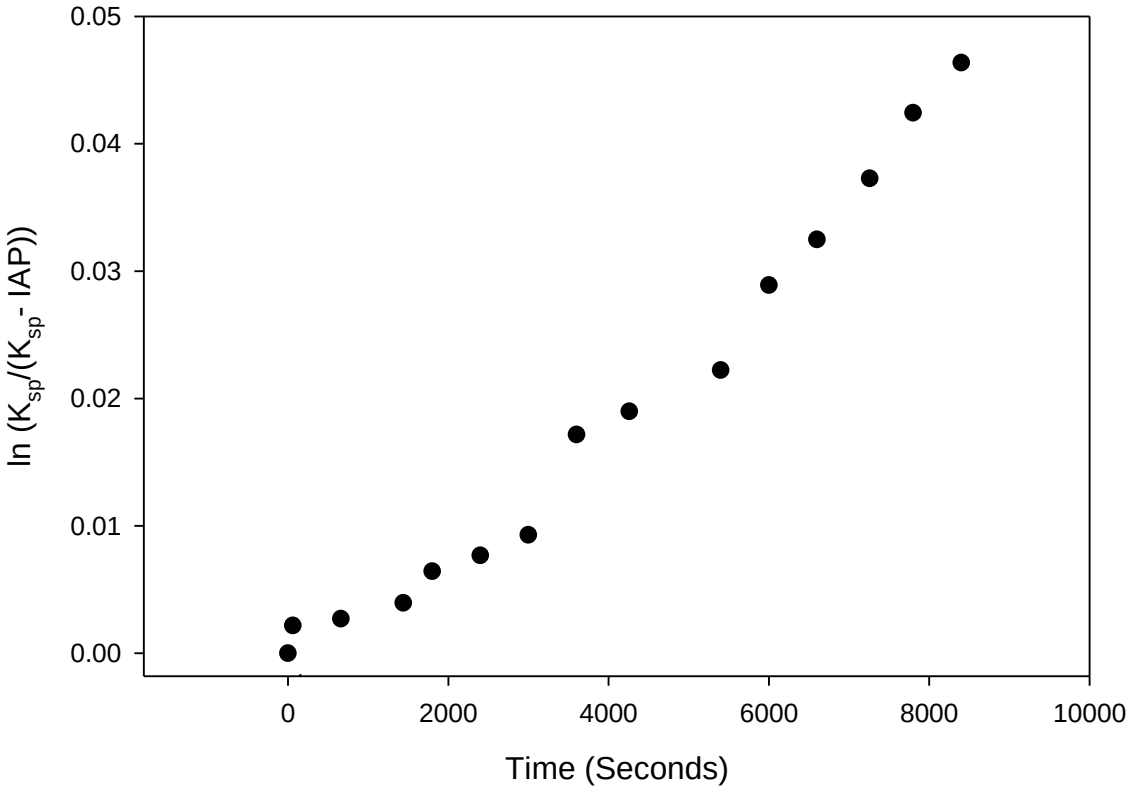

Appendix C: Raw Data Tables

Exp 48: pH 6.2, 20°C, 0.042m^2 , K_{sp} =$10^{-9.58}$, Pump Speed 5.2ml/sec

Sample #	Time (sec)	Ca (ppb)	W (ppb)	Ca, M	W, M	IAP	ln(Ksp/(Ksp-IAP))
D48-1	1	2.65	9.84	6.13E-09	1.44E-08	6.97E-17	2.65E-07
D48-2	10	11.04	18.54	1.15E-08	6.01E-08	5.48E-16	2.08E-06
D48-3	20	16.49	21.13	1.32E-08	8.97E-08	9.32E-16	3.54E-06
D48-4	36	14.54	27.24	1.70E-08	7.91E-08	1.06E-15	4.03E-06
D48-5	46	27.27	25.91	1.61E-08	1.48E-07	1.89E-15	7.19E-06
D48-6	64	22.11	28.37	1.77E-08	1.20E-07	1.68E-15	6.38E-06
D48-7	75	33.69	35.88	2.23E-08	1.83E-07	3.23E-15	1.23E-05
D48-8	89	37.94	28.17	1.75E-08	2.06E-07	2.86E-15	1.09E-05
D48-9	176	57.25	38.89	2.42E-08	3.11E-07	5.96E-15	2.26E-05
D48-10	223	64.08	44.84	2.79E-08	3.49E-07	7.69E-15	2.92E-05
D48-11	315	77.57	44.00	2.74E-08	4.22E-07	9.13E-15	3.47E-05
D48-12	356	84.07	52.48	3.27E-08	4.57E-07	1.18E-14	4.49E-05
D48-13	418	93.35	59.55	3.71E-08	5.08E-07	1.49E-14	5.65E-05
D48-14	493	102.75	52.49	3.27E-08	5.59E-07	1.44E-14	5.49E-05
D48-15	539	112.16	52.30	3.26E-08	6.10E-07	1.57E-14	5.97E-05
D48-16	601	120.79	57.69	3.59E-08	6.57E-07	1.86E-14	7.09E-05
D48-17	666	129.25	68.84	4.29E-08	7.03E-07	2.38E-14	9.05E-05
D48-18	735	137.70	64.72	4.03E-08	7.49E-07	2.38E-14	9.07E-05

Exp 49: pH 6.2, 20°C, 0.042m^2 , K_{sp} =$10^{-9.58}$, Pump Speed 29.4ml/sec

Sample #	Time (sec)	Ca (ppb)	W (ppb)	Ca, M	W, M	IAP	ln(Ksp/(Ksp-IAP))
D49-1	60	16.83	10.95	2.73E-07	9.15E-08	1.98E-14	7.51E-05
D49-2	600	13.63	21.12	5.27E-07	7.42E-08	3.09E-14	1.17E-04
D49-3	1500	45.01	24.40	6.09E-07	2.45E-07	1.18E-13	4.48E-04
D49-4	2400	54.22	24.53	6.12E-07	2.95E-07	1.43E-13	5.42E-04
D49-5	3540	62.70	26.10	6.51E-07	3.41E-07	1.75E-13	6.67E-04
D49-6	4320	71.21	31.76	7.92E-07	3.87E-07	2.42E-13	9.22E-04
D49-7	5220	79.90	31.73	7.92E-07	4.35E-07	2.72E-13	1.03E-03
D49-8	10260	110.88	42.00	1.05E-06	6.03E-07	4.99E-13	1.90E-03
D49-9	13980	127.29	40.76	1.02E-06	6.92E-07	5.56E-13	2.12E-03
D49-10	18960	147.27	57.76	1.44E-06	8.01E-07	9.12E-13	3.47E-03
D49-11	21420	154.54	60.38	1.51E-06	8.41E-07	1.00E-12	3.81E-03
D49-12	25140	166.64	57.98	1.45E-06	9.06E-07	1.04E-12	3.95E-03
D49-13	29580	180.49	56.79	1.42E-06	9.82E-07	1.10E-12	4.19E-03
D49-14	32100	190.42	57.67	1.44E-06	1.04E-06	1.18E-12	4.49E-03
D49-15	35760	201.33	59.44	1.48E-06	1.10E-06	1.28E-12	4.89E-03
D49-16	39720	210.57	63.62	1.59E-06	1.15E-06	1.44E-12	5.48E-03
D49-17	43380	218.97	70.39	1.76E-06	1.19E-06	1.65E-12	6.30E-03

Exp 52: pH 6.2, 20°C, 0.042m^2 , K_{sp} =$10^{-9.33}$, Pump Speed 19.4ml/sec

Sample #	Time (sec)	Ca (ppb)	W (ppb)	Ca, M	W, M	IAP	ln(Ksp/(Ksp-IAP))
D52-1	60	18.00	0.00	4.49E-07	0	6.31E-14	0
D52-2	600	12.04	48.63	3.00E-07	2.66E-07	6.36E-14	2.40E-04
D52-3	1140	14.86	39.72	3.71E-07	2.17E-07	1.17E-13	2.42E-04
D52-4	1740	25.05	43.35	6.25E-07	2.37E-07	1.87E-13	4.45E-04
D52-5	2400	32.40	53.48	8.08E-07	2.93E-07	2.39E-13	7.11E-04
D52-6	2940	38.05	58.16	9.49E-07	3.18E-07	2.14E-13	9.08E-04
D52-7	3600	30.51	65.17	7.61E-07	3.56E-07	2.72E-13	8.16E-04
D52-8	4200	35.07	71.79	8.75E-07	3.93E-07	2.86E-13	1.03E-03
D52-9	4800	32.30	82.10	8.06E-07	4.49E-07	3.40E-13	1.09E-03
D52-10	5460	36.63	86.10	9.14E-07	4.71E-07	4.14E-13	1.29E-03
D52-11	6000	39.39	97.39	9.83E-07	5.33E-07	3.95E-13	1.57E-03
D52-12	6600	38.52	95.03	9.61E-07	5.20E-07	2.04E-12	1.50E-03
D52-13	7200	179.26	105.47	4.47E-06	5.77E-07	6.08E-13	7.78E-03
D52-14	7920	52.98	106.41	1.32E-06	5.82E-07	6.43E-13	2.31E-03
D52-15	8400	51.59	115.56	1.29E-06	6.32E-07	8.07E-13	2.45E-03
D52-16	9600	62.21	120.24	1.55E-06	6.58E-07	1.03E-12	3.07E-03
D52-17	10800	69.73	136.51	1.74E-06	7.47E-07	1.31E-12	3.91E-03
D52-18	11400	73.59	164.65	1.84E-06	9.01E-07	1.28E-12	4.98E-03
D52-19	12000	70.55	168.50	1.76E-06	9.22E-07	6.31E-14	4.89E-03

Exp 59: pH 6.2, 35°C, 0.042m^2 , K_{sp} =$10^{-9.33}$

Sample #	Time (sec)	Ca (ppb)	W (ppb)	Ca, M	W, M	IAP	ln(Ksp/(Ksp-IAP))
D59-1	60	33.17	5.93	8.27E-07	3.22E-08	2.11E-14	4.51E-05
D59-2	720	65.90	64.11	1.64E-06	3.49E-07	4.53E-13	9.69E-04
D59-3	1260	65.10	128.46	1.62E-06	6.99E-07	8.97E-13	1.92E-03
D59-4	1800	80.36	170.23	2.01E-06	9.26E-07	1.47E-12	3.14E-03
D59-5	3000	89.49	232.83	2.23E-06	1.27E-06	2.23E-12	4.79E-03
D59-6	3600	96.11	267.41	2.40E-06	1.45E-06	2.76E-12	5.91E-03
D59-7	4200	102.68	295.28	2.56E-06	1.61E-06	3.25E-12	6.98E-03
D59-8	4500	115.19	334.39	2.87E-06	1.82E-06	4.13E-12	8.87E-03
D59-9	4920	111.61	343.22	2.78E-06	1.87E-06	4.11E-12	8.82E-03
D59-10	6000	117.30	194.25	3.09E-06	1.69E-06	4.12E-12	8.86E-03
D59-11	8100	123.88	310.42	3.18E-06	2.24E-06	5.65E-12	1.21E-02

Exp 61: pH 6.2, 20°C, 0.042m^2 , K_{sp} =$10^{-9.58}$, Pump Speed 108.3ml/sec

Sample #	Time (sec)	Ca (ppb)	W (ppb)	Ca, M	W, M	IAP	ln(Ksp/(Ksp-IAP))
D61-01	60	17.62	27.47	7.57E-07	1.46E-07	8.74E-14	2.58E-04
D61-02	660	30.58	61.26	1.25E-06	3.30E-07	3.26E-13	9.63E-04
D61-03	1440	43.45	89.24	1.85E-06	4.82E-07	7.04E-13	2.08E-03
D61-04	1800	41.96	96.23	1.70E-06	5.20E-07	7.01E-13	2.07E-03
D61-05	2400	58.53	116.63	2.40E-06	6.31E-07	1.20E-12	3.53E-03
D61-06	3000	49.16	137.55	2.03E-06	7.45E-07	1.20E-12	3.54E-03
D61-07	3600	59.43	159.02	2.47E-06	8.62E-07	1.68E-12	4.98E-03
D61-08	4260	58.55	164.95	2.49E-06	8.94E-07	1.76E-12	5.21E-03
D61-09	5400	73.93	200.92	1.65E-06	1.28E-06	1.66E-12	4.91E-03
D61-10	6000	77.99	233.29	2.91E-06	1.09E-06	2.51E-12	7.43E-03
D61-11	6600	72.44	236.35	3.21E-06	1.27E-06	3.21E-12	9.53E-03
D61-12	7260	84.69	272.97	2.94E-06	1.28E-06	2.97E-12	8.82E-03
D61-13	7800	79.46	270.78	3.56E-06	1.48E-06	4.17E-12	1.24E-02
D61-14	8400	97.06	282.19	3.16E-06	1.47E-06	3.68E-12	1.09E-02

Exp 62: pH 6.2, 20°C, 0.042m^2 , K_{sp} =$10^{-9.58}$, Pump Speed 91.6ml/sec

Sample #	Time (sec)	Ca (ppb)	W (ppb)	Ca, M	W, M	IAP	ln(Ksp/(Ksp-IAP))
D62-01	60	23.19	23.16	5.79E-07	1.26E-07	5.76E-14	2.19E-04
D62-02	540	53.61	56.73	1.34E-06	3.09E-07	3.26E-13	1.24E-03
D62-03	1200	85.41	86.23	2.13E-06	4.69E-07	7.90E-13	3.01E-03
D62-04	1740	93.06	106.32	2.32E-06	5.78E-07	1.06E-12	4.04E-03
D62-05	2400	102.08	120.54	2.55E-06	6.56E-07	1.32E-12	5.03E-03
D62-06	3000	112.70	133.44	2.81E-06	7.26E-07	1.61E-12	6.15E-03
D62-07	3600	124.07	152.84	3.10E-06	8.31E-07	2.03E-12	7.76E-03
D62-08	4200	127.86	164.71	3.19E-06	8.96E-07	2.26E-12	8.62E-03
D62-09	4800	139.32	185.36	3.48E-06	1.01E-06	2.77E-12	1.06E-02
D62-10	5400	154.68	195.76	3.86E-06	1.06E-06	3.25E-12	1.24E-02
D62-11	6000	149.47	216.43	3.73E-06	1.18E-06	3.47E-12	1.33E-02
D62-12	6600	170.06	229.38	4.24E-06	1.25E-06	4.18E-12	1.60E-02
D62-13	7200	161.60	245.71	4.03E-06	1.34E-06	4.26E-12	1.63E-02
D62-14	7800	172.73	259.22	4.31E-06	1.41E-06	4.80E-12	1.84E-02
D62-15	8400	166.21	262.17	4.15E-06	1.43E-06	4.67E-12	1.79E-02

Exp 63: pH 6.2, 20°C, 0.042m^2 , K_{sp} =$10^{-9.58}$

Sample #	Time (sec)	Ca (ppb)	W (ppb)	Ca, M	W, M	IAP	ln(Ksp/(Ksp-IAP))
D63-1	60	18.00	0	5.54E-07	2.29E-07	0	0
D63-2	300	12.04	48.63	7.32E-07	4.43E-07	1.00E-13	3.81E-04
D63-3	840	14.86	39.72	1.06E-06	6.57E-07	2.56E-13	9.75E-04
D63-4	1500	25.05	43.35	1.29E-06	8.45E-07	5.48E-13	2.09E-03
D63-5	1860	32.40	53.48	1.32E-06	9.96E-07	8.62E-13	3.28E-03
D63-6	2460	38.05	58.16	1.80E-06	1.17E-06	1.04E-12	3.96E-03
D63-7	3060	30.51	65.17	1.68E-06	1.27E-06	1.67E-12	6.36E-03
D63-8	3540	35.07	71.79	1.89E-06	1.38E-06	1.69E-12	6.45E-03
D63-9	4680	32.30	82.10	1.99E-06	1.70E-06	2.06E-12	7.86E-03
D63-10	5940	36.63	86.10	2.19E-06	1.88E-06	2.67E-12	1.02E-02
D63-11	6900	39.39	97.39	2.34E-06	2.07E-06	3.24E-12	1.24E-02

Exp 74: pH 7.0, 23°C, 0.042m^2 , K_{sp} =$10^{-9.53}$

Sample #	Time (sec)	Ca (ppb)	W (ppb)	Ca, M	W, M	IAP	ln(Ksp/(Ksp-IAP))
D74-1	60	47.53	157.70	1.35E-06	8.57E-07	5.76E-14	2.19E-04
D74-2	660	58.18	239.57	1.61E-06	1.30E-06	3.26E-13	1.24E-03
D74-3	1440	79.89	334.50	2.15E-06	1.82E-06	7.90E-13	3.01E-03
D74-4	1800	87.91	398.94	2.35E-06	2.17E-06	1.06E-12	4.04E-03
D74-5	2400	91.40	423.10	2.44E-06	2.30E-06	1.32E-12	5.03E-03
D74-6	3000	99.11	492.89	2.63E-06	2.68E-06	1.61E-12	6.15E-03
D74-7	3600	108.55	540.86	2.87E-06	2.94E-06	2.03E-12	7.76E-03
D74-8	4260	115.87	549.17	3.05E-06	2.99E-06	2.26E-12	8.62E-03
D74-9	5400	116.64	585.90	3.07E-06	3.19E-06	2.77E-12	1.06E-02
D74-10	6000	148.97	719.06	3.88E-06	3.91E-06	3.25E-12	1.24E-02
D74-11	6600	149.52	741.74	3.89E-06	4.03E-06	3.47E-12	1.33E-02
D74-12	7260	150.96	730.83	3.93E-06	3.98E-06	4.18E-12	1.60E-02
D74-13	7800	166.62	794.59	4.32E-06	4.32E-06	4.26E-12	1.63E-02
D74-14	8400	163.09	811.35	4.23E-06	4.41E-06	4.80E-12	1.84E-02

Exp 75: pH 8.1, 20°C, 0.042m^2 , K_{sp} =$10^{-9.58}$

Sample #	Time (sec)	Ca (ppb)	W (ppb)	Ca, M	W, M	IAP	ln(Ksp/(Ksp-IAP))
D75-01	60	13.6	42.08	3.39E-07	2.29E-07	6.14E-14	2.28E-04
D75-02	300	32.96	125.6	8.22E-07	6.83E-07	4.44E-13	1.65E-03
D75-03	600	41.28	181.28	1.03E-06	9.86E-07	8.03E-13	2.99E-03
D75-04	1200	53.44	252.16	1.33E-06	1.37E-06	1.45E-12	5.38E-03
D75-05	1800	60.64	312.32	1.51E-06	1.7E-06	2.03E-12	7.57E-03
D75-06	2400	70.4	362.08	1.76E-06	1.97E-06	2.73E-12	1.02E-02
D75-07	3000	72.64	381.92	1.81E-06	2.08E-06	2.98E-12	1.11E-02
D75-08	3600	80.48	405.92	2.01E-06	2.21E-06	3.50E-12	1.31E-02
D75-09	4200	86.4	452.64	2.16E-06	2.46E-06	4.19E-12	1.57E-02
D75-10	5400	177.28	768	4.42E-06	4.18E-06	1.46E-11	5.58E-02
D75-11	6600	100	504.96	2.5E-06	2.75E-06	5.42E-12	2.03E-02
D75-12	7800	107.36	548	2.68E-06	2.98E-06	6.31E-12	2.37E-02

Exp 76: pH 8.1, 20°C, 0.042m^2 , K_{sp} =$10^{-9.58}$

Sample #	Time (sec)	Ca (ppb)	W (ppb)	Ca, M	W, M	IAP	ln(Ksp/(Ksp-IAP))
D76-01	60	75.82	48.76	1.89E-06	2.65E-07	5.02E-13	2.35E-04
D76-02	300	104.79	128.14	2.61E-06	6.97E-07	1.82E-12	8.53E-04
D76-03	600	125.07	184.28	3.12E-06	1E-06	3.13E-12	1.46E-03
D76-04	1200	138.41	260.93	3.45E-06	1.42E-06	4.90E-12	2.30E-03
D76-05	1800	152.18	323.93	3.8E-06	1.76E-06	6.69E-12	3.13E-03
D76-06	2400	158.61	368.89	3.96E-06	2.01E-06	7.94E-12	3.72E-03
D76-07	3000	226.33	555.25	5.65E-06	3.02E-06	1.71E-11	8.01E-03
D76-08	3600	162.05	412.76	4.04E-06	2.25E-06	9.08E-12	4.25E-03
D76-09	4200	162.20	470.15	4.05E-06	2.56E-06	1.03E-11	4.85E-03
D76-10	5400	152.79	493.55	3.81E-06	2.68E-06	1.02E-11	4.80E-03
D76-11	6600	168.11	570.63	4.19E-06	3.1E-06	1.30E-11	6.11E-03
D76-12	7800	160.21	505.59	4.00E-06	2.75E-06	1.10E-11	5.16E-03

Exp 77: pH 6.2, 20°C, 0.042m^2 , K_{sp} =$10^{-9.58}$

Sample #	Time (sec)	Ca (ppb)	W (ppb)	Ca, M	W, M	IAP	ln(Ksp/(Ksp-IAP))
D77-01	300	27.31	90.06	6.81E-07	4.9E-07	2.64E-13	1.00E-03
D77-02	600	40.83	137.16	1.02E-06	7.46E-07	6.01E-13	2.29E-03
D77-03	1140	42.49	146.51	1.06E-06	7.97E-07	6.68E-13	2.54E-03
D77-04	1920	49.96	173.60	1.25E-06	9.44E-07	9.30E-13	3.54E-03
D77-05	2400	61.60	204.42	1.54E-06	1.11E-06	1.35E-12	5.15E-03
D77-06	3000	61.77	212.11	1.54E-06	1.15E-06	1.41E-12	5.36E-03
D77-07	3600	66.85	230.12	1.67E-06	1.25E-06	1.65E-12	6.29E-03
D77-08	4200	69.61	244.03	1.74E-06	1.33E-06	1.82E-12	6.95E-03
D77-09	4800	77.77	262.45	1.94E-06	1.43E-06	2.19E-12	8.36E-03
D77-10	5400	73.11	266.64	1.82E-06	1.45E-06	2.09E-12	7.98E-03
D77-11	7200	76.24	283.57	1.9E-06	1.54E-06	2.32E-12	8.85E-03
D77-12	8400	82.64	307.56	2.06E-06	1.67E-06	2.73E-12	1.04E-02

Exp 78: pH 6.2, 20°C, 0.042m^2 , K_{sp} =$10^{-9.58}$

Sample #	Time (sec)	Ca (ppb)	W (ppb)	Ca, M	W, M	IAP	ln(Ksp/(Ksp-IAP))
D78-01	300	63.49	141.78	1.58E-06	7.71E-07	1.22E-12	4.66E-03
D78-02	600	69.29	166.44	1.73E-06	9.05E-07	1.57E-12	5.97E-03
D78-03	1140	96.65	170.77	2.41E-06	9.29E-07	2.24E-12	8.55E-03
D78-04	1920	83.14	210.30	2.07E-06	1.14E-06	2.37E-12	9.06E-03
D78-05	2400	83.64	234.70	2.09E-06	1.28E-06	2.66E-12	1.02E-02
D78-06	3000	86.35	245.59	2.15E-06	1.34E-06	2.88E-12	1.10E-02
D78-07	3600	95.00	267.87	2.37E-06	1.46E-06	3.45E-12	1.32E-02
D78-08	4200	100.93	295.98	2.52E-06	1.61E-06	4.05E-12	1.55E-02
D78-09	4800	106.16	304.86	2.65E-06	1.66E-06	4.39E-12	1.68E-02
D78-10	5400	110.94	314.53	2.77E-06	1.71E-06	4.74E-12	1.82E-02
D78-11	7200	110.40	341.06	2.75E-06	1.86E-06	5.11E-12	1.96E-02
D78-12	8400	111.66	369.82	2.79E-06	2.01E-06	5.60E-12	2.15E-02

Exp 80: pH 6.2, 20°C, 0.042m^2 , K_{sp} =$10^{-9.58}$

Sample #	Time (sec)	Ca (ppb)	W (ppb)	Ca, M	W, M	IAP	ln(Ksp/(Ksp-IAP))
D80-01	60	51.21	9.89	1.28E-06	5.38E-08	5.43E-14	2.07E-04
D80-02	300	44.39	69.53	1.11E-06	3.78E-07	3.31E-13	1.26E-03
D80-01	720	57.93	166.15	1.45E-06	9.04E-07	1.03E-12	3.93E-03
D80-02	1260	70.25	225.98	1.75E-06	1.23E-06	1.70E-12	6.49E-03
D80-03	1860	78.97	272.04	1.97E-06	1.48E-06	2.30E-12	8.80E-03
D80-04	3000	91.18	332.33	2.28E-06	1.81E-06	3.25E-12	1.24E-02
D80-05	5640	112.63	389.85	2.81E-06	2.12E-06	4.71E-12	1.81E-02
D80-06	7200	122.45	510.37	3.06E-06	2.78E-06	6.70E-12	2.58E-02
D80-07	8940	132.92	558.01	3.32E-06	3.04E-06	7.95E-12	3.07E-02
D80-08	11820	157.34	588.23	3.93E-06	3.2E-06	9.92E-12	3.85E-02
D80-09	13860	154.58	686.76	3.86E-06	3.74E-06	1.14E-11	4.42E-02
D80-10	16380	162.32	813.18	4.05E-06	4.42E-06	1.42E-11	5.53E-02
D80-11	25020	211.48	669.44	5.28E-06	3.64E-06	1.52E-11	5.95E-02
D80-12	41700	251.33	947.62	6.27E-06	5.15E-06	2.45E-11	9.79E-02
D80-13	45360	264.07	1115.82	6.59E-06	6.07E-06	3.16E-11	1.28E-01
D80-14	48000	274.06	1248.99	6.84E-06	6.79E-06	3.67E-11	1.50E-01
D80-15	68700	283.47	1313.44	7.07E-06	7.14E-06	3.99E-11	1.65E-01
D80-16	69540	344.73	1208.75	8.6E-06	6.58E-06	4.47E-11	1.86E-01
D80-17	71100	317.91	1518.96	7.93E-06	8.26E-06	5.18E-11	2.19E-01
D80-18	72480	310.23	1380.06	7.74E-06	7.51E-06	4.59E-11	1.92E-01
D80-19	73440	332.47	1469.43	8.3E-06	7.99E-06	5.24E-11	2.22E-01
D80-20	76080	322.32	1571.00	8.04E-06	8.55E-06	5.43E-11	2.31E-01
D80-21	76500	324.94	1382.77	8.11E-06	7.52E-06	4.82E-11	2.02E-01
D80-22	76800	356.01	1690.76	8.88E-06	9.2E-06	6.46E-11	2.82E-01

Exp 82: pH 6.2, 20°C, 0.060m^2 , K_{sp} =$10^{-9.58}$

Sample #	Time (sec)	Ca (ppb)	W (ppb)	Ca, M	W, M	IAP	ln(Ksp/(Ksp-IAP))
D82-01	60	48.82	117.27	1.22E-06	6.38E-07	2.64E-12	1.29E-02
D82-02	300	84.43	140.59	2.11E-06	7.65E-07	3.36E-12	1.46E-02
D82-03	600	80.26	163.29	2.00E-06	8.88E-07	3.81E-12	1.36E-02
D82-04	1200	124.31	276.87	3.10E-06	1.51E-06	3.56E-12	2.37E-02
D82-05	1800	138.42	337.42	3.45E-06	1.84E-06	6.17E-12	1.69E-02
D82-06	2400	112.99	278.29	2.82E-06	1.51E-06	4.41E-12	2.10E-02
D82-07	3000	121.35	310.96	3.03E-06	1.69E-06	5.46E-12	2.51E-02
D82-08	3600	129.17	336.71	3.22E-06	1.83E-06	6.53E-12	2.08E-02
D82-09	4200	139.56	365.80	3.48E-06	1.99E-06	5.42E-12	2.02E-02
D82-10	4800	135.62	362.57	3.38E-06	1.97E-06	5.25E-12	2.33E-02
D82-11	5400	146.75	391.68	3.66E-06	2.13E-06	6.07E-12	2.13E-02
D82-12	6000	152.28	410.23	3.80E-06	2.23E-06	5.56E-12	1.29E-02
D82-13	6600	152.39	397.05	3.80E-06	2.16E-06	2.64E-12	1.46E-02

Exp 83: pH 6.2, 8°C, 0.042m^2 , K_{sp} =$10^{-9.81}$

Sample #	Time (sec)	Ca (ppb)	W (ppb)	Ca, M	W, M	IAP	ln(Ksp/(Ksp-IAP))
D83-01	60	23.19	23.16	3.39E-07	2.4E-07	6.43E-14	3.01E-05
D83-02	300	53.61	56.73	4.3E-07	3.07E-07	1.05E-13	4.89E-05
D83-03	600	85.41	86.23	5.24E-07	3.73E-07	1.54E-13	7.22E-05
D83-04	1200	93.06	106.32	6.3E-07	4.47E-07	2.23E-13	1.04E-04
D83-05	1800	102.08	120.54	8.32E-07	5.65E-07	3.71E-13	1.74E-04
D83-06	2400	112.70	133.44	7.92E-07	5.78E-07	3.62E-13	1.69E-04
D83-07	3000	124.07	152.84	9.65E-07	6.56E-07	5.00E-13	2.34E-04
D83-08	3600	127.86	164.71	8.58E-07	6.36E-07	4.31E-13	2.02E-04
D83-09	4200	139.32	185.36	1.1E-06	7.05E-07	6.15E-13	2.88E-04
D83-10	4800	154.68	195.76	1.03E-06	7.47E-07	6.08E-13	2.84E-04
D83-11	5400	149.47	216.43	1.09E-06	7.56E-07	6.51E-13	3.05E-04
D83-12	6000	170.06	229.38	1.1E-06	7.74E-07	6.72E-13	3.14E-04
D83-13	6600	161.60	245.71	1.24E-06	8.47E-07	6.43E-14	3.01E-05
D83-14	7200	172.73	259.22	1.35E-06	9.27E-07	1.05E-13	4.89E-05
D83-15	7800	166.21	262.17	1.32E-06	8.77E-07	1.54E-13	7.22E-05

Exp 84: pH 6.2, 8°C, 0.042m^2 , K_{sp} =$10^{-9.81}$

Sample #	Time (sec)	Ca (ppb)	W (ppb)	Ca, M	W, M	IAP	ln(Ksp/(Ksp-IAP))
D84-01	60	14.32	30.44	3.57E-07	1.66E-07	4.67E-14	2.19E-05
D84-02	300	20.93	42.58	5.22E-07	2.32E-07	9.56E-14	4.47E-05
D84-03	600	21.92	64.58	5.47E-07	3.51E-07	1.52E-13	7.10E-05
D84-04	1200	31.40	103.95	7.83E-07	5.65E-07	3.50E-13	1.64E-04
D84-05	1800	34.50	128.17	8.61E-07	6.97E-07	4.74E-13	2.22E-04
D84-06	2400	38.81	154.74	9.68E-07	8.42E-07	6.44E-13	3.01E-04
D84-07	3000	43.13	167.45	1.08E-06	9.11E-07	7.74E-13	3.62E-04
D84-08	3600	40.50	183.26	1.01E-06	9.97E-07	7.96E-13	3.72E-04
D84-09	4200	45.81	193.48	1.14E-06	1.05E-06	9.51E-13	4.45E-04
D84-10	4800	53.12	219.57	1.33E-06	1.19E-06	1.25E-12	5.85E-04
D84-11	5400	48.43	218.73	1.21E-06	1.19E-06	1.14E-12	5.31E-04
D84-12	6000	50.24	232.02	1.25E-06	1.26E-06	1.25E-12	5.85E-04
D84-13	6600	53.86	251.47	1.34E-06	1.37E-06	1.45E-12	6.80E-04
D84-14	7200	58.38	274.99	1.46E-06	1.5E-06	1.72E-12	8.05E-04
D84-15	7800	51.95	249.13	1.3E-06	1.36E-06	1.39E-12	6.49E-04

Exp 86: pH 10.5, 24^{o}C, 0.042m^{2} , K_{sp} =10$^{-9.52}$

Sample #	Time (sec)	Ca (ppb)	W (ppb)	Ca, M	W, M	IAP	ln(Ksp/(Ksp-IAP))
D86-01	60	20.44	117.74	5.10E-07	6.40E-07	2.58E-13	8.55E-04
D86-02	300	24.74	158.01	6.17E-07	8.59E-07	4.19E-13	1.39E-03
D86-03	600	37.53	235.18	9.36E-07	1.28E-06	9.47E-13	3.14E-03
D86-04	1200	45.79	320.31	1.14E-06	1.74E-06	1.57E-12	5.22E-03
D86-05	1800	55.97	372.60	1.40E-06	2.03E-06	2.24E-12	7.43E-03
D86-06	2400	58.37	403.98	1.46E-06	2.20E-06	2.53E-12	8.41E-03
D86-07	3000	64.10	405.61	1.60E-06	2.21E-06	2.79E-12	9.27E-03
D86-08	3600	73.39	504.06	1.83E-06	2.74E-06	3.97E-12	1.32E-02
D86-09	4200	76.84	524.99	1.92E-06	2.86E-06	4.33E-12	1.44E-02
D86-10	4800	83.94	562.37	2.09E-06	3.06E-06	5.06E-12	1.69E-02
D86-11	5400	88.96	580.52	2.22E-06	3.16E-06	5.54E-12	1.85E-02
D86-12	6000	93.10	625.50	2.32E-06	3.40E-06	6.24E-12	2.09E-02
D86-13	6600	90.92	625.22	2.27E-06	3.40E-06	6.10E-12	2.04E-02
D86-14	7200	108.24	686.28	2.70E-06	3.73E-06	7.97E-12	2.67E-02
D86-15	7800	108.32	725.65	2.70E-06	3.95E-06	8.43E-12	2.83E-02

Exp 87: pH 8.2, 20°C, 0.042m^2 , K_{sp} =$10^{-9.58}$

Sample #	Time (sec)	Ca (ppb)	W (ppb)	Ca, M	W, M	IAP	ln(Ksp/(Ksp-IAP))
D87-01	60	18.92	99.52	4.72E-07	5.41E-07	2.56E-13	1.20E-04
D87-02	300	22.85	136.26	5.7E-07	7.41E-07	4.22E-13	1.98E-04
D87-03	600	31.04	194.79	7.75E-07	1.06E-06	8.21E-13	3.84E-04
D87-04	1200	45.31	276.16	1.13E-06	1.5E-06	1.70E-12	7.95E-04
D87-05	1800	47.63	315.68	1.19E-06	1.72E-06	2.04E-12	9.55E-04
D87-06	2400	55.56	364.74	1.39E-06	1.98E-06	2.75E-12	1.29E-03
D87-07	3000	67.34	418.09	1.68E-06	2.27E-06	3.82E-12	1.79E-03
D87-08	3600	68.34	445.75	1.71E-06	2.42E-06	4.13E-12	1.94E-03
D87-09	4200	70.86	488.18	1.77E-06	2.66E-06	4.69E-12	2.20E-03
D87-10	4800	80.57	521.77	2.01E-06	2.84E-06	5.71E-12	2.67E-03
D87-11	5400	79.28	535.85	1.98E-06	2.91E-06	5.77E-12	2.70E-03
D87-12	6000	89.49	612.11	2.23E-06	3.33E-06	7.43E-12	3.48E-03
D87-13	6600	89.00	598.75	2.22E-06	3.26E-06	7.23E-12	3.39E-03
D87-15	7800	102.51	678.80	2.56E-06	3.69E-06	9.44E-12	4.43E-03

Exp 88: pH 10.5, 20°C, 0.042m^2 , K_{sp} =$10^{-9.58}$

Sample #	Time (sec)	Ca (ppb)	W (ppb)	Ca, M	W, M	IAP	ln(Ksp/(Ksp-IAP))
D88-01	300	22.02	126.87	4.72E-07	5.41E-07	3.00E-13	1.14E-03
D88-02	600	25.46	162.58	5.7E-07	7.41E-07	4.44E-13	1.69E-03
D88-03	1200	38.02	238.22	7.75E-07	1.06E-06	9.71E-13	3.70E-03
D88-04	1800	47.70	333.65	1.13E-06	1.5E-06	1.71E-12	6.51E-03
D88-05	2400	60.32	401.51	1.19E-06	1.72E-06	2.60E-12	9.92E-03
D88-06	3000	63.84	441.85	1.39E-06	1.98E-06	3.03E-12	1.16E-02
D88-07	3600	67.69	428.34	1.68E-06	2.27E-06	3.11E-12	1.19E-02
D88-08	4200	74.92	514.56	1.71E-06	2.42E-06	4.13E-12	1.58E-02
D88-09	4800	80.04	546.87	1.77E-06	2.66E-06	4.69E-12	1.80E-02
D88-10	5400	88.64	593.88	2.01E-06	2.84E-06	5.65E-12	2.17E-02
D88-11	6000	92.67	604.71	1.98E-06	2.91E-06	6.01E-12	2.31E-02
D88-12	6600	96.98	651.57	2.23E-06	3.33E-06	6.78E-12	2.61E-02
D88-13	7200	96.01	660.25	2.22E-06	3.26E-06	6.80E-12	2.62E-02
D88-14	7800	115.00	729.17	2.56E-06	3.69E-06	8.99E-12	3.48E-02
D88-15	8400	108.32	725.65	4.72E-07	5.41E-07	3.00E-13	1.14E-03

Exp 89: pH 10.5, 20^{o}C, 0.042m^{2} , K_{sp} =10$^{-9.58}$

Sample #	Time (sec)	Ca (ppb)	W (ppb)	Ca, M	W, M	IAP	ln(Ksp/(Ksp-IAP))
D89-01	300	19.75	100.35	4.93E-07	5.46E-07	2.13E-13	9.94E-05
D89-02	600	23.68	137.09	5.91E-07	7.46E-07	3.48E-13	1.63E-04
D89-03	1200	31.87	195.61	7.95E-07	1.06E-06	6.69E-13	3.13E-04
D89-04	1800	46.15	276.99	1.15E-06	1.51E-06	1.37E-12	6.41E-04
D89-05	2400	48.46	316.51	1.21E-06	1.72E-06	1.64E-12	7.70E-04
D89-06	3000	56.39	365.57	1.41E-06	1.99E-06	2.21E-12	1.03E-03
D89-07	3600	68.17	418.92	1.7E-06	2.28E-06	3.06E-12	1.43E-03
D89-08	4200	69.17	446.58	1.73E-06	2.43E-06	3.31E-12	1.55E-03
D89-09	4800	71.69	489.01	1.79E-06	2.66E-06	3.76E-12	1.76E-03
D89-10	5400	81.40	522.60	2.03E-06	2.84E-06	4.56E-12	2.14E-03
D89-11	6000	80.11	536.68	2E-06	2.92E-06	4.61E-12	2.16E-03
D89-12	6600	90.32	612.94	2.25E-06	3.33E-06	5.94E-12	2.78E-03
D89-13	7200	89.83	599.58	2.24E-06	3.26E-06	5.78E-12	2.71E-03
D89-14	8400	103.34	679.63	2.58E-06	3.7E-06	7.53E-12	3.53E-03

Exp 90: pH 6.2, 30°C, 0.042m^2 , K_{sp} =$10^{-9.41}$

Sample #	Time (sec)	Ca (ppb)	W (ppb)	Ca, M	W, M	IAP	ln(Ksp/(Ksp-IAP))
D90-01	60	76.99	117.79	1.92E-06	3.77E-07	5.72071E-13	2.18E-03
D90-02	660	74.39	145.47	1.86E-06	4.84E-07	7.10428E-13	2.70E-03
D90-03	1440	88.66	184.12	2.21E-06	5.93E-07	1.03602E-12	3.95E-03
D90-04	1800	111.65	230.33	2.79E-06	7.67E-07	1.68843E-12	6.44E-03
D90-05	2400	107.46	276.26	2.68E-06	9.51E-07	2.01406E-12	7.69E-03
D90-06	3000	111.62	301.83	2.78E-06	1.11E-06	2.43306E-12	9.29E-03
D90-07	3600	150.07	448.72	3.74E-06	1.51E-06	4.477E-12	1.72E-02
D90-09	4260	149.41	477.90	3.73E-06	1.68E-06	4.94498E-12	1.90E-02
D90-10	5400	160.33	527.01	4E-06	1.83E-06	5.78338E-12	2.22E-02
D90-11	6000	179.79	634.78	4.49E-06	2.11E-06	7.49268E-12	2.89E-02
D90-12	6600	188.59	670.65	4.71E-06	2.26E-06	8.40866E-12	3.25E-02
D90-13	7260	198.54	729.24	4.95E-06	2.46E-06	9.62585E-12	3.73E-02
D90-14	7800	213.56	784.95	5.33E-06	2.6E-06	1.09267E-11	4.24E-02
D90-15	8400	220.99	785.79	5.51E-06	2.74E-06	1.19177E-11	4.64E-02

Appendix D. Calculation of the Solubility Product, K_{sp}, of Scheelite for Various Temperatures

(Calculations are based off of section 8.2 in "Geochemical Thermodynamics" by Nordstrom and Munoz, 1994.)

To determine the effect of temperature on the solubility product for scheelite, the free energy (ΔG) is related to the entropy (ΔS) and enthalpy (ΔH) by

$$\Delta G^o = \Delta H^o - T\Delta S^o \quad (1)$$

The free energy of reaction (ΔG^o_r) is also related to the solubility product by

$$\Delta G^o_r = -RT\ln K_{sp} \quad (2)$$

where R is the gas constant 8.314 J/mol*K and the temperature, T, is in Kelvin. By substituting we get

$$\ln K_{sp} = -\Delta H^o_r/RT + \Delta S^o_r/R \quad (3)$$

which can then be rewritten as

$$\ln K_{sp} = (A/T) + B \quad (4)$$

where $A = \Delta H^o_r/R$ and $B = \Delta S^o_r/R$. If the entropies and enthalpies of formation for the products and reactants in a reaction are known and the heat capacity is assumed to be zero, then the solubility product may be solved for. Table 1 contains the entropy and enthalpy values for Ca^{2+}, WO_4^{2-}, and scheelite.

Table 1.

	ΔH_f J/mol*K	ΔS_f	Source
Ca^{2+}	-542660	-55.23	Naumov et al., 1974
WO_4^{2-}	-1073360	97.49	Naumov et al., 1974
Scheelite	1645150	126.40	Robie et al., 2008

For example, when determining the K_{sp} for scheelite at 20°C (293.15K), first the entropy of reaction (ΔS^o_r) and enthalpy of reaction (ΔH^o_r) were calculated by taking the difference of the products and the reactants from the dissolution of scheelite.

$$\Delta S^o_r = \Sigma \text{ products} - \Sigma \text{ reactants} \quad (5)$$

$$= (97.49 \text{ J/mol*K}) + (-55.23 \text{ J/mol*K}) – (126.40 \text{ J/ mol*K})$$

$$= -84.14 \text{ J/mol*K}$$

$$\Delta H^{o}_{r} = \Sigma \text{ products} - \Sigma \text{ reactants} \quad (6)$$

$$= (-1{,}073{,}360 \text{ J/mol*K}) + (-542{,}660 \text{ J/mol*K}) – (1{,}645{,}150 \text{ J/ mol*K})$$

$$= -3{,}261{,}170 \text{ J/mol*K}$$

Plugging the values from equations 5 and 6 into equation 3 gives

$$\ln K_{sp} = (((-29{,}130 \text{ J/mol*K}) / (8.314 \text{ J/mol*K}))/(293.15\text{K}))+((-84.14 \text{ J/mol*K})/$$

$$(8.314 \text{ J/mol*K})) \quad (7)$$

$$= -22.07 \text{ J/mol*K}$$

Following, $K_{sp} = 2.60\text{x}10^{-10}$ or $10^{-9.58}$. All of the K_{sp} calculated for experiments are shown in Table 2.

Table 2.

Temperature ^{o}C	Temperature (K)	Ln K	Ksp	Log Ksp
8	281.15	-22.58	$1.56\text{x}10^{-10}$	-9.81
20	293.15	-22.07	$2.63\text{x}10^{-10}$	-9.58
21	294.15	-22.03	$2.70\text{x}10^{-10}$	-9.57
22	295.15	-21.99	$2.81\text{x}10^{-10}$	-9.55
23	296.15	-21.95	$2.93\text{x}10^{-10}$	-9.53
24	297.15	-21.91	$3.05\text{x}10^{-10}$	-9.52
30	303.15	-21.68	$3.89\text{x}10^{-10}$	-9.41
35	308.15	-21.49	$4.64\text{x}10^{-10}$	-9.33